OUKA
The University of Osaka
Institutional Knowledge Archive

Title	Distribution of Temperature and Human-Originated Contaminant in Hospital Ward with Displacement Ventilation
Author(s)	Choi, Narae
Citation	大阪大学, 2021, 博士論文
Version Type	VoR
URL	https://doi.org/10.18910/81925
rights	
Note	

The University of Osaka Institutional Knowledge Archive : OUKA

https://ir.library.osaka-u.ac.jp/

The University of Osaka

Doctoral Dissertation

Distribution of Temperature and Human-Originated Contaminant in Hospital Ward with Displacement Ventilation

Narae Choi

December 2020

Graduate School of Engineering,
Osaka University

Acknowledgement

First and foremost I am sincerely grateful to my supervisor Prof. Toshio Yamanaka for his continuous support and for giving me the opportunity to fulfil this study. Whenever I got lost in the research, Prof. Yamanaka guided me to the next step with his overall insights and amazing ideas in this field.

I am also deeply grateful to Prof. Yoshiyuki Shimoda for providing insightful discussions and suggestions about this research. I would like to offer my special thanks to Associate Prof. Tomohiro Kobayashi, for his valuable suggestions, encouragement and criticism throughout this work.

I would like to extend my sincere thanks to Emeritus Prof. Kazunobu Sagara and Dr. Yoshihisa Momoi for their shrewd advice and feedback on my research. I also truly grateful to for the dedicated guidance and inspiration provided by Prof. Hisashi Kotani, who passed away on December 17, 2017.

My sincere thanks also goes to Dr. Eunsu Lim, who has been and will be my emotional prop and who always supported me both happy and troubled times. I would also like to thank Dr. Akihisa Takemura for pertinent advice on the research and life.

I profoundly appreciate the hard work of my co-authors and their substantial contribution in this thesis. I would not have been able to complete this research without them. Thanks Tomoya Suzuki, Junya Yamada, Tatsuya Inagaki, Taisei Ihama and Miho Wakasa. Although we had to spend a long time in the experimental room, I could enjoy it thanks to them. I am truely delighted to have worked with them. In additon, I would also like to say big thank you for all members and students in our laboratory. It is their kind help that have made my daily life in the laboratory a wonderful time.

In the end, I would like to thank my beloved family who have been very patient and always believed and supported me. My parents have always been on my side as a powerful anchor. To come back to Osaka university and study for a doctorate was a very momentous decision for me and my husband. I am extremely grateful to him for encouraging me to go out into the world and pursue my dreams. I also thank to my friends in South Korea, Japan, Shanghai and Manila. Our fragrant memories had kept me going through it all.

Narae Choi

Osaka in December 2020

Contents

NOMENCLATURE

1 INTRODUCTION 1

1.1 Background 2

1.2 What is Displacement Ventilation? 2

1.3 Literature Review 4

1.3.1 Temperature Distribution in a Displacement-ventilated Room 4

1.3.2 Contaminant Concentration Distribution and Stratification Height in a Displacement-ventilated Room 6

1.3.3 Ventilation Effectiveness 8

1.3.4 Displacement Ventilation in a Hospital Ward and Particle Transportation 8

1.3.5 Influence of Disturbances 10

1.3.6 Cooling and Heating System 10

1.4 Objectives 11

1.5 Outline of This Study 13

References 15

2 PREDICTION MODELS FOR TEMPERATURE AND CONTAMINANT CONCENTRATION DISTRIBUTION 21

2.1 Purpose 22

2.2 Prediction of Vertical Temperature Distribution 22

2.1.1 Mundt Model 22

2.1.2 Nielsen Model 23

2.1.3 Xu and Yamanaka Model 24

2.1.4 Mateus and Da Graça Model 25

2.1.5 Zonal Model 26

2.3 Prediction of Vertical Contaminant Concentration Distribution 28

2.3.1 Simplified Model 28

2.3.2 Zonal Model 29

2.3.3 Improved Zonal Model 30

2.4 Plume Rates above Heat Sources 32

2.5 Conclusion 33

References 33

3 DISPLACEMENT-VENTILATED WARD WITH RADIANT PANEL 35

3.1 Purpose 36

3.2 Experimental Investigation in Displacement-ventilated Single-bed Ward with Radiant Panel 36

3.2.1 Experimental Setup 36

3.2.2 Experimental Conditions 39

3.2.3 Experimental Results 39

3.3 Personal Exposure 44

3.3.1 Experimental Setup 44

3.3.2 Experimental Conditions 44

3.3.3 Measured and Predicted Results of Personal Exposure in a Displacement-ventilated ward with Radiant Panel 44

3.3.4 Personal Exposure of the Different Location in the room 48

3.4 Model Validation 49

3.5 Chapter Discussion and Conclusion 53

References 54

Published Papers related to Chapter 3 55

4 INFLUENCE OF VERTICAL CONVECTION AIRFLOW ALONG A VERTICAL SURFACE 57

4.1 Purpose 58

4.2 Experimental Investigation in Single-bed Ward 59

4.2.1 Experimental Setup 59

4.2.2 Experimental Conditions 60

4.2.3 Experimental Results 61

4.3 Experimental Investigation in Four-bed Ward 63

4.3.1 Experimental Setup 63

4.3.2 Experimental Conditions 64

4.3.3 Expreimental Results 65

4.3.3.1 Influence of downward convection flow along the cold wall 66

4.3.3.2 Influence of upward convection flow along the warm wall 71

4.3.4 Influence of downward convective airflow along the wall on the contaminant concentration in the lower part of the room 74

4.3.5 Heat loss and the contaminant concentration in the lower part of the room 75

4.4 Model Validation 77

4.5 Chapter Discussion and Conclusion 80

References 81

Published Papers related to Chapter 4 82

5 INFLUENCE OF INTERNAL PARTITION CURTAINS 84

5.1 Purpose 85

5.2 Experimental Investigation in a Single-bed Ward 86

5.2.1 Experimental Setup 86

5.2.2 Experimental Conditions 88

5.2.3 Experimental Results 88

5.3 Experimental Investigation in a Four-bed Ward 92

5.3.1 Experimental Setup 92

5.3.2 Experimental Conditions 94

5.3.3 Temperature Distribution 95

5.3.4 Contaminant Concentration Distribution 96

5.3.5 Personal Exposure of Lying, Sitting and Standing person 98

5.3.6 Supplied Airflow Rate into the Partition Curtains 100

5.3.7 Prediction of the Contaminant Concentration inside the Curtain with Contaminant Emission 101

5.3.8 Location of the Supply Inlet 103

5.4 Chapter Discussion and Conclusion 108

References 109

Published Papers related to Chapter 5 110

6 CONCLUSIONS 111

Published Papers 116

Nomenclature

A	Surface area [m^2]
$a + a_t$	Molecular and turbulent heat diffusion coefficient [m^2/s]
B	Width [m]
C	Normalized contaminant concentration [-]
C_b	Contaminant concentration at the breathing height outside the breathing zone [-]
C_{exp}	Contaminant concentration of the inhaled air [-]
C_l	Contaminant concentration in the locked-up air [-]
C_{st}	Contaminant concentration at the contaminant interface [-]
c_p	Specific heat at a constant air pressure [J/kg K]
D_p	Distance between the panel and bed [m]
F	View factor
F_{MO}	Fraction of the convective heat generations in the occupied zone [-]
g	Acceleration of gravity [m^2/s]
H_p	Height of the panel (from the floor to the bottom end of the panel) [m]
I_M	Entrained degreee of mixing to the supply airflow [-]
l	Thickness [m]
M	Contaminant emission [m^3/s]
N	Number of contaminant sources [-]
$D + D_t$	Molecular and turbulent diffusion coefficient of the contaminant [m^2/s]
P_c	Convective heat flux (W)
P_{loss}	Heat loss (W)
P_{total}	Total heat generation in the experimental room (W)
T	Temperature [°C]
T_0	Room air temperature at the height of the thermal plume generated by the lying manikin [°C]
T_m	Temperature of the ambient air around the plume [°C]
T_n	Normalized temperature [-]
T_r	Room air temperature [°C]
Q	Airflow rate [m^3/h]

$Q_d(y)$	Downward airflow rate along the wall at height y [m^3/h]
$Q_{dr}(y)$	Downward airflow rate at height y [m^3/h]
$Q_p(y)$	Total thermal plume airflow rate at height y [m^3/h]
$Q_u(y)$	Upward airflow rate along the wall at height y [m^3/h]
$Q_{ur}(y)$	Upward airflow rate at height y [m^3/h]
q	Airflow rate [m^3/s]
Δy	Vertical width of the small wall part [m]
y	Height above the floor [m]
y_{exp}	Height of the breathing zone [m]
y_l	Height of the contaminant stagnation [m]
y_o	Height of the thermal plume generated by the lying person (manikin) [m]
y_{st}	Height of the contaminant interface height (stratification height) [m]
y_{vl}	Height of the virtual heat source [m]
α_c	Convective heat transfer coefficient [W/m^2K]
α_r	Radiative heat transfer coefficient [W/m^2K]
β	Thermal expansion coefficient of air [K^{-1}]
κ	Dimensionless temperature of the air near the floor ($\kappa = (T_{af} - T_s) / (T_e - T_s)$) [-]
η	Height ratio of the interface to the contaminant interface layer
η_e	Effectiveness of entrainment in the human boundary layer
λ	Thermal conductivity [W/mK]
ρ	Air density at normal room temperature [kg/m^3]

Subscription

ac	Near the ceiling
af	Near the floor
ah	Near heat source
ai	Near Wall (i)
ave-1.1m	Average value from the floor to 1.1m in height
bl	Black lamp
c	Ceiling surface
cf	Convective heat
co	Outer surface of ceiling
d	Lower zone of the contaminant interface layer

d-n	Average in the lower zone of the contaminant interface (from floor to neutral height)
e	Exhaust air
f	Floor surface
fo	Outer surface of floor
h	Person simulator (the lying cylinder)
m	Measured value at a point in the room
mx	Mixing layer
o	Outside the chamber
oc	Outer chamber
p	Radiant panel
r	Radiative heat
s	Supply air
u	Upper zone of the contaminant interface layer
w	Wall
wo	Outer surface of wall

Chapter 1.
Introduction

1 Introduction

1.1 Background

The aging population in Japan has dramatically increased more than any other developed country. The statistics Bureau, Ministry of Internal Affairs and Communications in Japan reported that those who are 65 or over made up the 35.6 million and 28.1% of the total population in Sep. 2018. It is so far the highest proportion in the world. This has increased demand for hospital and welfare facilities for the elderly, and the indoor environment of these facilities has begun to attract considerable attention. A hospital ward is a place where inpatients live and get treated, and they spend most of their time in the infirmary. For this reason, both high indoor air quality and comfortable environment are required. The indoor environment of the ward has an impact on their quality of life and the mood of their family and visitors. The hospital environment affects patient and staff outcomes (Ulrich et al. (2004)[1-1)], Rowlands et al. (2008)[1-2)]) Because it is also a workplace for hospital staff, uncomfortable and unhealthy environments may demotivate and stress staff, as well as patients. Unpleasant odors are one of the most bothersome problems regarding indoor environmental quality (IEQ) in hospital wards (Hellgren et al. (2008)[1-3)]). Horiguchi et al. (2015)[1-4)] surveyed the odor perception of nurses in Japanese hospitals and reported that odor management in hospital rooms and at nurses' stations would improve the working conditions for nurses. According to a survey by Itakura et al. (2007)[1-5)], more than 81% of the nursing staff sensed odor problems, and 67.2% of nurses required their improvement. Since air quality is perceived by olfactory and chemical sense (Fanger et al. (1988)[1-6)]), the odor environment is also a crucial factor in the evaluation of IEQ (Wargocki et al. (2006)[1-7)]). Furthermore, odors have been proven to influence cognitive performance and emotions because the olfactory system is directly connected to the limbic structures (Rouby et al. (2002)[1-8)], Millot et al.(2002)[1-9)]) Hence, improvement of the odor environment in a ward is considered an important challenge. To control indoor odor problems, researchers in academia and industry have proposed methods, such as local exhaust ventilation (Knutson (2003)[1-10)]), deodorants, and air fresheners (Beck et al. (1982)[1-11)]). However, the best solution for the odor problem in hospital wards is yet to be determined.

1.2 What is Displacement Ventilation?

Displacement ventilation (DV) was first introduced to a welding industry in Nordic country in 1978 (Yuan et al. (1998)[1-12)].). In the early days, DV had been generally used for industrial facilities with large heat load to offer high air quality in Scandinavia. However, it has been increasingly applied to a non-industrial premises (Svensson et al. (1989)[1-13)]) since the 1980s and it is also used in the United States (Hu et al. (1999)[1-14)]).

Figure 1.1 presents the schematic illustration of DV and **Figure 1.2** shows MV for comparison. DV is well-known for its high effectiveness compared to traditional mixing ventilation (MV) (Seppänen et al. (1989,

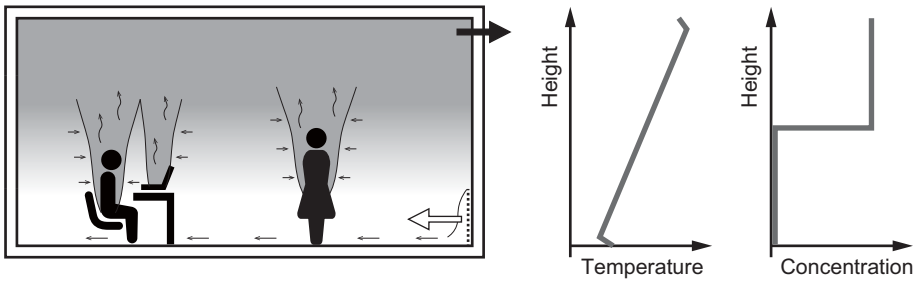


Figure 1.1 Schematic illustration, temperature and contaminant concentration distribution of displacement ventilation (DV)

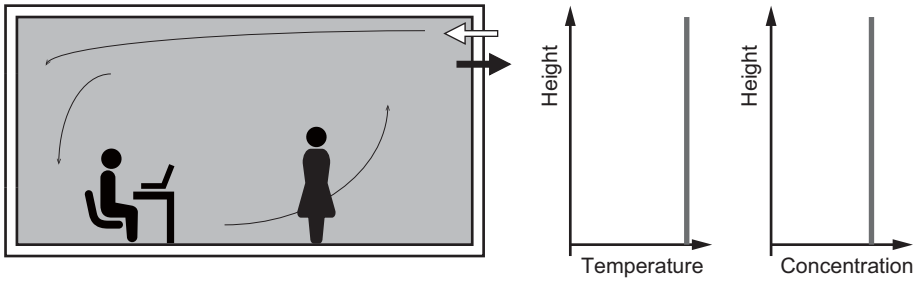


Figure 1.2 Schematic illustration, temperature and contaminant concentration distribution of mixing ventilation (MV)

2008)[1-15,16)], Lin et al. (2005)[1-17)]). Furthermore, DV has also been reported to be an energy-efficient ventilation system, especially in the cooling season (Zhivov et al. (1998)[1-18], Lin et al. (2011)[1-19)], Ahmed et al. (2016)[1-20)]). In rooms with DV, cool and fresh air is introduced near the floor with low velocity. Upward convective plumes are produced around heat sources and ascend to the ceiling while entraining the ambient air. Gaseous pollutants entrained by plumes do not descend because of the vertical temperature gradient and are efficiently exhausted near the ceiling (Kosonen et al. (2017)[1-21)], Mundt et al. (1995)[1-22)]) Hence, DV is particularly useful when contaminant sources are also heat sources. The lower part of the room is filled with the cool and fresh air while the old contaminated air is diplaced upward (Breum et al. (1992)[1-23)], Nielsen (1993)[1-24)]). The room is vertically divided into two zone: the lower clean zone and the upper contaminated zone. For this reason, DV can offer the better air quality to the lower occupied zone. Additionally, less cooling is needed because the cooled air is supplied in the room with DV. However, DV is not always preferable to mixing ventilation (Kosonen et al. (2017)[1-21)]). DV is considered to be able to provide a better environment rather than the mixing ventilation when the contaminant is warmer than the ambient air and the supply air temperature is lower than the surrounding air. Thus, it is not recommended to use when the heating load is the main problem of the room. Furthermore, DV is sensitve to disturbances such as walking occupants and partitions. The height of the room is also important and DV is more suitable to the tall room.

Nielsen (2011)[1-25)] defined the indoor air distribution pattern of cooling mode using three-dimensional chart, which is calle "Family tree". This chart is composed of three axis: the supply airflow rate (Q_s), the difference between the exhaust and supply air temperature (ΔT_s), and the ratio between the total area of the supply inlet and wall area (the surface area where the supply inlet is located) (α_o/A). When $\Delta T_s/Q_s^2$ is large, the covective flow is dominant while inlet momentum is dominant if $\Delta T_s/Q_s^2$ is small. For MV, is smaller than 10^{-3} for MV and $6 \cdot 10^{-3}$ for typical DV (Kosonen et al. (2017)[1-21)], Nielsen (2007)[1-26)]). **Figure 1.3** presents the DV in the "family tree". DV needs large area of supply inlet to achieve a low momentum flow.

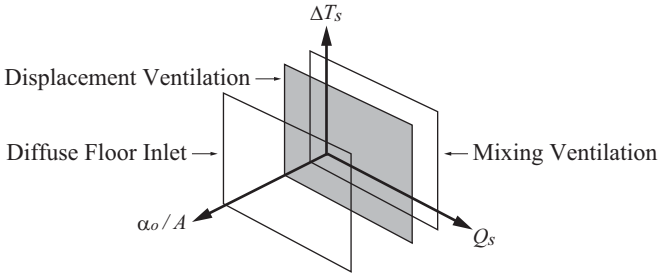


Figure 1.3 Different room air distribution for cooling with low level suppy openings

1.3 Literature Review

1.3.1 Temperature Distribution in a Displacement-ventilated Room

Thermal comfort should also be considered for a comfortable indoor environment. In the room with DV, the positive vertical temperature gradient exists while the temperature in the room is nearly unifrom with the MV. Since its inception, the temperature distribution in the displacement-ventilated room has been investigated in large amount of research. Chen et al. (1988)[1-27)] and Li et al. (1992)[1-28)] found that the air temperature near the floor decreases as the supply airflow rate gets larger. Skistad (1994)[1-39)] examined convection airflows and temperature distribution in a room with DV. Mundt (1995)[1-22)], (1996)[1-30)] focused on the heat transfer balance in the room, especially near the floor, and investigated the vertical temperature gradient. Because the cooled supply air is introduced to the lower part of the room, the air temperature near the floor is relatively low compared to the upper part of the room and there is a potential draught risk. Local discomfort due to a vertical temperature gradient is often considered as a disadvantage of DV (Melikov et al. (1989)[1-31)]). Hence the air temperature near the floor is one of the important factors to decide the supply air temperature and supply airflow rate. A dimensionless air temperature near the floor κ is presented as

$$\kappa = \frac{T_{af} - T_s}{T_e - T_s} \qquad \cdots(1\text{-}1)$$

κ is the relative air temperature near the floor and it varies with types of heat sources in the room. Nielsen (1996)[1-32)] and Brohus and Ryberg (1999)[1-33)] investigated the temperature distribution in the displacement-ventilated room. In their study, κ varied between 0.3 and 0.65 (**Figure 1.3**). κ was nearly 0.3 with a point heat source and κ was 0.58 when sedentary persons are the main heat source. X-axis of the figure indicates temperature ratio (normalized temperature) and it can be defined:

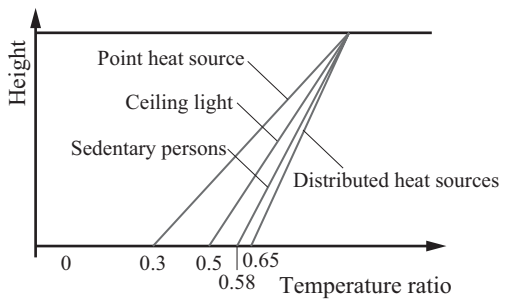


Figure 1.4 κ for different types of heat sources (Kosonen et al. (2017)[1-21)], Nielsen (1996)[1-26)] and Brohus and Ryberg (1999)[1-27)])

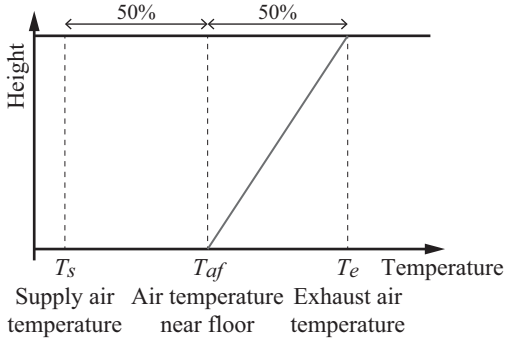


Figure 1.5 The 50% rule of vertical temperature distribution in a room with DV (Kosonen et al. (2017)[1-21)])

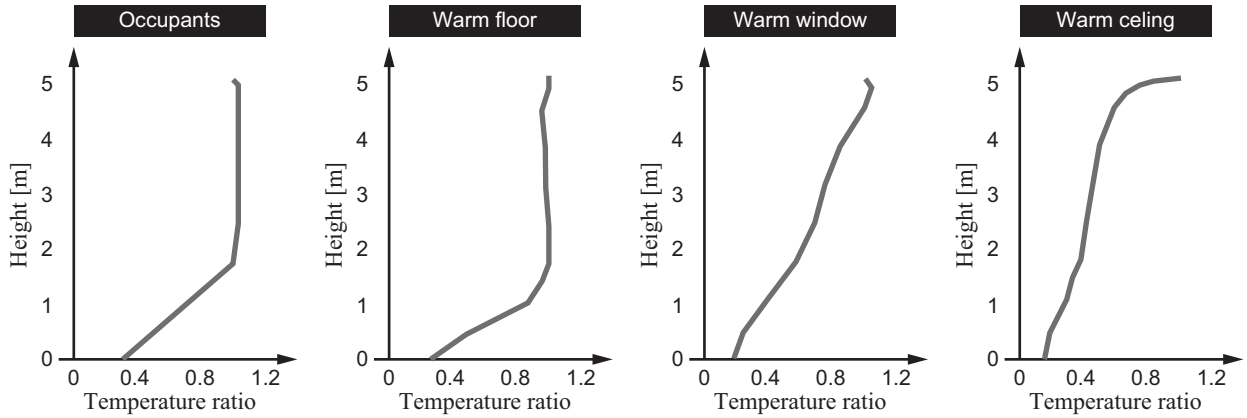


Figure 1.5 Schematic illustration, temperature and contaminant concentration distribution of mixing ventilation (MV) (Kosonen et al. (2016)[1-34])

$$Temperature\ ratio\ (T_n) = \frac{T - T_s}{T_e - T_s} \quad \cdots(1\text{-}2)$$

If there are many different heat sources in the displacement-ventilated room, κ can be simply assumed as 0.5 ("50% rule", **Figure 1.4**)[1-21]. Skistad (1994)[1-29] suggested this simplified temperature profile. The "50% rule" indicates that the half of the toal temperature increase between the supply and exhaust air temperature occurs near the floor owing to the heat transfer from the floor surface.

Vertical temperature distribution is also influnced by types of heat sources. Kosonen et al. (2016)[1-34] studied the vertical temperature distribution with different heat sources and room height conditions. **Figure 1.5** presents the measured results of their experiments. When occupants or a warm floor are the dominant heat sources, the positive temperature gradient exists the lower part of ther room (occupied zone) while the air temperature of the upper part was nearly consistent. On the other hand, the vertical temperature profile was nearly linear when the heated window was the only heat source. However, the air temperature was stratified if other dominant heat elements (occupants) also existed in the occupied zone. When there was heated ceiling, the air temperature mainly increased in the upper part of the room. In order to avoid thermal discomfort derived from the vertical temeprature gradient, the suppy air temperature of DV cannot be very low. Hence, the ancillary cooling system is needed in the room with large cooling load. Rees et al. (2013)[1-35] examined the temperature distribution in the displacement-ventilated room with chilled ceiling. In all cases, the air temperature gradiens were in the lower part of the room; however the temperature gradient was evidently reduced in the upper part, which was similar to the MV. Causone et al. (2010)[1-36] studied the DV combined with floor cooling. The relative air temperature near the floor was lower than general DV, hence, the large vertical temperature difference occured and the "50% rule" could not be applied for this system.

To appropriately apply DV to hospital wards, the indoor temperature must be forecasted during the design phase. Previous studies have already developed several models to predict the vertical temperature profile of a displacement ventilated room. The two-node model developed by Mundt (1996)[1-30] is the most well-known of these models. In the two-node model, the vertical temperature profile is linearized between the floor and ceiling levels. The Nielsen model (Nielsen (2007)[1-26]) assumes that the air temperature is constant in the upper zone of neutral height. Rees and Haves (2001)[1-37] proposed the multi-nodal model which consists of

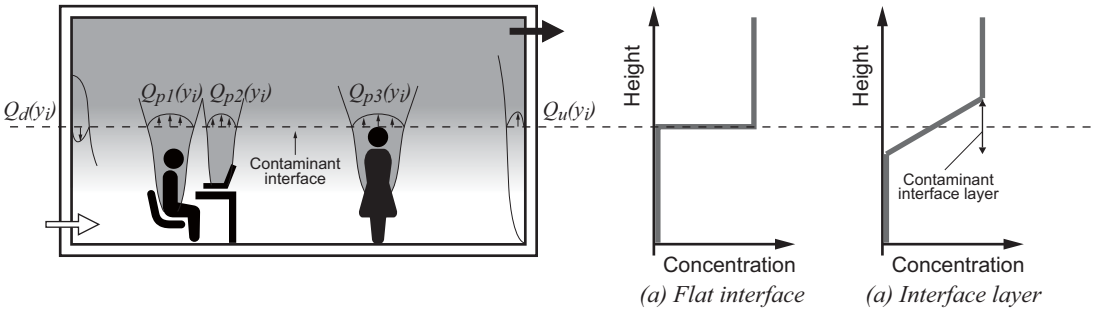


Figure 1.6 Contaminant concentration in a room with DV and contaminant interface

11 nodes: 4 room air nodes, 4 nodes of the air flow in the plume and 3 surface nodes. The three-node model suggested by Mateus and da Graça (2015)[1-38] further improved the accuracy of the predicted temperature distribution.

1.3.2 Contaminant Concentration Distribution and Stratification Height in a Displacement-ventilated room

Whether the pollutants are heat sources or not is a crucial factor for the contaminant concentration in the displacement-ventilated room. If the contaminant source is also a heat source and is not denser than the air, the contaminated air would be transported directly to the upper part of the room and exhausted efficiently. However, if the pollutants are large particles and denser than the air, the contaminant concentration in the occupied zone would not be low and it might even higher than the MV. In the general displacement-ventilated room with warm or hot contaminant sources, the contaminant concentration can be vertically divided into two zones: the lower fresh zone and the upper polluted zone. The interface between two zones is formed at the neutral height (stratification height) y_i where the supply airflow rate Q_s and the sum of convective airflow rates (the upward and downward convection airflow rates along walls, and total plume airflow rates, denoted as Q_u, Q_d, and Q_p, respectively) are equal (**Figure 1.6**, Sandberg et al. (1989)[1-39], Nielsen (2007)[1-26]):

$$Q_s = Q_p(y_i) + Q_u(y_i) - Q_d(y_i) \quad \cdots(1\text{-}3)$$

The contaminant concentration in the lower part of the contaminant interface is low and the concentration in the space upper than interface is nearly closed to the exhaust air. When there is no downward convection airflow, the air quality in the lower part is as good as the supply air. The neutral height is often considered as a flat line (**Figure 1.6(a)**), although there is an intermediate stratified layer between the lower zone and the upper zone because of molecular and turbulent diffusion in actual situations (**Figure 1.6(b)**). There is an intermediate stratified layer between the two zones (contaminant interface layer), rather than them being clearly separated.

If all of convection airflow in the room is able to be forecasted, the neutral height could be accurately calculated. Xing and Awbi (2002)[1-40] measured the neutral height in a experimental chamber with various heat load. The measured height was compared with the predicted height and it agreed well. Yamanaka et al. (2007)[1-41] and Suzuki et al. (2008)[1-42] estimated the neutral height from the plume rates of the heat sources in the room and the calculated results matched well with the measured results. Several studies suggested the

equation for estimating the neutral height (stratification height). Nielsen assumed that the neutral height is located at the height where the plume above the heat source lose the buoyancy.

$$y_{mx} = 0.62 \cdot {P_{cf}}^{\frac{2}{5}} \cdot \left(T_e - T_{af}\right)^{-\frac{3}{5}} \quad \cdots(1\text{-}4)$$

Mateus and da Graça assumed that the heat source in a room are the point source and it is placed near the floor. The neutral height in their model is calculated by

$$y_{mx} = 23.95\left(\frac{{q_s}^3}{P_{cf}}\right)^{\frac{1}{5}} \quad \cdots(1\text{-}5)$$

DV is particularly efficient when the contamiant is also a heat source. If the contaminant is emitted without positive buoyancy in the lower part of the room, the contaminant concentration would not be stratified. Cermark and Melikov (2006)[1-43] examined the contaminant concentration in a room with pollutant near the floor. Because the pollutants were not heat sources and the contaminant concentration profile was close to the MV except for near the floor. On the other hand, if there is a stronger heat source than a contaminant source, the contaminated air will be locked-up in the middle of the room and cannot reach the ceiling (**Figure 1.7**). This lock-up phenomenon in DV is first revealed by Stymne et al. (1991)[1-44]. Bjørn and Nielsen (2002)[1-45] found the exhaled air from the human could be locked-up and it might be inhaled directly by another person in the displacement-ventilated room. Although the contaminant concentration in the lower part of the room is significantly low in a room with DV; however, there is a risk of worse personal exposure rather than MV. To take advantage of DV, this lock-up phenomenon should be revealed.

In terms of predicting the contaminant concentration distribution in a room with DV, there are relatively few studies compared to the temperature models. It is often considered that the contaminant concentration in the lower part of the neutral height (stratification height, mixing height) is low and the upper part is high. However, the diffusion across the neutral height should be considered to predict the actual contaminant concentration profile. Lin and Lin (2014)[1-45] suggested two-layer stratification model and studied on the thickness of the intermediated stratified layer as well. Yamanaka et al. (2007)[1-41] suggested a zonal model for predicting the vertical contaminant concentration distribution in a room with DV. Since the zonal model takes into account the diffusion across the interface, the contaminant interface has a thickness, which is close to the contaminant concentration distribution under real conditions. Suzuki et al. (2008)[1-42] suggested an improved zonal model to predict the contaminant concentration distribution when the contaminated air is locked up. Inagaki et al. (2012)[1-47] and Yamanaka et al. (2012)[1-48] developed a coupled zonal model that can predict the temperature and contaminant concentration profiles simultaneously.

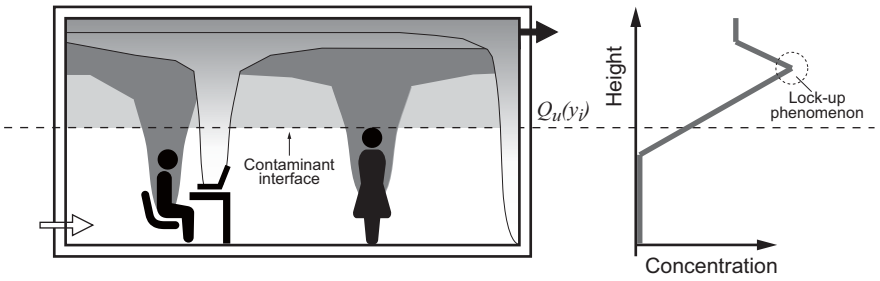


Figure 1.7 Lock-up phenomenon in a room with DV

1.3.2 Ventilation Effectiveness

The contaminant removal effectiveness ε^c and air change efficiency ε^a (Mundt et al. (2004)[1-49]) are often used to evaluate the ventilation effectiveness of DV.

$$\varepsilon^c = \frac{C_e - C_s}{C_{mean} - C_s} \quad \cdots(1\text{-}6)$$

$$\varepsilon^a = \frac{\tau_n}{\overline{\tau_r}} \cdot 100 = \frac{\tau_n}{2 \cdot \bar{\tau}} \cdot 100 \quad \cdots(1\text{-}7)$$

The contaminant removal effectiveness in a room with DV is considered to be larger than 1. With ideal piston flow, the air change efficiency is 100%. The air change efficiency of DV is known to be between 50 and 100% and it is generally higher (mostly 60-70%) than MV (50%).

The normalized concentration at the breath level of the person is also used as ventilation effectiveness (Chen and Glicksman (2003)[1-50]).

$$\eta_h = \frac{C_h - C_s}{C_e - C_s} \quad \cdots(1\text{-}8)$$

It seems to be similar to the inverse of the contaminant removal effectiveness. However, it evaluates the contaminant concentration at a specific height while the ε^c estimates the mean concentration in the room or in the occupied zone.

The interface layer of a displacement ventilated room exists above the occupied zone. While lying or sitting occupants inhale clean air in the lower zone of the interface layer, the breathing zone of standing occupants is occasionally located in the upper zone. Brohus and Nielsen (1996)[1-51] carried out full-scale measurements of personal exposure and found that standing occupants could inhale cleaner air than the contaminant concentration at the same height. There is the boundary layer around the body and the contaminant concentration inside the layer is low because it goes up while entraing the air from floor to the breathing level. They proposed an index for ventilation effectiveness ${\varepsilon_{exp}}^c$ which is called personal exposure index. This index takes into account that person inhaled the air inside the boundary layer. However, it should be noticed that this index may not suitable when there are moving persons in a room. (**Figure 1.8**)

$${\varepsilon_{exp}}^c = \frac{C_e - C_s}{C_{exp} - C_s} \quad \cdots(1\text{-}9)$$

If the neutral heigh is known, personal exposure can be calculated by

$$C_{exp} = C_e - \frac{y_i}{y_{exp}}\left(C_e - C_f\right) \qquad y_i < y_{exp} \quad \cdots(1\text{-}10)$$

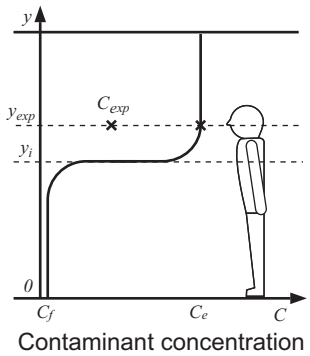


Figure 1.8 Personal exposure

1.3.4 Displacement Ventilation in a Hospital Ward and Particle Transportation

Because DV can provide clean air to the occupied zone in a room, many studies have been examined the applicability of DV to hospital wards (Beggs et al. (2008)[1-52]). However, since severe acute respiratory syndrome (SARS) affected the world in 2003 (Qian et al. (2009)[1-53]), most of the studies have only focused

on whether DV can prevent droplet infection or not.

According to some research, DV is effective at reducing the risk of airborne infection. Hillerbrant and Ljungqvist (1990)[1-54] examined the performance of mixing, displacement and downward airflow for the operating room and proved that DV has a superior performance. Yin et al. (2009)[1-55] conducted the experiment to compare DV with MV in terms of the infectious disease transmission. They used SF_6 gas to simulated the infectious contaminant and found that DV could provide the better air quality to the breathing zone rather than MV. Berlanga et al. (2018)[1-56] demonstrated that the exhaled contaminant could go up with the plume of the source manikin successfully when the manikin that exhaled contaminant air was facing up. Li et al. (2011)[1-57] examined the exposure risk for the co-occupant under displacement, mixing and underfloor ventilation by the numerical study. As a result, it was found that DV could provide better air quality when the droplet residuals are smaller than 5 μm and the co-occupant is located a certain distance from the source. However, if the contaminants are large, the efficiency of DV got worse. There are also several studies have found that DV has a higher exposure risk than other ventilation systems. Qian et al. (2006)[1-58] investigated hospital wards with three different ventilation systems: displacement, mixing, and downward ventilation. They used CO_2 to simulate the droplet nuclei from the patient. DV was effective if the contaminated air was exhaled upward. However, their results showed that DV had worse efficiency in removing infectious droplets than other ventilation systems when the lying patient exhaled facing sideways. The exhaled jet from the source manikin penetrated a long distance along the exhaled direction. Villafruela et al. (2019)[1-59] revealed that exhaled air could be locked-up at the inhale height in a ward.

The movement of various sizes of particles in a room with DV may be an important key to judge the suitability of DV for preventing nosocomial infection. Mundt (2001)[1-60] evaluated the ventilation efficiency of DV, when the contaminant sources were particles and emitted without buoyancy force. Although the resuspension risk of particles was little, it needs further study because the particles larger than 0.5 μm were only investigated and the particle concentration inside the plume fluctuated according to the location of the contamiants. Lai and Cheng (2007)[1-61] examined droplet nuclei dispersion and transport in a room with DV by computational fluid dynamics (CFD). They focused on two droplet nuclei size, 0.01 and 10μm and found that large droplets float in the lower part of the room. Mundt (2008)[1-62] studied the several sizes of particle concentration in the plume with DV and MV, when the particles were distributed near the floor. The results indicated DV has a higher exposure risk. From these results, it seems to be crucial to examine the entrainment of the particles to the boundary layer around the human (the convection airflow). There are some studies on particle transport of the convection flow around the human. Rim and Novoselac (2009)[1-63] investigated the particulate and gaseous contaminants in the thermal plume around the sitting manikin under mixed and stratified airflow patterns. They found that the convection airflow around the human can transport the particulated contaminants near the floor to the inhale zone. Licina et al. (2015)[1-64] also examined the contaminant concentration inside the thermal plume (the human convective boundary layer (CBL))around the person, when the particles were emitted near the floor or by cough. The measured results indicated that the airborne particles released near the floor was transported by CBL. On the other hand, the impact of CBL was not considerble when the particles were released by cough.

The suitability of DV is still a matter of controversy, especially if droplet or airborne transmission is the primary concern in wards. Li et al. (2011)[1-65] summarized the studies on displacement ventilation in hospital environments. They stated three unfavorable conditions for DV in hopitals. The first is that DV does not have a good efficiency with denser pollutants such as large droplet. The second is when the contaminants are horizontally emitted with momentum but without positive buoyancy force. In this case, the contaminants would stay long in the lower part of the room. The last is disturbances such as moving person in hospitals. For these reasons, they did not recommend DV for hospitals in the meantime and further studies are needed. To assess the suitability of DV for the ward in terms of preventing nosocomial infection, the exhaled particle by coughing or speaking should be also investigated. However, most study carried out their experiment using tracer gas to simulate the droplet or drople nuclei, or used CFD without the experimental results. Hence, further researches are needed before applying DV to a ward for the purpose of reducing infection risk.

1.3.5 Influence of Disturbances

The contaminant concentration in the displacement-ventilated room is sensitive to disturbances (Kosonen et al. (2017)), whereas the temperature distribution is nearly impervious because of the stable temperature gradient. Mundt (1994)[1-66] studied the influence of the door opening and closing, and person entering on the stability of the contaminant concentration distribution. As a result, opening and closing door led a significant decrease in the local effectiveness; however, the air quality in the breathing zone was still good. Moving person also affects the contaminant concentration. Mattsson et al. (1997)[1-67] simulated the displacement ventilated room with moving person. When the person simulator moved with not slow speed (larger than 0.6 m/s), both of the ventilation effectiveness and the air quality in the breathing zone decreased considerably. Mazumdar et al. (2010)[1-68] also investigated the influence of moving object, but using CFD and for a ward. The contaminant concentration was not significantly influenced by the moving objects; however, if the location of the object was close, the concentration changed considerably.

The partitions and layout also affect the contaminant concentration in a room with DV. Lau and Chen (2007)[1-69] investigated the impact of furniture arrangement and partition location on indoor environment in the displacement-ventilated room by CFD and it was revealed that those parameters had a significant influence on thermal comfort and air quality. Ahn et al. (2018)[1-70] also proved that the internal partition affected the air quality and energy consumption in a room with DV. Lin et al (2007)[1-71] found that the location of opening affected on air quailty of DV.

1.3.6 Cooling and Heating System

Since the supply air temperature of DV cannot be very low, the complementary cooling system is need if there is great cooling load. On the contrary, the supply air temperature should be lower than the target room temperature in a room with DV. Hence, the ancillary heating system is required during heating season. If there is active air movements inside the room with DV, the temperature and contaminant distribution will be affected and no longer stratified. For this reason, the radiant cooling and heating system can be more suitable

rather than the air conditioning system with fans.

Several studies explored to find an appropriate cooling or heating system for DV. Chilled ceiling might be the most studied complementary cooling system of DV. However, it might be counter productive, because the temperature gradient in a displacement-ventilated room is positive and the air temperature near the ceiling is high. Alamadari et al. (1998)[1-72)] proved that the chilled ceiling affects air temperature near the ceiling and causes the downward airflow. Tan et al. (1998)[1-73)] studied about each ratio of the cooling load handled by DV and chilled ceiling. In their study, it was recommended that DV remove at least 33% of cooling load in the room and the vertical temperature gradient should be larger than 2 °C/m. Novoselac and Srebic (2002)[1-74)] reviewed the studies about the chilled ceiling with DV and affirmed that the ratio of cooling load of DV and the chilled ceiling is a crucial parameter. Rees and Haves (2013)[1-75)] and Mateus and da Graça (2015)[1-76)] developed the prediction model for temperature distribution in the displacement-ventilated room with chilled ceiling. Aside from the chilled ceiling, passive chilled beam (PCB) has been also investigated as a cooling system with DV. Because PCB do not use fan and it has silent operation, it is considered that PCB may be a good complementary cooling system of DV in non-industrial building. Shan and Rim (2018)[1-77)] examined the thermal comfort and ventilation performance of combined PCB and DV systems using CFD. Zhu et al. (2019)1-78) also investigated indoor environment of DV-PCB system by validated CFD model. They revealed that PCB could minimize the vertical temperature difference and removed the cooling load in a room effectively. However, as the cooling capacity of PCB got larger, the downdraught risk also increased and the indoor air quality got worse. Floor cooling and heating was also studied by Causone et al. (2010)[1-79)] and Wu et al. (2013)[1-80)]. When floor heating was used, the air temperature near the floor is higher than the general DV in their experiment while the high air quality in the lower part of the room was maintained. However, because floor cooling increases the vertical air temperature difference, it should be carefully used with DV.

1.4 Objectives

An unpleasant odor in hospital wards is one of the most perplexing problems for indoor environments. An uncomfortable environment due to odor leads to a myriad of problems that contribute to the stress levels of patients, healthcare workers, and visitors. Unpleasant odors in hospital wards are diffused from human bodies or their discharges, and the human body is also a heat source. Displacement ventilation (DV) is known for providing high air quality to the occupied zone, especially when contaminant is emitted from a heat source. Thus, DV may be an effective way to remove heat and odor from the wards. The aim of this study is to explore the potential application of DV to the hospital ward, in order to provide high air quailty to a ward and create a comfortable indoor environment.

The validity of DV for a hospital ward is verified mainly by experimental method in this study. There is large amount of studies on applicability of DV to the wards; however few studies focused on reducing unpleasant odor or thermal comfort in a ward. Although the suitability of DV for preventing nosocomial infections is still a matter of controversy and it requires further study, it is clear that DV is superior to other ventilation

systems when the contaminant is combined with the plume from a heat source. The target pollutants of this study were unpleasant odors in the general wards and nursing facilities, not in the infection isolation wards, and it was expected that unpleasant odors could be removed efficiently with DV. Most hospitals contain a greater number of general wards compared with infection isolation wards, and unpleasant odors in general wards (e.g., cancer ward, long-term care ward) are now highly problematic.

Because the supply air temperature of DV should be lower than the room air temperature, the complementary heating system is required when there is heating load in the room. Additionally, the cooling capacity of DV is limited, the ancillary cooling system is need if the cooling load is large. hospital wards in Japan are generally multiple-bed wards, it is difficult to design the thermal environment to satify all patients in a ward. Patients are sensitive to thermal environment and the preferable thermal condition of each patient would be different. Radian panel is personally controllable and the thermal comfort is also better than convective heating system. Although it is expected that the radiant panel is compatible with DV, there are few studies about using radiant panel as a complementary system for the DV. This study proposes using radiant panel, and the influence of the radiant panel on the indoor environment in a room with DV is examined. To find the proper condition of radiant panel, several parameters related to radiant panel were adopted. Since it is known that the lock-up phenomenon occurs if there is stronger heat source than the contaminant source, the conditions that cause the lock-up phenomenon is analyzed.

If there is heat loss or heat gain through the wall, the vertical convection airflow is generated along a wall. Downward and upward airflow may have a great influence on the neutral height and the contaminant concentration profile in a room with DV. If DV is used in a room containing a window or a poorly insulated wall, the convention airflow along the vertical surface during the cold and hot season will affect the indoor environment of the room.To prevent deterioration of air quality in the occupied zone and to remove the unpleasant odor efficiently in a ward, the convection airflow along a vertical suface should be studied. Hence, the influence of this downward and upward airflow on indoor air quality in a displacement-ventilated ward is examined in this study. The temperature and contaminant concentration distributions are measured under various conditions regarding the temperature difference between the wall surface and room air.

As it was mentioned in Section 1.3.5, the layout, internal partition, the location of contaminant source significantly affect the contaminant concentration distribution in the displacement-ventilated room. If DV is installed in the multiple-bed hospital wards without examining the influence of internal partition curtains, the indoor environment could be different from expectations. This study investigates the indoor environment in a displacement-ventilated hospital ward containing internal partition curtains. The temeprature and contaminant concentration with and without curtain is measured and the influence of curtain on the efficiency of removing contaminant is analyzed.

For the design of an indoor air environment, it is essential to correctly predict the air temperature and contaminant concentration distribution. Previous studies have already developed various models to predict the vertical temperature and contaminant concentration profile of a displacement ventilated room. However, which model is suitable for the hospital wards is not known yet. Unlike the office building, the dominant

heat sources in a ward are lying patients. Because the convection airflow above the lying person is different from the sitting person, the temperature and concentration distributions would also be different. In this study, several models are validated to find the appropriate model for a ward with DV.

1.5 Outline of This Study

This work is consisted of six chapters. **Figure 1.9** shows the outline and flowchart of this study.

Chapter 1. Introduction

In this chapter, the background of this study was described and the basic knowledge of displacement ventilation (DV) was illustrated. The literatures regarding the temperature and contaminant concentration distribution, ventilation effectiveness, influence of disturbance and cooling or heating system in a room with DV and DV in the hopital environments are also reviewed.

Chapter 2. Prediction of Temperature and Contaminant Concentration Distributions

This chapter introduced several prediction models for vertical temperature and contaminant concentration profiles in the displacement-ventilated room. The theory and calculation method of each model was explained and the differences between the models were also given. Additionally, the equations for convection airflow rate of the various heat sources in this study were presented.

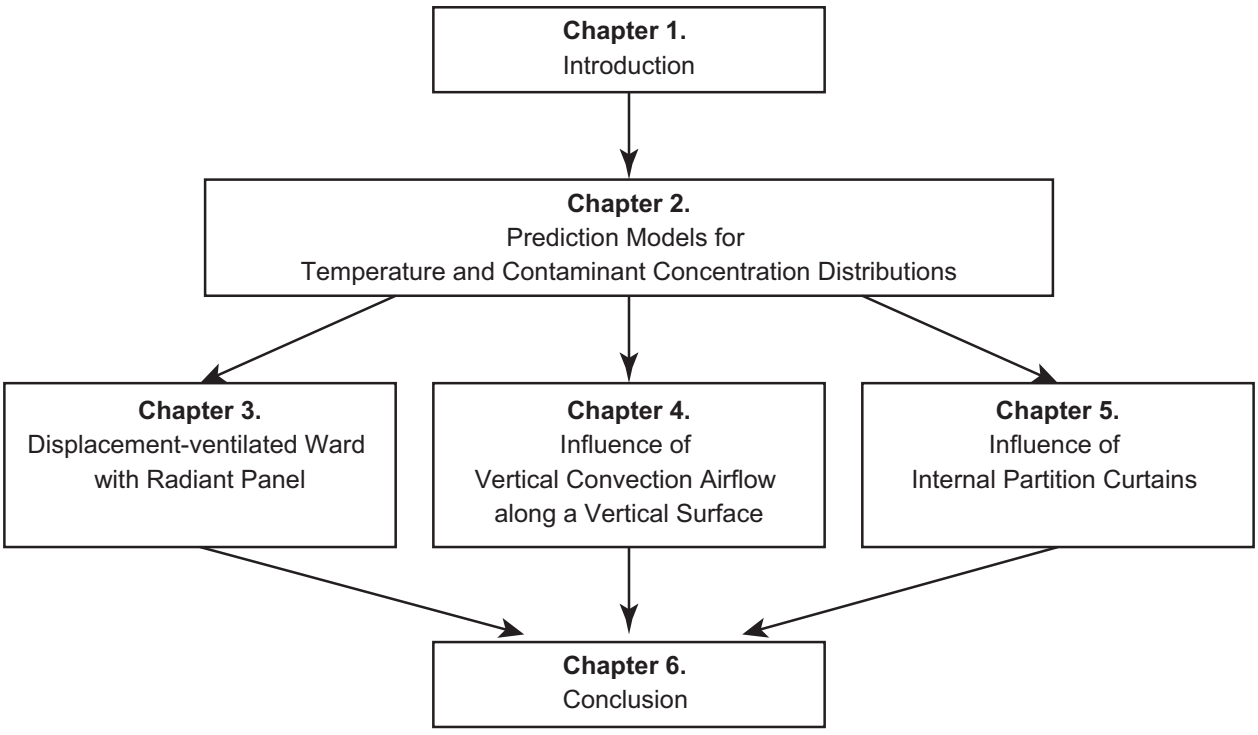


Figure 1.9 Outline of this study

Chapter 3. Displacement-ventilated Ward with Radiant Panel

This chapter presented the experimental results of the temperature and contaminant concentration distributions in the displacement-ventilated single-bed ward with radiant panel. To examine the influence of the radiant panel, several conditions related to panel were varied. The lock-up phenomenon and personal exposure of standing person were also investigated. Furthermore, the prediction model was validated with experimental results.

Chapter 4. Influence of Vertical Convection Airflow along a Vertical Surface

This chapter focused on the influence of downward and upward airflow along a cold or warm wall in a room with DV. The measurements were carried out in single-bed and four-bed displacement-ventilated ward under different heat loss or gain through the wall. The conditions that the temperautre and contaminant concentration distributions were not stratified in were analyzed. The simpified model for predicting the contaminant concentration in the displacement-ventilated room with downward airflow (proposed in Chapter 2) was valitdated. Additionally, the calculated results using zonal model were compared with the measured results.

Chapter 5. Influence of Internal Partition Curtains

This chapter presented the experimental study on the impact ot the internal partition curtains in a ward. The temperature and contaminant concentration profiles inside and outside the partition curtains were measured and compared with the measured results without the curtains. Supplied airflow rate inside the curtain was also analyzed and the predictability of the contaminant concentration inside the curtain with contaminant source was investigated.

Chapter 6 . Conclusion

This chapter summarized the findings and outcome of this study. The uncertainty and limitation of this work were discussed and the further study was also mentioned.

References

1-1) R. Ulrich, X. Quan, C. Zimring, A. Joseph, R. Choudhary (2004) : The role of the physical environment in the hospital of the 21st Century: A once in a lifetime opportunity. *Report to the Center for Health Design for the "Designing the 21st Century Hospital Project"*, The Center for Health Design, Concord, CA.

1-2) J. Rowlands (2008) : How does the environment impact on the quality of life advanced cancer patients? A qualitative study with implications for ward design, *Palliat. Med*. 22, pp.768–774.

1-3) UM. Hellgren, M. Lahitinen (2008) : Indoor-air-related complaints and symtoms among hospital workers, *Scandinavian Journal of Work, Environment and Health, Supplement*, 4, pp.58-63.

1-4) M. Horiguchi, E. Shudo, K. Sato, M. Nakamura, W. Sai, T. Ohinata (2015) : Nurse odor perception in various Japanese hospital settings, *Int. J. Nurs. Sci*. 2, pp.355–360.

1-5) T. Itakura, M. Mitsuda (2007) : Survey of characteristics of the odor in medical facilities, *The 6th International Conference on Indoor Air Quality, Ventilation & Energy Conservation in Buildings IAQVEC 2007*, Oct. 28 - 31, Sendai, Japan.

1-6) P. O. Fanger (1988) : Introduction of the olf and the decipol units to quantify air pollution perceived by humans indoors and outdoors, *Energy Build*. vol.12, pp.1–6.

1-7) P. Wargocki, O. Seppänen, J. Andersson, A. Boerstra, D. Clements-Croome, K. Fitzner, S. O. Hanssen (2006) : REHVA Guidebook No. 6: Indoor Climate and Productivities in Offices, REHVA, Brussels.

1-8) C. Rouby, B. Schaal, D. Dubois, R. Gevais, A. Holley, K (2002) : Olfaction, taste, and cognition, Cambridge University Press, Cambridge.

1-9) JL. Millot, G. Brand, N. Morand (2002) : Effects of ambient odors on reaction time in humans, *Neuroscience Letters*, 322, pp.79-82.

1-10) G.W. Knutson (2003) : Ventilation for odor control, *ASHRAE J*. 45(4), 36.

1-11) W. C. Beck, R. H. Meyer (1982) : Health care environment: The user's viewpoint, CRC Press, Boca Raton, FL.

1-12) X. Yuan, Q. Chen, L . R. Glicksman (1998) : A critical review of displacement ventilation, *ASHRAE Trans*. 104 (Part 1A) pp.78-90.

1-13) A. G. L. Svensson (1989) : Nordic experience of displacement ventilation systems, *ASHRAE Trans. 95* (Part 2), pp.1013-1017.

1-14) S. Hu, Q. Chen, L. R. Glicksman (1999) : Comparison of energy consumption between displacement and mixing ventilation systems for different US buildings and climates, *ASHRAE Trans*. 95. 105(2), pp.453-464.

1-15) O. A. Seppänen, W. J. Fisk, J. Eto, D. T. Grimsrud (1989) : Comparison of conventional mixing and displacement air-conditioning and ventilating systems in U.S. commercial buildings, *ASHRAE Trans*. 95, pp.1028-1040.

1-16) Z. Lin, T. T. Chow, K. F. Fong, C. F. Tsang, Q. Wang (2005) : Comparison of performances of displacement and mixing ventilations. Part II: indoor air quality. *International Journal of Refrigeration* 28(2), pp.288-305.

1-17)O. A. Seppänen (2008) : Ventilation Strategies for Good Indoor Air Quality and Energy EfficiencInternational Journal of Ventilation 6:4, pp.297-306.

1-18)A. M. Zhivov, A. A. Rymkevich, Comparison of heating and cooling energy consumption by HVAC system with mixing and displacement air distribution for a restaurant dining area in different climates, *ASHARE Trans*. 104 (2) (1998) 473-484

1-19)Z. Lin, C.K. Lee, S. Fong, T.T. Chow, T. Yao, A.L.S. Chan, Comparison of annual energy performances with different ventilation methods for cooling, *Energy Build*. 43 (1) (2011) 130–136.

1-20)A. Q. Ahmed, S. Gao, A.K. Kareem, A numerical study on the effects of exhaust locations on energy consumption and thermal environment in an office room served by displacement ventilation, *Energy Convers. Manag*. 117 (2016) 74–85.

1-21)R. Kosonen, A. Melikov, E. Mundt, P. Mustakallio, P. V. Nielsen, REHVA Guidebook No. 23: Displacement Ventilation, REHVA, Brussels, 2017.

1-22)E. Mundt, Displacement ventilation systems: Convection flow and temperature gradients, *Build. Environ*. 30(1) (1995) 129–133.

1-23)N. O. Breum, Flow fields of simulated body odor in an office ventilated from the displacement design principle, Proceedings of Roomvent '92, Aalborg, Denmark, Vol. 3 (1992) 181-194.

1-24)P. V. Nielsen, Displacement ventilation: Theory and design, Aalborg University, Aalborg, 1993.

1-25)P. V. Nielsen, The "family tree" of air distribution systems, *Proceedings of ROOMVENT 2011, 12th International Conference on Air Distribution in Rooms*, Trondheim, Norway

1-26)P. V. Nielsen, Analysis and design of room air distribution systems, *HVAC&R Research* (2007) 13(6) 987-997.

1-27)Q. J. Chen, J. van de Kooi, A. Meyers, Measurements and computations of ventilation efficiency and temperature efficiency in a ventilated room, *Energy Build*. 12(2) (1988) 85-99.

1-28)Y. Li, M. Sandberg, L. Fuchs, Vertical temperature profiles in rooms ventilated by displacement: Full-scale measurement and nodal modelling, *Indoor Air*. 2 (1992) 225-243.

1-29)H. Skistad, Displacement Ventilation, Research Studies Press Ltd., Baldock, 1994.

1-30)E. Mundt, The Performance of Displacement Ventilation – Experimental and Theoretical Studies, PhD thesis, Royal Institute of Technology, Stockholm, 1996.

1-31)A. K. Melikov, J. B. Nielsen, Local thermal discomfort due to draft and vertical temperature difference in rooms with displacement ventilation, *ASHRAE Trans*. 96 (1989) 1050–1057.

1-32)P. V. Nielsen, Temperature distribution in a displacment-ventilated room, *In Roomvent '96: Proceedings of the 5th International Conference on Air Distribution in room*, Yokohama, Japan (1996) Vol.3 232-330.

1-33)H. Brohus, H. Ryberg, The kappa model - a simple model for the approximate determination of vertical temperature distribution in rooms, Department of Building Technology and Structural Engineering, Aalborg University (1999)

1-34)R. Kosonen, N. Lastovets, P. Mustakallio, G. C. da Graça, N. M. Mateus, M. Rosenqvist, The effect of typical buoyant flow elements and heat load combinations on room air temperature profile with

displacement ventilation, *Build. Environ*. 108 (2016) 207–219.

1-35)S. J. Rees, P. Haves, An experimental study of air flow and temperature distribution in a room with displacement ventilation and a chilled ceiling, *Building and Environment*. 59 (2013) 358-368

1-36)F. Causone, F. Baldin, B. W. Olesen, S. P. Corgnati, Floor heating and cooling combined with displacement ventilation: Possibilities and limitations, *Energy Build*. 42(12) (2010) 2338–2352.

1-37)S. J. Rees, P. Haves, A nodal model for displacement ventilation and chilled ceiling systems in office spaces. *Building and Environment*. 36(6) (2001) 753–762.

1-38)N. M. Mateus, G. C. da Graça, A validated three-node model for displacement ventilation, *Building and Environment*. 84 (2015) 50–59.

1-39)M. Sandberg, C. Blomqvist, Displacement ventilation in office rooms, *ASHRAE Trans*. 95(2) (1989) 1041-1049.3

1-40)H. Xing, H. B. Awbi (2002) : Measurement and calculation of the neutral height in a room with displacement ventilation, *Building and Environment*. 37, pp.961-967

1-41)T. Yamanaka, H. Kotani, M. Xu (2007) : Zonal models to predict vertical contaminant distribution in room with displacement ventilation accounting for convection flows along walls, *Roomvent: 10th International Conference on Air Distribution in Rooms*, FINVAC, Helsinki.

1-42)T. Suzuki, K. Sagara, T. Yamanaka, H. Kotani, A. Iwamura, T. Yamashita (2008) : Prediction of vertical profile of contaminant concentration in displacement-ventilated sickroom with radiant panel, *Transactions of the Society of Heating, Air-conditioning and Sanitary Engineers of Japan*, No. 141, pp.19-27 (In Japanese).

1-43)R. Cermark, A. K. Melikov (2006) : Air quality and thermal comfort in an office with underfloor, mixing and displacement ventilation, *International Journal of Ventilation*. 5:3, pp.323-352.

1-44)H. Stymne, M. Sandberg, M. Mattsson (1991) : Dispersion pattern of contaminants in a displacement ventilated room - implications for demand control, *In proceedings of 12th AIVC conference*, Ottawa, Canada.

1-45)E. Bjørn, P. V. Nielsen (2002) : Dispersion of exhaled air and personal exposure in displacement ventilated rooms, *Indoor Air*. 12, pp.147-164.

1-46)Y. J. P. Lin, C. L. Lin (2014) : A study on flow stratification in a space using displacement ventilation, *International Journal of Heat and Mass Transfer*. 73, pp.67-75.

1-47)T. Inagaki, T. Yamanaka, K. Sagara, H. Kotani, Y. Momoi, M. Shinozaki (2012) : Temperature and Contaminant Concentration Profiles in Four-Beds Sickroom with Displacement Ventilation (Part4) CFD Analysis of indoor airflow and application of zonal model, *Technical papers of annual meeting, the Society of Heating, Air-Conditioning and Sanitary Engineers of Japan*, pp.1751-1754 (In Japanese).

1-48)T. Yamanaka, K. Hisashi, S. Kazunobu, Y. Momoi, T. Inagaki, M. Shinozaki, Temperature and contaminant concentration in sick room with displacement ventilation, in: Proceedings of the 9th International Forum and Workshop on Combined Heat, Air, Moisture and Pollutant Simulations (CHAMPS 2012), IIS, Tokyo, 2012

1-49)E. Mundt, H. M. Mathisen, P. V. Nielsen, A. Moser (2004) : Ventilation effectiveness, REHVA

Guidebook No.2.

1-50)Q. Chen, L. Glicksman (2003) : System performance evaluation and design guidelines for displacement ventilation, American Society of Heating, Refrigerating and Air-Conditioning Engineers, Inc., Atlanta, GA, 2003.

1-51)H. Brohus, P. V. Nielsen, Personal exposure in displacement ventilated rooms, *Indoor Air* 6 (1996) 157–167.

1-52)C. B. Beggs, K. G. Kerr, C. J. Noakes, E. A. Hathway, P. A. Sleigh (2008) : The ventilation of multiple-bed hospital wards: Review and analysis, *Am. J. Infect. Control* 36(4), pp.250–259.

1-53)H. Qian, Y. Li, P. V. Nielsen, X. Huang (2009) : Spatial distribution of infection risk of SARS transmission in a hospital ward, *Building and Environment*. 44 (8), pp.1651–1658.

1-54)B. Hillerbrant, B. Ljungqvist (1990) : Comparison between three air distribution systems for operating rooms, *Swiss Contamination Control*. No. 4a, pp.336-339.

1-55)Y. Yin, W. Xu, J. K. Gupta, A. Guity, P. Marmion, A. Manning, B. Gulick, X. Zhang, Q. Chen (2009) : Experimental study on displacement and mixing ventilation systems for a patient ward, *HVAC&R Research*. 15(6), pp.1175–1191.

1-56)F. A. Berlanga, M. Ruiz de Adana, I. Olmedo, J. M. Villafruela, J. F. San Jose, F. Castro (2018) : Experimental evaluation of thermal comfort, ventilation performance indices and exposure to airborne contaminant in an airborne infection isolation room equipped with a displacement air distribution system, *Energy Build*. 158, pp.209–221.

1-57)X. Li, J. Niu, N. Gao (2011) : Spatial distribution of human respiratory droplet residuals and exposure risk for the co-occupant under different ventilation methods, HVAC&R Res. 17(4), pp.432–445.

1-58)H. Qian, Y. Li, P. V. Nielsen, C. E. Hyldgaard, T. W. Wong, A. T. Y. Chwang (2006) : Dispersion of exhaled droplet nuclei in a two-bed hospital ward with three different ventilation systems, *Indoor Air*. 16, pp.111–128.

1-59)J. M. Villafruela, I. Olmedo, F. A. Berlanga, M. Ruiz de Adana (2019) : Assessment of displacement ventilation systems in airborne infection risk in hospital rooms, *PLoS ONE*. 14(1), e0211390

1-60)Mundt (2001) : Non-buoyant pollutant sources and particles in displacement ventilation, *Building and Environment*. 36, pp.829-836

1-61)A. C. K. Lai, Y. C. Cheng (2007) : Study of expiratory droplet dispersion and transport using a new Eulerian modeling approach, Atmospheric Environment. 41(35), pp.7473-7484.

1-62)E. Mundt (2008) : Air quality in the near zone of humans with different ventilation stratigies, *The 29th AIVC Conference*, Kyoto, Japan

1-63)D. Rim, A. Novoselac (2009) : Transport of particulate and gaseous pollutants in the vicinity of a human body, *Building and Environment*. 44, pp.1840-1849.

1-64)D. Licina, A. Melikov, J. Pantelic, C. Sekhar, K. W. Tham (2015) : Human convection flow in spaces with and without ventilation: personal exposure to floor-released particles and cough-released droplets, *Indoor Air*. 25, pp.672-682

1-65)Y. Li, P.V. Nielsen, M. Sandberg (2011) : Displacement ventilation in hospital environments, ASHRAE

Journal. 53(6), pp.86–88.

1-66)E. Mundt (1994) : Contamination distribution in displacement ventilation - Influence of disturbances, *Building and Environment*. 29(3), pp.311-317.

1-67)M. Mattsson, E. Bjorn, M. Sandberg, P. V. Nielsen (1997) : Simulating people moving in displacement ventilated rooms, *Proceedings of Healthy Buildings 1997*, pp.495-500.

1-68)S. Mazumdar, Y. Yin, A. Guity, P. Marmion, B. Gulick, Q. Chen (2010) : Impact of moving objects on contaminant concentration distributions in an inpatient ward with displacement ventilation, *HVAC&R Research* 16(5), pp.545-563.

1-69)J. Lau, Q. Chen (2007) : Floor-supply displacement ventilation for workshops, *Building and Environment*. 42, pp.1718–1730.

1-70)H. Ahn, D. Rim, L. J. Lo (2018) : Ventilation and energy performance of partitioned indoor spaces under mixing and displacement ventilation, *Building Simulation*. 11, pp.561-574.

1-71)Z. Lin, T. T. Chow, C. F. Tsang (2007) : Effect of door opening on the performance of displacement ventilation in a typical office building, *Building and Environment*. 42, pp.1335-1347

1-72)F. Alamadari, P. F. Butler, P. F. Grigg, M. R. Shaw (1998) : Chilled ceiling and displacement ventilation, *Renewable Energy*. 15, pp.300-305.

1-73)H. Tan, T. Murata, K. Aoki, T. Kurabuchi (1998) : Cooled ceiling / displacement ventilation hybrid air conditioning system - design criteria, Proceeding of Roomvent '98. 1, pp.77-84.

1-74)A. Novoselac, J. Srebric (2002) : A critical review on the performance and design of combined cooled ceiling and displacement ventilation systems, Energy and Building. 34(5), pp.497–509.

1-75)S. J. Rees, P. Haves (2013) : An experimental study of air flow and temperature distribution in a room with displacement ventilation and a chilled ceiling, *Building and Environment*. 59, pp.358–368.

1-76)N. M. Mateus, G. C. da Graça (2015) : Simplified modeling of displacement ventilation systems with chilled ceilings, *Building and Environment*. 108, pp.44–54.

1-77)W. Shan, D. Rim (2018) : Thermal and ventilation performance of combined passive chilled beam and displacement ventilation systems, *Energy and Building*. 158, pp.466-475.

1-78)Z. Shi, Z. Lu, Q. Chen (2019) : Indoor airflow and contaminant transport in a room with coupled displacement ventilation and passive-chilled-beam systems, *Building and Environment*. 161, 106244.

1-79)F. Causone, F. Baldin, B. W. Olesen, S. P. Corgnati (2010) : Floor heating and cooling combined with displacement ventilation: Possibilities and limitations, *Energy and Building*. 42(12), pp.2338–2352.

1-80)X. Wu, B. W. Olesen, L. Fang, J. Zhao (2013) : A nodal model to predict vertical temperature distribution in a room with floor heating and displacement ventilation, Building and Environment. 59, pp.626-634.

Chapter 2.
Prediction Models for Temperature and Contaminant Concentration Distribution

2 Prediction Models for Temperature and Contaminant Concentration Distribution

2.1 Purpose

In a room with displacement ventilation (DV), the air temperature is vertically stratified and the air temperature near the floor (the lower part of the room) is low compared with mixing ventilation. The possibility of the cold draught near the floor is often considered as a disadvantage of DV, because it can cause thermal discomfort (Kosonen et al. (2017)[2-1)]). To provide thermally comfortable indoor environment in a room with DV, the prediction of the vertical air temperature profile at the design stage is particularly important. Hence, previous studies have already developed several models to predict the vertical temperature profile of a displacement ventilated room. On the other hand, the contaminant concentration stratification is one of the strongest merits of using DV. Air quality in the lower part of the contaminant concentration is as fresh as supply air. To make the best use of DV, the prediction of contaminant concentration profile in the room is also crucial. However, there are relatively few models for predicting the contaminant concentration distribution.

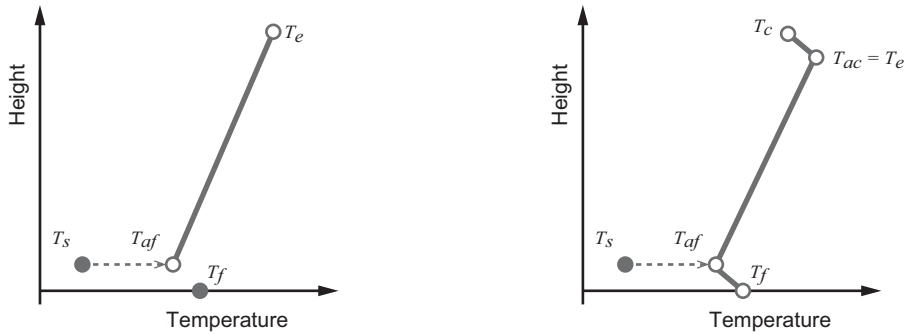
In this chapter, the detail of several prediction models is introduced. Additionally, the methods for calculating the plume rate of several types of heat sources are also explained.These models are validated in Chapter 3, 4 and 5 with the measured results to find appropriate model for predicting vertical temperature and contaminant concentration profiles in a ward with DV.

2.2 Prediction of Vertical Air Temperature Profile

2.2.1 Mundt Model

Mundt (Mundt (1996)[2-2)]) suggested the simplified model and the extended model for predicting vertical temperature profile in a room with DV. The simplified model is the most recognized temperature prediction model of DV. Both simplified and extended models assume that the temperature profile near the floor and ceiling is linear (**Figure 2.1**). Mundt model considers the increase of temperature near the floor caused by the heat transfer from the floor surface to the supplied air.

In the simplified model (**Figure 2.1 (a)**), the floor surface gains radiative heat energy from the ceiling. The heat gain from the ceiling is transferred to the air near the floor by convection, and it it equal to the heat transfer to the supply air. The ceiling surface temperature is assumed to be equal to the exhaust air temperature (T_e). The air temperatre near the floor is the height of 0.1 m in this model.



(a) Simplified model ***(b) Extended model***

Figure 2.1 Mundt model (linearlized model) (Mundt (1996)[2-2])

$$\alpha_r \cdot A_f \cdot (T_e - T_f) = \alpha_{cf} \cdot A_f \cdot (T_f - T_{af}) \quad \cdots(2\text{-}1)$$

$$c_p \cdot \rho \cdot Q_s \cdot (T_{af} - T_s) = \alpha_{cf} \cdot A_f \cdot (T_f - T_{af}) \quad \cdots(2\text{-}2)$$

Because the total heat in the room is balanced, the following equation can be given.

$$P_{total} = c_p \cdot \rho \cdot Q_s \cdot (T_e - T_s) \quad \cdots(2\text{-}3)$$

In the extended model (**Figure 2.1 (b)**), the heat gain or loss through the ceiling and floor, and the radiative heat transfer from the wall are additionally considered. Equation (2-2) and (2-3) are also used. The heat balance of the floor can be expressed by

$$\alpha_{cf}(T_{af} - T_f) + \left(\frac{1}{\sum_{k=1}^{n} \frac{l_{f(k)}}{\lambda_{f(k)}}}\right)(T_{fo} - T_f) + \frac{P_{rh-f} + P_{rp-f}}{A_f} + \alpha_r(T_{c+w} - T_f) = 0 \quad \cdots(2\text{-}4)$$

Likewise, the heat balance of the ceiling can be obtained.

$$\alpha_{cc}(T_{ac} - T_c) + \left(\frac{1}{\sum_{k=1}^{n} \frac{l_{c(k)}}{\lambda_{c(k)}}}\right)(T_{co} - T_c) + \frac{P_{rh-c} + P_{rp-c}}{A_f} + \alpha_r(T_{c+w} - T_c) = 0 \quad \cdots(2\text{-}5)$$

The air temperature near the ceiling (T_{af}) is assumed to be equal to the exhaust temperature (T_e) in the extended model.

This linearized model is considered to work well when a warm window or ceiling is a dominant heat source in the room (Kosonen et al. (2017)[2-1]). However, if there are other heat sources in the lower part of the room such as occupants, the air temperature is not linearized but stratified. Hence, the Mundt model could not accurately predict the air temperature of the occupant zone in these cases.

2.2.2 Nielsen Model

Nielsen's model (Nielsen (1995)[2-3], (2003)[2-4]) assumes that the air temperature is constant in the upper zone of the neutral height (**Figure 2.2**). In this model, the room is vertical divided into two layers, and the upper part of the stratification height is called the mixing layer. The air temperature is linearlized between near the floor (T_{af}) and the mixing height (T_e). In this model, the air temperature near the floor is determined by **Figure 2.3**, the type of heat source and Eq. (2-3). **Figure 2.3** is the experimental results and it shows the relation between the relative temperature near the floor κ (dimensionless temperature) and Archimedes number in a

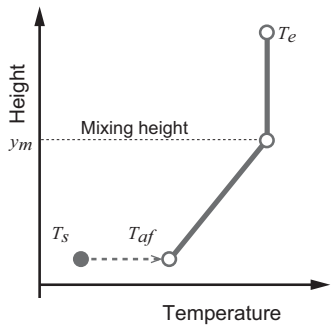


Figure 2.2 Nielsen model

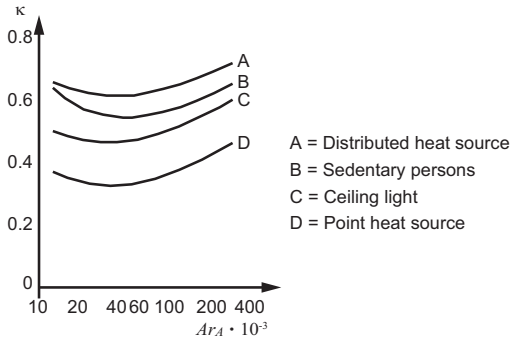


Figure 2.3 Relative temperature near the floor and Archimedes number (Nielsen (1995)[2-3])

displacement-ventilated room (Nielsen (1995)[2-3]). The Archimedes number in this figure can be expressed by

$$Ar_A = \beta \cdot g \cdot H \cdot \frac{T_r - T_s}{\left(\frac{q_s}{A_f}\right)^2} \quad \cdots(2\text{-}6)$$

The mixing height is obtaind by

$$y_{mx} = 0.62 \cdot P_{cf}{}^{\frac{2}{5}} \cdot \left(T_e - T_{af}\right)^{-\frac{3}{5}} \quad \cdots(2\text{-}7)$$

When the dominant heat sources are located in the lower part of the displacement-ventilated room, the room air temperature is stratified and the air temperature in the upper part of the room is close to the mixing ventilation. Hence, it could be expected that the Nielsen model may agree well with the temperature distributions in a room with DV. However, several studies (Kosonen et al. (2017)[2-5], Latrovet et al. (2020)[2-6]) found that the predicted results of Nielsen model does not match with the measured temperature distributions, because the calculated mixing heights were significantly higher than the measured results. The interface between two different zones in a room with DV is known to form at the neutal height where the supply airflow rate is equal to the sum of upward and downward convection airflows in the room. However, the Nielsen model assumes that the mixing height exists at the height where the plume from the heat sources lose the buoyancy force and this height might be higher than the actual mixing height.

2.2.3 Xu and Yamanaka Model

Although Mundt model takes account of the convective and radiative heat transfer, the heat balance at wall surface is not well considered and the radiative heat transfer is roughly calculated. Xu (2001)[2-7] proposed the detailed model considering convective and radiative heat transfer at each surface to predict the vertical temperature profile in a room with DV. Eq. (2-2) and (2-3) of Mundt model are also used in this model. Heat loss or gain throught the walls, floor and ceiling is calculated by the temperature difference between outer and inner surface and heat transmission coefficiency. The radiative heat transfer is estimanted by the temperature difference between two surfaces and view factor.

Because the heat transfer at floor surface is balanced, the following equation is obtained.

$$A_f\alpha_{cf}(T_{af}-T_f)+A_c\alpha_r F_{c-f}(T_c-T_f)+\sum_{i=1}^{n}A_{wi}\alpha_r F_{wi-f}(T_{wi}-T_f) +A_h\alpha_r F_{h-f}(T_h-T_f)+A_f K_f(T_{fo}-T_f)=0 \quad \cdots(2\text{-}8)$$

Likewise, the convective and radiative heat transfer at the ceiling surface is also balanced.

$$A_c\alpha_{cc}(T_{ac}-T_c)+A_f\alpha_r F_{f-c}(T_f-T_c)+\sum_{i=1}^{n}A_{wi}\alpha_r F_{wi-c}(T_{wi}-T_c) +A_h\alpha_r F_{h-c}(T_h-T_c)+A_c K_c(T_{co}-T_c)=0 \quad \cdots(2\text{-}8)$$

The heat transfer balance of the inner surface wall (i) can be obtained as well.

$$A_{wi}\alpha_{cwi}(T_{ai}-T_{wi})+A_c\alpha_r F_{c-wi}(T_c-T_{wi})+A_f\alpha_r F_{f-wi}(T_f-T_{wi}) +\sum_{j=1}^{n}A_{wj}\alpha_r F_{wj-wi}(T_{wj}-T_{wi})+A_h\alpha_r F_{h-wi}(T_h-T_{wi})+A_{wi}K_{wi}(T_{wio}-T_{wi})=0 \quad \cdots(2\text{-}10)$$

In this model, the heat transfer balance at the surface of the heat source is also considered. Human is assumed as a heat source in the room in the following equation. If there are other heat sources in the room, it should be taken accounted as well.

$$A_h\alpha_{ch}(T_{ah}-T_h)+A_c\alpha_r F_{c-h}(T_c-T_h)+A_f\alpha_r F_{f-h}(T_f-T_h) +\sum_{i=1}^{n}A_{wi}\alpha_r F_{wi-h}(T_{wi}-T_h)+P_h=0 \quad \cdots(2\text{-}11)$$

If the heat loss and gain through the walls, floor and ceiling is considered, Eq. (2-3) should be revised. The heat balance of the whole room can be expressed by

$$Q_s c_p\rho(T_s-T_{ac})+A_f K_f(T_{fo}-T_f)+A_c K_c(T_{co}-T_c)+\sum_{i=1}^{n}A_{wi}K_{wi}(T_{wio}-T_{wi})+P_h=0 \quad \cdots(2\text{-}12)$$

The air temperature near the heat source (T_{ah}) and near the wall (i) can be calculated using follow equations. yah is the height of the heat source, and yai is the height at the middle of the wall.

$$T_{ah}=T_{af}+\frac{y_{ah}}{y_c}(T_{ac}-T_{af}) \quad \cdots(2\text{-}13)$$

$$T_{ai}=T_{af}+\frac{y_{ai}}{y_c}(T_{ac}-T_{af}) \quad \cdots(2\text{-}14)$$

2.2.4 Mateus and Da Graça Model

Mateus and da Graça (2015)[2-8), 2-9)] proposed the three-node temperature prediction model. This model is considered to have a better accuracy than Mundt and Nielsen model. In this model, the temperature values at three different heights are calculated: near the floor, 0. 65m (the representative height of the occupied zone) and the mixing height. They pointed out that Mundt model underpredicts the air temperature near the floor. The significant difference of this model from Mundt and Nielsen model is considering the supplied air entraing ambient air. Because of the entrained air, the air temperature near the floor is predicted higher than Mundt model. There are two new parameters I_M and F_{MO} in this model. I_M indicates entrained degree of mixing and F_{MO} means fraction of the convective heat generations in the occupied zone.

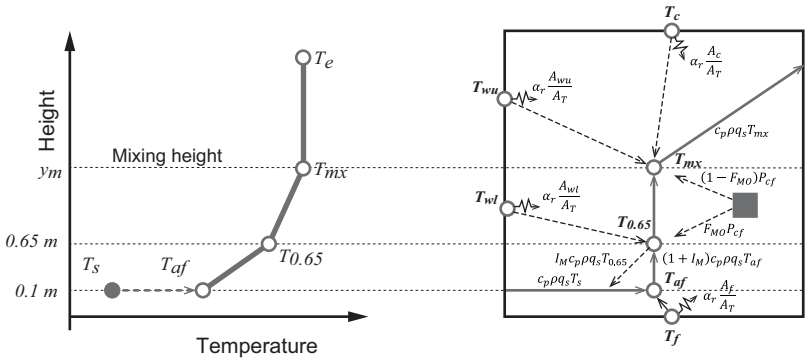


Figure 2.4 Mateus and da Graça model (Mateus and da Graça (2015)[2-8])

Because the convective heat is balanced at each node, the following equations can be obtained:

$$c_p\rho q_s T_s + I_M c_p\rho q_s T_{0.65} + \alpha_{cf,f} A_f\left(T_f - T_{af}\right) = (1+I_M)c_p\rho q_s T_{af} \quad \cdots(2\text{-}15)$$

$$(1+I_M)c_p\rho q_s T_{af} + P_{cf}F_{MO} + \alpha_{cf,wl}A_{wl}(T_{wl} - T_{0.65}) = c_p\rho q_s T_{0.65} \quad \cdots(2\text{-}16)$$

$$c_p\rho q_s T_{0.65} + P_{cf}(1-F_{MO}) + \alpha_{cf,c}A_c(T_c - T_{mx}) + \alpha_{cf,wu}A_{wu}(T_{wu} - T_{mx}) = c_p\rho q_s T_{mx} \quad \cdots(2\text{-}17)$$

T_{mx} is also equal to T_e in this model. The heat balance at each surface (ceiling, floor and wall) can be expressed by

$$\alpha_{cf,c}(T_c - T_{mx}) + \alpha_{r,c}\left(T_c - \frac{T_f A_f + T_{wl}A_{wl} + T_{wu}A_{wu}}{A_t - A_c}\right) = \frac{P_{r,c}}{A_c} \quad \cdots(2\text{-}18)$$

$$\alpha_{cf,f}\left(T_f - T_{af}\right) + \alpha_{r,f}\left(T_f - \frac{T_c A_c + T_{wl}A_{wl} + T_{wu}A_{wu}}{A_t - A_f}\right) = \frac{P_{r,f}}{A_f} \quad \cdots(2\text{-}19)$$

$$\alpha_{cf,wl}(T_{wl} - T_{oc}) + \alpha_{r,wl}\left(T_{wl} - \frac{T_c A_c + T_f A_f + T_{wu}A_{wu}}{A_t - A_{wl}}\right) = \frac{P_{r,wl}}{A_{wl}} \quad \cdots(2\text{-}20)$$

$$\alpha_{cf,wu}(T_{wu} - T_{oc}) + \alpha_{r,wu}\left(T_{wu} - \frac{T_c A_c + T_f A_f + T_{wl}A_{wl}}{A_t - A_{wu}}\right) = \frac{P_{r,wu}}{A_{wu}} \quad \cdots(2\text{-}21)$$

The neutral height (mixing height) y_{mx} is calculated using following equation. In this equation, the heat source in the room assumed to be a point source located at the floor level.

$$y_{mx} = 23.95\left(\frac{{q_s}^3}{P_{cf}}\right)^{\frac{1}{5}} \quad \cdots(2\text{-}22)$$

The room air temperatures at three nodes and surface temperatures can be calculated using above equations.

2.2.4 Zonal Model

The first zonal model was suggested by Yamanaka et al. (2007)[2-10](Section 2.3.1) to predict the contaminant concentration in a displacement-ventilated room. This model accounts for molecular and turbulent diffusion across the interface; thus, there is a stratified layer at neutral height. In this model, the room is vertically divided into four zones (**Figure 2.5, 2.7**). Zone (1) is the upper mixed zone where the contaminant concentration is equal to the exhaust air concentration. The neutral height exists at the boundary between zones (2) and (3), and these two zones constitute the stratified contaminant interface layer. Zone (4) is filled

with clean air and the concentration of this zone depends on the downward airflow in the room. If downward convection airflow does not exist in the room, the contaminant concentration of zone (4) is equal to that of the supply air. Inagaki et al. (2012)[2-11] and Yamanaka et al. (2012)[2-12] applied the zonal model to predict the vertical temperature profile in a room with DV as well. This model also divides the room into four zones vertically and predicts the air temperature from the heat balance of each zone.

The temperature near the floor and the exhaust air temperature can be obtained based on Mundt's model (Eq. (2-2), (2-3)). The stratification height (the mixing height) can be calculated using follow equation.

$$Q_s = Q_P(y_{st}) + Q_u(y_{st}) - Q_d(y_{st}) \quad \cdots(2\text{-}23)$$

The following equations can be obtained by the heat income and outgoing balance of each zone.

Zone (2) :

$$T_u c_p \rho Q_{dr}(y_u) = T_2 c_p \rho Q_{dr}(y_u) + (a + a_t) c_p \rho \frac{\partial T}{\partial y} A_f \quad \cdots(2\text{-}24)$$

Zone (3) :

$$T_d c_p \rho Q_{ur}(y_d) + (a + a_t) c_p \rho \frac{\partial T}{\partial y} A_f = T_3 c_p \rho Q_{ur}(y_d) \quad \cdots(2\text{-}25)$$

Zone (4) :

$$T_d c_p \rho \left(Q_s + Q_d(y_d)\right) = T_u c_p \rho Q_d(y_u) + T_2 c_p \rho (Q_d(y_{st}) - Q_d(y_u)) + T_3 c_p \rho (Q_{ur}(y_d) - Q_{ur}(y_{st})) \quad \cdots(2\text{-}26)$$

In this study, the diffusion coefficient $a + a_t$ was set to 0.0005 m^2/s from the previous studies (Inagaki et al. (2012)[2-11], Yamanaka et al. (2012)[2-12]). The calculation method of vertical convection airflow rate along a wall was revised in this study. If the wall temperature is lower than the room air temperature across the entire wall surface, the contaminated air entrained to the downward airflow along the wall flows into the lowest zone of the room (zone (4)). In contrast, when the overall temperature of the wall is higher than the air temperature, the upward airflow enters the uppermost zone (zone (1)). On the other hand, if the upper part of the wall surface is cooler and the lower part is warmer than the room air, there will be a downward airflow from the top and an upward airflow from the floor, which will flow to the zone where the wall surface temperature and air temperature are equal.

The average temperatures in Zone (2) and (3) (T_2 and T_3) can be obtained by

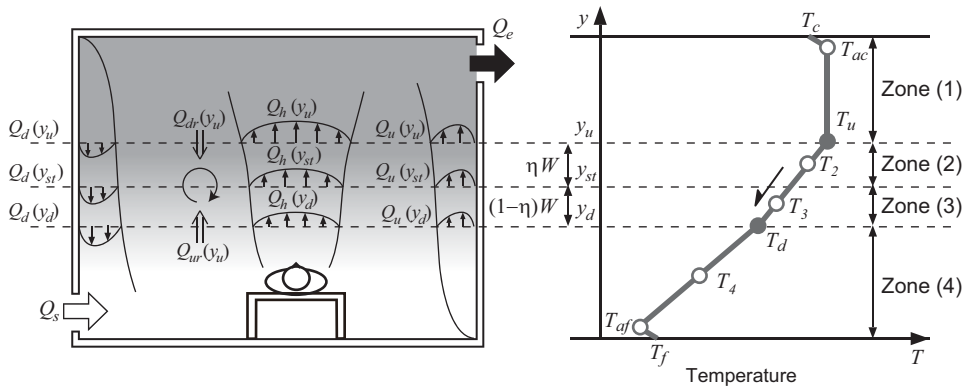


Figure 2.5 Zonal model for temperature profile in a room with DV (Inagaki et al. (2012)[2-11])

$$T_2 = (T_u - T_d)\left(1 - \frac{\eta}{2}\right) + T_d \quad \cdots(2\text{-}27)$$

$$T_3 = (T_u - T_d)\left(\frac{1 - \eta}{2}\right) + T_d \quad \cdots(2\text{-}28)$$

$$T_4 = \frac{T_d + T_{af}}{2} \quad \cdots(2\text{-}29)$$

If the convection airflow rates at all heights can be calculated, the temperature values T_{af}, T_d, T_u could be predicted by this model.

2.3 Prediction of Vertical Contaminant Concentration Profile

2.3.1 Simplified Model

This simplified model for prediction the vertical contaminant concentration profile in a room with DV is firstly proposed by Xu et al. (2001)[2-13] (**Figure 2.6**). If the upward and downward convection airflow rates in the room are known, the contaminant concentration profile could be simply forecasted by this model. In a room with DV, the contaminant interface is formed at a height where the upward flow rate and supply airflow rate are equivalent:

$$Q_s = Q_P(y_{st}) + Q_u(y_{st}) - Q_d(y_{st}) \quad \cdots(2\text{-}30)$$

Hence, the height of the contaminant interface is affected by convection airflow. Because downward convection airflow along the wall transports contaminated air from the upper part of the room to the lower part, it has a considerable effect on contaminant concentration in the lower zone (C_d). With the incoming and outgoing contaminants being equal, the following contaminant balance equation can be obtained for the lower zone

$$Q_s \cdot C_s + Q_d(y_{st}) \cdot C_e = \left(Q_p(y_{st}) + Q_u(y_{st})\right) \cdot C_d \quad \cdots(2\text{-}31)$$

The normalized contaminant concentration of the supply air is 0 and the exhaust air is 1. Hence, the equation can be expressed by

$$Q_d(y_i) = \left(Q_p(y_{st}) + Q_u(y_{st})\right) \cdot C_d \quad \cdots(2\text{-}25)$$

If the vertical airflow rate along the wall surface is known, the contaminant contamination below the contaminant interface can be predicted by the following equation:

$$C_d = \frac{Q_d(y_{st})}{Q_s + Q_d(y_{st})} \quad \cdots(2\text{-}32)$$

Because the height of the contaminant interface can be calculated by Eq.(2-30), the contaminant concentration profile can be simply predicted by 2 equations in this model.

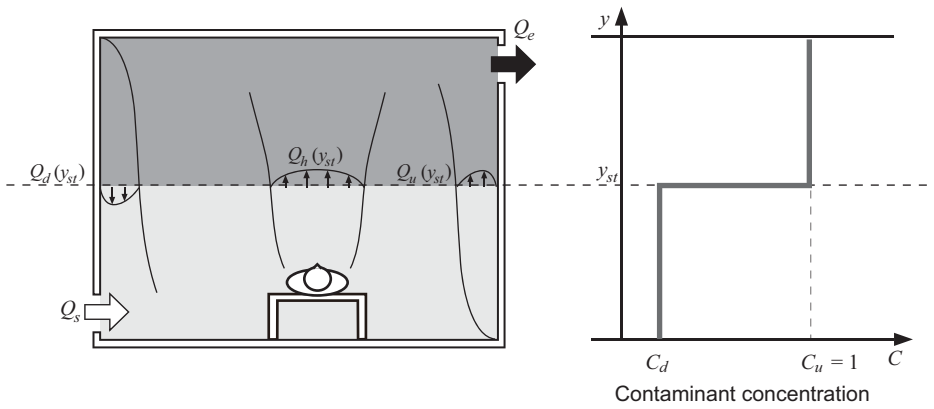


Figure 2.6 Simplified model for contaminant concentration profile in a room with DV

2.3.2 Zonal Model

In the simplified model, the contaminant interface was assumed as a flat line. However, in the general displacement-ventilated room, there is an intermediate stratified layer between the two zones (contaminant interface layer), rather than them being clearly separated. Yamanaka et al. (2007)[2-10] developed a zonal model that considers diffusion. The model accounts for molecular diffusion and turbulent diffusion across the interface in order to approach the actual concentration distribution. Hence, the contaminant interface was considered to be a layer with a vertical width. The model also considers the upward and downward flows along the walls.

As shown in **Figure 2.7**, the room is vertically divided into four zones in this model. Because the incoming and outgoing contaminants are equal in each zone, the following contaminant balance equations can be obtained for each zone (Zone (2) – (4)). y_{st} can be calculated by Eq.(2-23). In this study, the diffusion coefficient $D + D_t$ was set to 0.0005 m^2/s from the previous studies (Suzuki (2008)[2-14]).

Zone (2) :

$$C_u Q_{dr}(y_u) = C_2 Q_{dr}(y_u) + (D + D_t)\frac{\partial C}{\partial y} A_f \quad \cdots(2\text{-}33)$$

Zone (3) :

$$C_d Q_{ur}(y_d) + (D + D_t)\frac{\partial C}{\partial y} A_f = C_3 Q_{ur}(y_d) \quad \cdots(2\text{-}34)$$

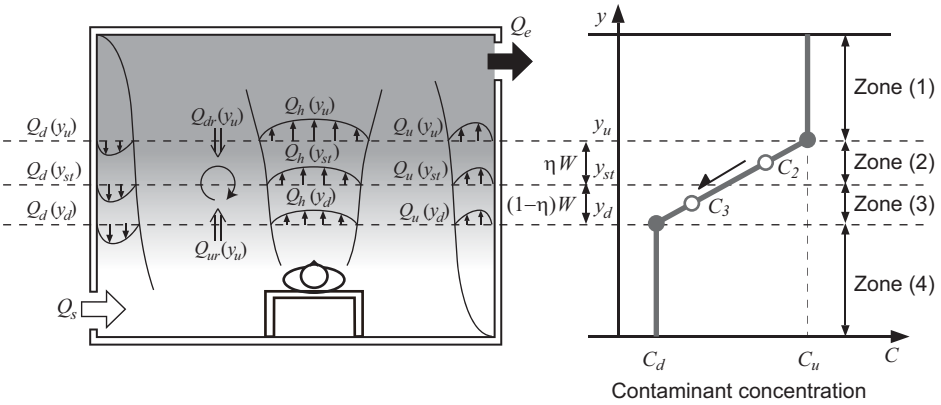


Figure 2.7 Zonal model for contaminant concentration profile in a room with DV (Yamanaka et al. (2007)[2-10])

Zone (4) :

$$C_d(Q_s + Q_d(y_d)) = C_u Q_d(y_u) + C_2(Q_d(y_{st}) - Q_d(y_u)) + C_3(Q_{ur}(y_d) - Q_{ur}(y_{st})) \quad \cdots(2\text{-}35)$$

For the whole room, the contaminant balance can be expressed by

$$C_u = C_e = \frac{NM}{Q_s} \quad \cdots(2\text{-}36)$$

The average concentrations in Zone (2) and (3) (C_2 and C_3) can be obtained by

$$C_2 = (C_u - C_d)\left(1 - \frac{\eta}{2}\right) + C_d \quad \cdots(2\text{-}37)$$

$$C_3 = (C_u - C_d)\left(\frac{1-\eta}{2}\right) + C_d \quad \cdots(2\text{-}38)$$

2.3.3 Improved Zonal Model

If a contaminated plume is weaker than plumes from other heat sources, the contaminated air cannot rise directly to the ceiling and will be locked-up at the middle height in the room. Although this may not be an unusual situation for a displacement ventilated room, there have been few prediction models that have considered this phenomena. Suzuki et al. (2008)[2-14] proposed the improved zonal model to predict the concentration distribution with contaminant stagnation. Inagaki et al. (2011)[2-15] revised the calculation method of the height where the contaminated air is locked-up.

As shown in Fig. 11, a room comprises five zones. The contaminant plume is locked up at the height yl. Half of the contaminated air is assumed to go into zone (2), and the other half is assumed to go into zone (3). The contaminant balance equation of each zone is given below.

Zone (2) :

$$\begin{aligned} &C_u Q_{dr}(y_u) + \frac{1}{2}\{M + C_d Q_h(y_d) + C_4(Q_h(y_{st}) - Q_h(y_d)) + +C_3(Q_h(y_l) - Q_h(y_{st}))\} \\ &= C_2 Q_{dr}(y_l) + C_2\left\{\left(Q_p(y_u) - Q_p(y_l)\right) + \left(Q_d(y_l) - Q_d(y_u)\right) + \left(Q_u(y_u) - Q_u(y_l)\right)\right\} \end{aligned} \quad \cdots(2\text{-}39)$$

Zone (3) :

$$\begin{aligned} &C_2 Q_{dr}(y_l) + \frac{1}{2}\{M + C_d Q_h(y_d) + C_4(Q_h(y_{st}) - Q_h(y_d)) + +C_3(Q_h(y_l) - Q_h(y_{st}))\} \\ &= (D + D_t)\frac{\partial C}{\partial y} A_f + C_3\left\{\left(Q_p(y_l) - Q_p(y_{st})\right) + \left(Q_d(y_{st}) - Q_d(y_l)\right) + \left(Q_u(y_l) - Q_u(y_{st})\right)\right\} \end{aligned} \quad \cdots(2\text{-}40)$$

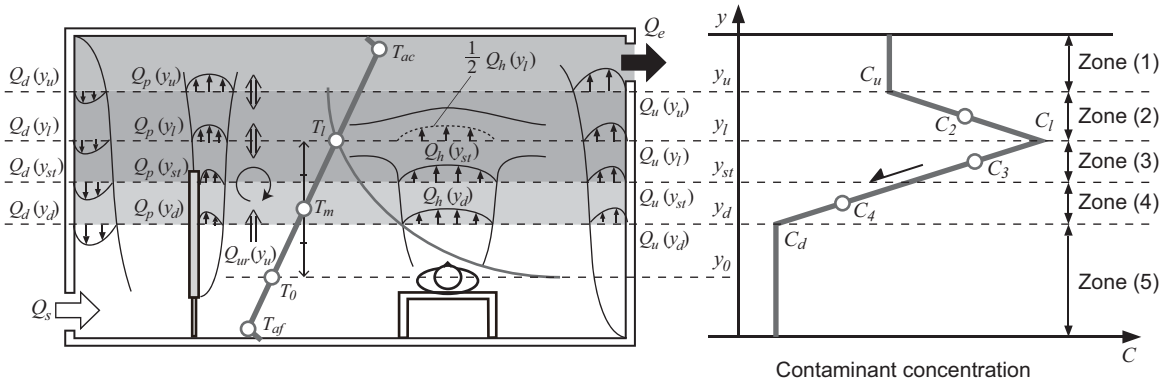


Figure 2.8 Improved zonal model for contaminant concentration profile in a room with DV (Suzuki et al. (2008)[2-14])

Zone (4) :

$$C_d Q_{ur}(y_d) + (D + D_t)\frac{\partial C}{\partial y}A_f = C_4\left\{\left(Q_p(y_{st}) - Q_p(y_d)\right) + \left(Q_h(y_{st}) - Q_h(y_d)\right) + \left(Q_d(y_d) - Q_d(y_{st})\right) + \left(Q_u(y_{st}) - Q_u(y_d)\right)\right\} \quad \cdots(2\text{-}41)$$

Zone (5) :

$$C_u Q_d(y_u) + C_2\left(Q_d(y_l) - Q_d(y_u)\right) + C_3\left(Q_d(y_{st}) - Q_d(y_l)\right) + C_4\left(Q_d(y_d) - Q_d(y_{st})\right) = C_d Q_{ur}(y_d) + C_d\left(Q_p(y_d) + Q_h(y_d) + Q_u(y_d)\right) \quad \cdots(2\text{-}42)$$

For the whole room, the contaminant balance can be expressed by

$$C_u = C_e = \frac{NM}{Q_s} \quad \cdots(2\text{-}43)$$

The plumes are considerably affected by temperature stratification. The plume would stop rising at the height where the plume temperature and the ambient temperature are equal. In original model (Suzuki et al. (2008)[2-14]), the height where contaminated air is locked-up is calculated using following equation suggested by Mundt (1996)[2-2]. Mundt (1996)[2-2] studied the maximum height of the plume and the height where the plume loses the buoyancy force of the plume..

$$y_l = 0.35 \cdot {P_{cf}}^{\frac{1}{3}} \cdot \left(\frac{\partial T}{\partial y}\right)^{\frac{1}{2}} \quad \cdots(2\text{-}44)$$

This equation is for the line source and if the plume is generated from the point heat source, the height where the plume stops rising is given by

$$y_l = 0.74 \cdot {P_{cf}}^{\frac{1}{4}} \cdot \left(\frac{\partial T}{\partial y}\right)^{-\frac{3}{8}} \quad \cdots(2\text{-}45)$$

To calculate the stagnation height more accurately, Inagaki et al. (2011)[2-15] suggested another calculation method. If the plume airflow rate is assumed to increase linearly, the average temperature of the temperature at the height where the plume is generated and the temperature at the height where the plume is stagnated could be used for the temperature of the entrained air. The air temperature inside the plume at height (yl) can also be expressed as follows (Inagaki et al. (2011)[2-15]):

$$T_p(y_l) = T_m + \frac{P_h}{Q_h(y_l)\rho C_p} = T_{af} + \frac{\partial T}{\partial y}\cdot\left(\frac{y_l + y_0}{2} - y_{af}\right) + \frac{P_h}{Q_h(y_l)\rho C_p} \quad \cdots(2\text{-}46)$$

The plumes are locked up when there is no difference between the temperature inside the plume and the ambient temperature. Hence, the height where the plume is stagnant can be derived as follows [20]:

$$T_{af} + \frac{\partial T}{\partial y}\cdot\left(\frac{y_l + y_0}{2} - y_{af}\right) + \frac{P_h}{Q_h(y_l)\rho C_p} = T_{af} + \frac{\partial T}{\partial y}y_l \quad \cdots(2\text{-}47)$$

C_2, C_3, C_4, and C_{st} can be expressed as follows:

$$C_2 = \frac{C_u + C_l}{2} \quad \cdots(2\text{-}48)$$

$$C_3 = \frac{C_l + C_{st}}{2} \quad \cdots(2\text{-}49)$$

$$C_4 = \frac{C_{st} + C_d}{2} \quad \cdots(2\text{-}50)$$

$$C_{st} = (C_l - C_d)\left(\frac{y_{st} - y_d}{y_l - y_d}\right) + C_d \quad \cdots(2\text{-}51)$$

Solving these equations yields C_u, C_l, C_d, y_u, and y_d, which can be used to obtain the predicted vertical concentration profile.

2.4 Plume Rates above Heat Sources

In this section, the methods for calculating plume rates from various types of the heat sources in a ward are introduced. The plume rates in this study were estimated using existing and empirical equations in the previous studies.

The plume rate from the point heat source can be given by following equation (Skistad (1994)[2-16)]). In this study, the black lamp was used to simulate the electric devices in a ward. The plume rate of the black lamp was calculated using this equation.

$$Q_p(y) = 0.005 P_{cf}^{\frac{1}{3}} y^{\frac{5}{3}} \quad \cdots(2\text{-}52)$$

The convection flow rate along the walls was estimated using the equation of the plume rate along the vertical surface when the temperature difference between the surface and room air is known (Skistad (1994)[2-16)], Eckert and Jackson (1951)[2-17)])

$$Q_p(y) = 0.00275|\Delta T|^{0.4} y^{1.2} \quad \cdots(2\text{-}53)$$

However, the temperature difference between the wall surface and room air fluctuates with height. The following differentiated equation is used to forecast the air flow rate (Yamanaka et al. (2007)[2-10)]):

$$\Delta Q_u(y) = \Delta Q_d(y) = 0.0033|\Delta T|^{\frac{2}{5}} y^{\frac{1}{5}} B_w \Delta y \quad \cdots(2\text{-}54)$$

In Chapter 3, the radiant panel was used as a complementary heating and cooling system in a room with DV. When the plume rate along the panel is calculated, the radiant panel is considered to be a vertical plane surface. Thus, the air flow rate along the radiant panel is obtained by (Skistad (1994)[2-16)])

$$Q_p(y) = 0.022 P_{cf}^{\frac{1}{3.5}} y^{0.857} B \quad \cdots(2\text{-}55)$$

The thermal plume above the panel is estimated with the virtual source method. The virtual line source is located where the flow rates from the virtual line source and the panel would be the same at the top of the panel. The following equation is used (Suzuki et al. (2008)[2-14)]):

$$Q_p(y) = 0.14 P_{cf}^{\frac{1}{3}} (y - y_{vl}) B \quad \cdots(2\text{-}56)$$

In Chapter 3, 4 and 5, the person simulators are used to simulate the lying patients in the ward. The human shaped manikin was utilized in Chapter 3. However, the cylinder type heating source was used in Chapter 4 and 5. A lying down manikin in Chapter 3 is regarded as a linear heat source. According to previous research [16], the length of the linear source was set to 0.5 m and 0.8 m below the real location. The convection flow rate from a lying body is given by (Suzuki et al. (2008)[2-14)], Ueba et al. (2005)[2-18)])

$$Q_p(y) = 82.43(y - 0.3) + 24.72 \quad \cdots(2\text{-}57)$$

The plume rate above lying cylinder in Chapter 4 and 5 was calculated using empirical equation. Shinozaki et al. (2012)[2-19] measured the air velocity above the cylinder heated at 100 W and estimated the plume rate of the cylinder.

$$Q_p(y) = 0.04y + 0.0245 \quad \cdots(2\text{-}58)$$

2.5 Conclusion

In this Chapter, several prediction models to predict the vertical temperature and contaminant concentration profiles in a room with DV are introduced. Additionally, simplified model for prediction concentration is proposed. The described models in this chapter are validated in Chapter 3 and 4 by comparison with the experimental results.

References

2-1) R. Kosonen, A. Melikov, E. Mundt, P. Mustakallio, P. V. Nielsen (2017) : REHVA Guidebook No. 23: Displacement Ventilation, REHVA, Brussels.

2-2) E. Mundt (1996) : The Performance of Displacement Ventilation – Experimental and Theoretical Studies, PhD thesis, Royal Institute of Technology, Stockholm.

2-3) P. V. Nielsen (1995) : Vertical temperature distribution in a room with displacement ventilation, i*n: IEA Annex 26: Energy Efficient Ventilation of Large Enclosures*, IEA, Paris.

2-4) P. V. Nielsen (2003) : Temperature and air veloctity distribution in rooms ventilated by displacement ventilation, *Proceedings of the 7th International Symposium on Ventilation for Contaminant Control*, Sapporo, Japan, pp.691-696.

2-5) R. Kosonen, N. Lastovets, P. Mustakallio, G. C. da Graça, N. M. Mateus, M. Rosenqvist (2016) : The effect of typical buoyant flow elements and heat load combinations on room air temperature profile with displacement ventilation, *Building and Environment*. 108, pp.207–219.

2-6) M. Xu (2001) : Study on the prediction of contaminant concentration distribution in rooms with displacement ventilation, Doctoral Thesis, Osaka University.

2-7) N. Lastovets, R. Kosonen, P. Mustakllio, J. Jokisalo, A. Li (2020) : Modelling of room air temperature profile with displacement ventilation, *Internation Journal of Ventilation*, 19:2, pp.112-126.

2-8) N. M. Mateus, G. C. da Graça (2015) : A validated three-node model for displacement ventilation, *Building and Environment*, 84, pp.50-59.

2-9) N. M. Mateus, G. C. da Graça (2015) : Simplified modeling of displacement ventilation systems with chilled ceilings, *Building and Environment*, 108, pp.44–54.

2-10) T. Yamanaka, H. Kotani, M. Xu (2007) : Zonal models to predict vertical contaminant distribution in room with displacement ventilation accounting for convection flows along walls, *Roomvent: 10th International Conference on Air Distribution in Rooms*, FINVAC, Helsinki.

2-11) T. Inagaki, T. Yamanaka, K. Sagara, H. Kotani, Y. Momoi, M. Shinozaki (2012) : Temperature and Contaminant Concentration Profiles in Four-Beds Sickroom with Displacement Ventilation (Part4) CFD Analysis of indoor airflow and application of zonal model, *Technical papers of annual meeting, the*

Society of Heating, Air-Conditioning and Sanitary Engineers of Japan, pp.1751-1754 (In Japanese).

2-12)T. Yamanaka, K. Hisashi, S. Kazunobu, Y. Momoi, T. Inagaki, M. Shinozaki, Temperature and contaminant concentration in sick room with displacement ventilation, in: Proceedings of the 9th International Forum and Workshop on Combined Heat, Air, Moisture and Pollutant Simulations (CHAMPS 2012), IIS, Tokyo, 2012

2-13)M. Xu, T. Yamanaka, H. Kotani, T. Higashimoto (2001) : Effect of cooled or heated wall on vertical distribution of temperature and contaminant concentration in rooms with displacement ventilation, *Transaction of AIJ. Journal of architecture, planning and environmental engineering*. No.544, pp.17-23

2-14)T. Suzuki, K. Sagara, T. Yamanaka, H. Kotani, A. Iwamura, T. Yamashita (2008) : Prediction of vertical profile of contaminant concentration in displacement-ventilated sickroom with radiant panel, *Transactions of the Society of Heating, Air-conditioning and Sanitary Engineers of Japan*, No. 141, pp.19-27 (In Japanese).

2-15)T. Inagaki, T. Yamanaka, K. Sagara, H. Kotani, Y. Momoi, T. Yamashita (2011) : Prediction of vertical profile of temperature and contaminant concentration in sickroom with displacement ventilation (Part 2) Prediction model of vertical profile of temperature and contaminant concentration, *Technical papers of annual meeting, the Society of Heating, Air-Conditioning and Sanitary Engineers of Japan*, pp. 2021–2024 (in Japanese).

2-16)H. Skistad (1994) : Displacement Ventilation, Research Studies Press Ltd., Baldock, 1994.

2-17)E.R.G. Eckert, T.W. Jackson (1951) : Analysis of turbulent-free convection boundary layer on flat plate, NACA Report No. 1015, NACA, Cleveland.

2-18)Y. Ueba, K. Sagara, T. Yamanaka, H. Kotani, T. Hamaguchi, T. Yamashita (2005) : Semi-personal air-conditioning system for sickroom by displacement ventilation with radiant cooling and heating, *Summaries of Technical Papers of Annual Meeting of AIJ*, pp.1013-1014 (In Japanese).

2-19)M. Shinozaki, T. Yamanaka, K. Sagara, H. Kotani, Y. Momoi, T. Inagaki (2012) : Temperature and contaminant concentration profiles in four-bed sickroom with displacement ventilation (Part 3) Experiment results and thermal plume velocity above lying person simulator, *Technical papers of annual meeting, the Society of Heating, Air-Conditioning and Sanitary Engineers of Japan*, pp.1747-1750 (In Japanese).

Chapter 3.
Displacement-ventilated Ward with Radiant Panel

3 Displacement-ventilated Ward with Radiant Panel

3.1 Purpose

Thermal comfort should also be considered for a comfortable indoor environment. Local discomfort due to a vertical temperature gradient is often considered as a disadvantage of DV[3-1)]. Moreover, DV cannot be used as a heating system[3-2)], so a complementary heating and cooling system is needed. Inpatients in hospital wards usually lie in a bed, so the vertical temperature gradient would not affect their thermal comfort. However, patients are also more susceptible to the thermal environment than healthy people, and each patient may have different levels of thermal sensitivity depending on their condition[3-3, 4)]. Since there was a restriction on the ratio of the one-patient ward, most hospital wards in Japan have more multiple beds. Hence, an individually controllable heating and cooling system is desirable. In this chapter, a vertical radiant panel that can be personally controlled by a patient was proposed for an ancillary heating system to acquire a thermally comfortable environment. The measurements were carried out to investigate the temperature and contaminant concentration profiles were measured in a full-scale displacement ventilated room with a vertical radiant panel.

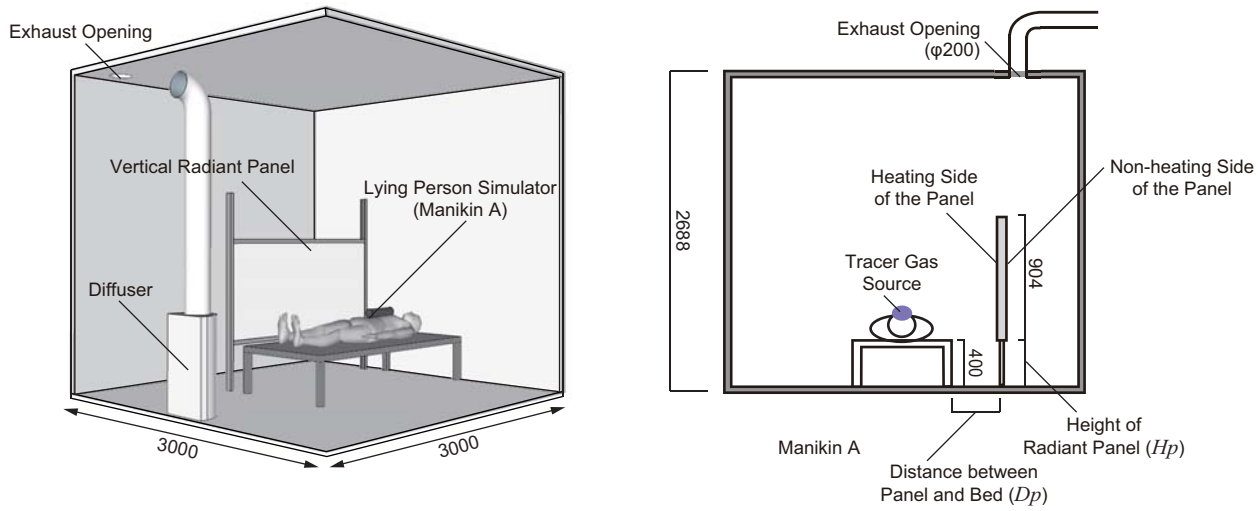
On the other hand, the contaminant interface layer of a displacement ventilated room exists above the occupied zone. While lying or sitting occupants inhale clean air in the lower zone of the interface layer, the breathing zone of standing occupants is occasionally located in the upper zone. Brohus and Nielsen [15] carried out full-scale measurements of personal exposure and found that standing occupants could inhale cleaner air than the contaminant concentration at the same height because they inhale air inside the boundary layer around bodies. Healthcare providers work on their feet, so it is critical to examine the personal exposure of standing occupants in wards to solve the odor problem.

3.2 Experimental Investigation in Displacement-ventilated Single-bed Ward with Radiant Panel

3.2.1 Experimental Setup

Experiments were carried out in an environmental chamber with a length of 3000 mm, width of 3000 mm, and height of 2688 mm. The experimental arrangement is shown in **Figure 3.1**. All envelopes (four walls, ceiling, and floor) were insulated with a 50mm thick polystyrene layer. Inner surfaces of all envelopes were coated with mat black to consider the influence of the radiation. The surroundings of the chamber were kept at 23–26 °C throughout the experiments except for the underfloor. **Figure 3.2** shows the supply inlet. Fresh air was supplied from a semicircular wall-mounted diffuser (D = 400 mm, T = 260 mm, H = 750 mm) that was located on the floor in the middle of the wall. The supply air temperature was maintained at 25 °C. The

exhaust grill had 200φ holes and was on the ceiling near the wall where the diffuser was placed. A manikin was placed on the bed to simulate the lying patient (manikin A, lying down, **Figure 3.3**). The manikins were wrapped in polyvinyl chloride (PVC) heating cable at equal intervals and put in sweat suits. The heat generation from manikin A was controlled at 40 W to represent the sensible heat load of the lying patient. CO_2 was used as the tracer gas to simulate the odor from the human body and was distributed from a tube on manikin A. Because the odor is the passive gaseous contaminant, CO_2 emission point was covered with sponge to make the initial moment as small as possible. The CO_2 flow rate was controlled at 0.5 L/min with a mass flow controller. For the vertical radiant panel, hot water was provided from a water tank installed outside the chamber. The surface of panel was made of steel plate and one side of the panel was only heated. The surface temperature of the radiant panel was monitored, and the water temperature was controlled to achieve the target surface temperature with the heater and cooler inside the water tank. The detail of the radiant panel is shown in **Figure 3.4**. The surface temperatures were measured at 11 points and the target surface temperature was the mean measured temperature of these measurement points.



(a) Schematic view of the experimental room (b) Section view of the experimental room, [mm]

Figure 3.1 Schematic and section view of the experimental room

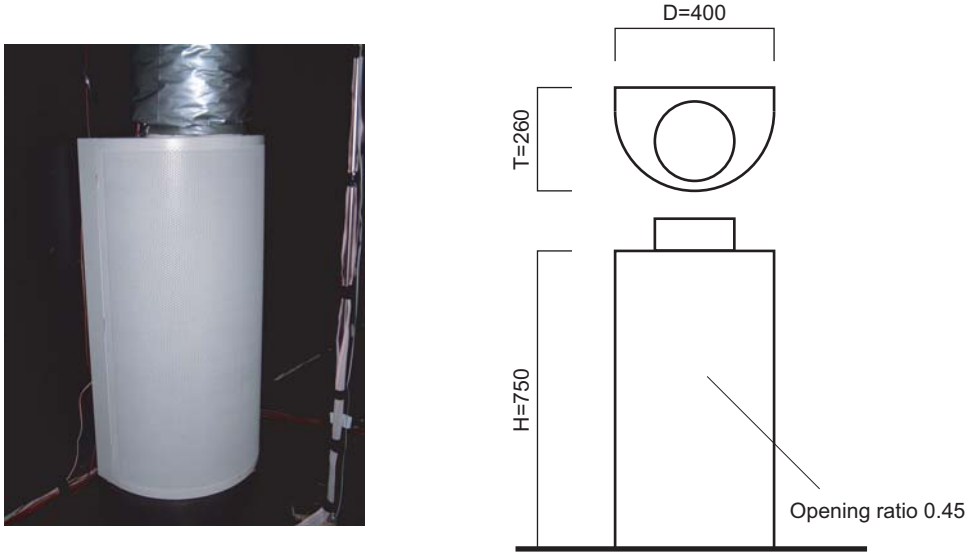


Figure 3.2 Schematic and section view of the experimental room



Figure 3.2 Manikin A

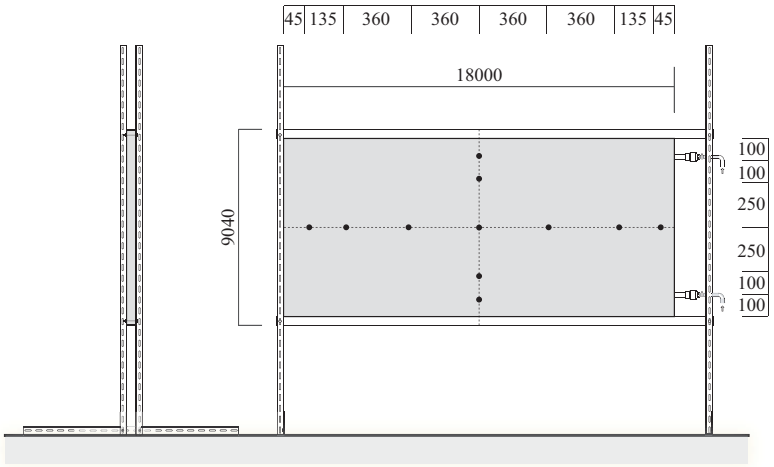
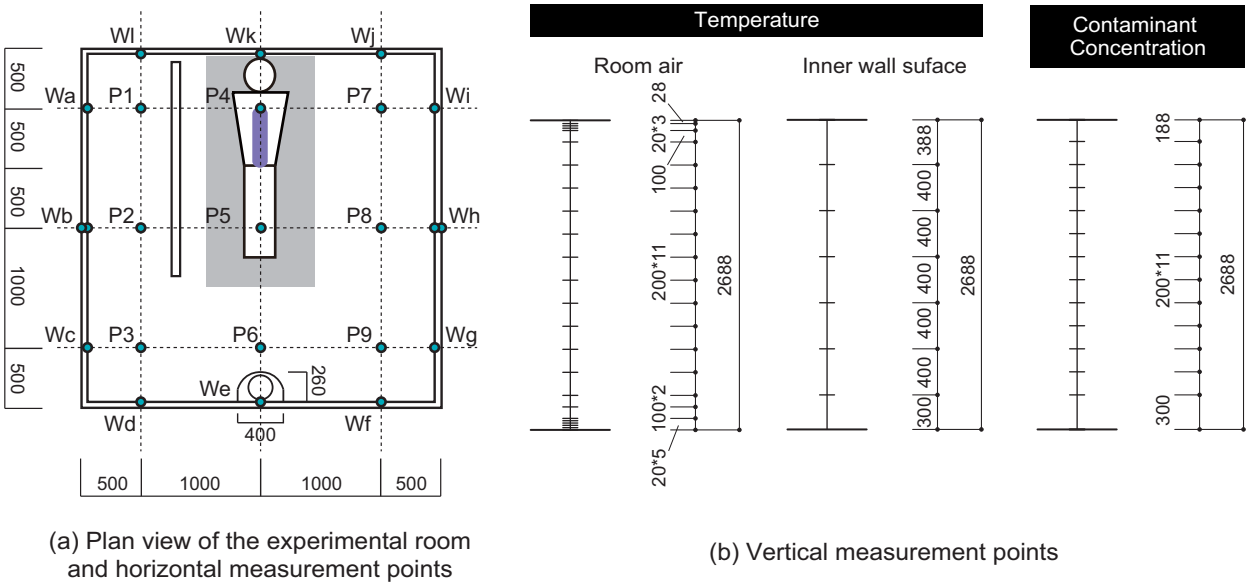


Figure 3.3 Radiant paenl



(a) Plan view of the experimental room and horizontal measurement points

(b) Vertical measurement points

Figure 3.4 Horizontal and vertical measurement points

Figure 3.4 shows the horizontal and vertical measurement points for the temperature and CO_2 concentration. The air and wall surface temperatures were measured using T-type thermocouples (φ = 0.32 mm). There were 9 measurement points for the air temperature on the horizontal plane (P1–P9) and 22 points on the vertical line for 198 points in total. The inner wall surface temperature was measured at 12 points on the horizontal plane (Wa–Wl) and 6 points on the vertical line for a total of 72 points. Because P4 and P5 were located on the manikin A, the number of vertical measure points were smaller than other measurement points. The inner surface temperatures of the floor and ceiling were also measured. The external surface temperatures of each envelope were measured to calculate the heat loss through the envelopes. The contaminant concentrations were measured at 7 points on the horizontal plane (P1–P3 and P6–P9) and 12 points in the vertical direction. Non-dispersive infrared (NDIR) gas analysers were used to measure CO_2 concentration. The gas analysers were calibrated before the measurement and the reproducibility was confirmed. The measurements were performed after the temperature and concentration in the room reached a steady state.

Table 3.1 Experimental conditions

Cases	Supply airflow rate	Distance between the panel and bed	Height of the panel	Temperature of the panel surface
	Q_s [m^3/h]	D_p [m]	H_p [m]	T_p [°C]
Case 1	100	0	0.4	40
Case 2	200	0	0.2	40
Case 3	200	0	0.4	23
Case 4	200	0	0.4	30
Case 5	200	0	0.4	40
Case 6	200	0	0.8	40
Case 7	200	0.05	0.4	40
Case 8	200	0.1	0.4	40
Case 9	200	0.2	0.4	40
Case 10	200	0.4	0.2	40
Case 11	200	0.4	0.4	40
Case 12	200	0.4	0.8	40
Case 13	300	0	0.4	40
Case 14	300	0.4	0.4	40

3.2.2 Experimental Conditions

Table 3.1 presents the experimental conditions. The influences of several factors associated with the radiant panel on the temperature and concentration profile were investigated in the experiments. The following parameters were considered: distance from the panel to the bed (D_p), height of the lower end of the panel (H_p), surface temperature of the panel (T_p), and supply airflow rate (Q_s). In order to identify the positional relation between the panel and the bed, D_p and H_p were changed. Since the contaminant air was locked when D_p = 0.4 m in the pilot study, D_p was altered within the range of 0 m ~ 0.4 m. H_p was set to 0.4 m, as high as the bed. Both H_p = 0.2 and 0.8 m were also chosen to examine when the lower end of the panel is lower or higher than the bed. The radiant panel was heated at 40 °C, which is higher than the human body temperature but not high enough to cause a danger from burns. The panel surface temperature was controlled at 23 °C for cooling and 30°C for the neutral condition for reference. Q_s = 200 m^3/h was chosen as the standard condition because it was confirmed that the interface was formed higher than the breathing zone of lying and sitting person in the pilot study. Because the supply airflow rate affects the height of the contaminant interface, Q_s =100 and 300 m^3/h were also adopted to carry out the measurement under the several height conditions of the contaminant interface.

3.2.3 Experimental Results

In the experimental results, the horizontal axis of the vertical temperature profiles represents the temperature difference from the supply air temperature. The normalized concentration was used for the vertical concentration distribution and is defined as

$$C = \frac{C_m - C_s}{C_e - C_s} \quad \cdots(3\text{-}1)$$

Table 3.2 Experimental conditions to examine the influence of the vertical radiant panel

Cases	Heat loss through the envelopes	Heat generation of the radiant panel	Heat generation of the manikin A
	[W]	[W]	[W]
Case 1	131	170	40
Case 2	112	173	40
Case 3	44	-23	40
Case 4	75	77	40
Case 5	97	154	40
Case 6	110	160	40
Case 7	97	158	40
Case 8	64	158	40
Case 9	63	144	40
Case 10	111	175	40
Case 11	57	147	40
Case 12	95	141	40
Case 13	99	179	40
Case 14	96	154	40

Although the temperature outside the chamber was controlled, it was still influenced by the outdoor temperature. Furthermore, it was not possible to control the underfloor air temperature. Therefore, the impact of heat loss through the envelopes slightly differed depending on the outdoor temperature in all cases. Heat loss and heat generation values of each case are presented in **Table 3.2**. The floor consisted of polystyrene board (0.05 m), plywood panel (0.009 m), tile carpet (0.006 m) and FRC (fiber reinforced concrete) panel (0.017 m) and the heat transmission coefficient was 0.629 kcal/m2h°C. The walls and ceiling were made of polystyrene board (0.05 m) and the heat transmission coefficient was 0.721 kcal/m2h°C. The mean values of the measured inner and outer surface temperature of each wall, floor, and ceiling were used to calculate the heat loss through the envelopes. Heat generation from the panel was calculated using the differences between the inlet and outlet water temperatures as follows;

$$P_p = c_p r V (T_{in} - T_{out}) \quad \cdots(3\text{-}2)$$

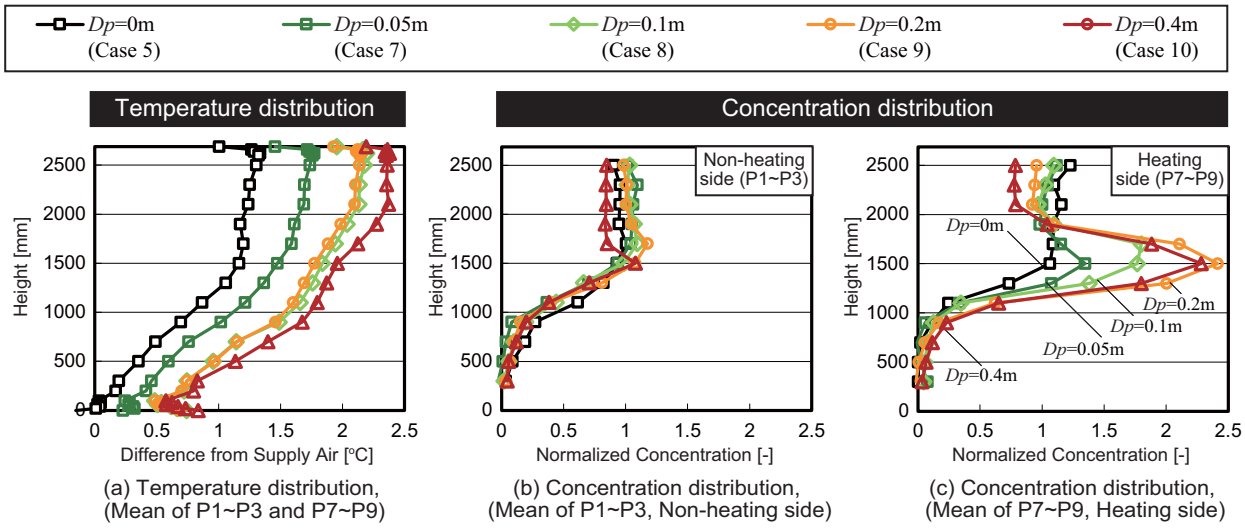


Figure 3.5 Measured temperature and concentration profiles (paratmeter: distance between the panel and bed D_p)

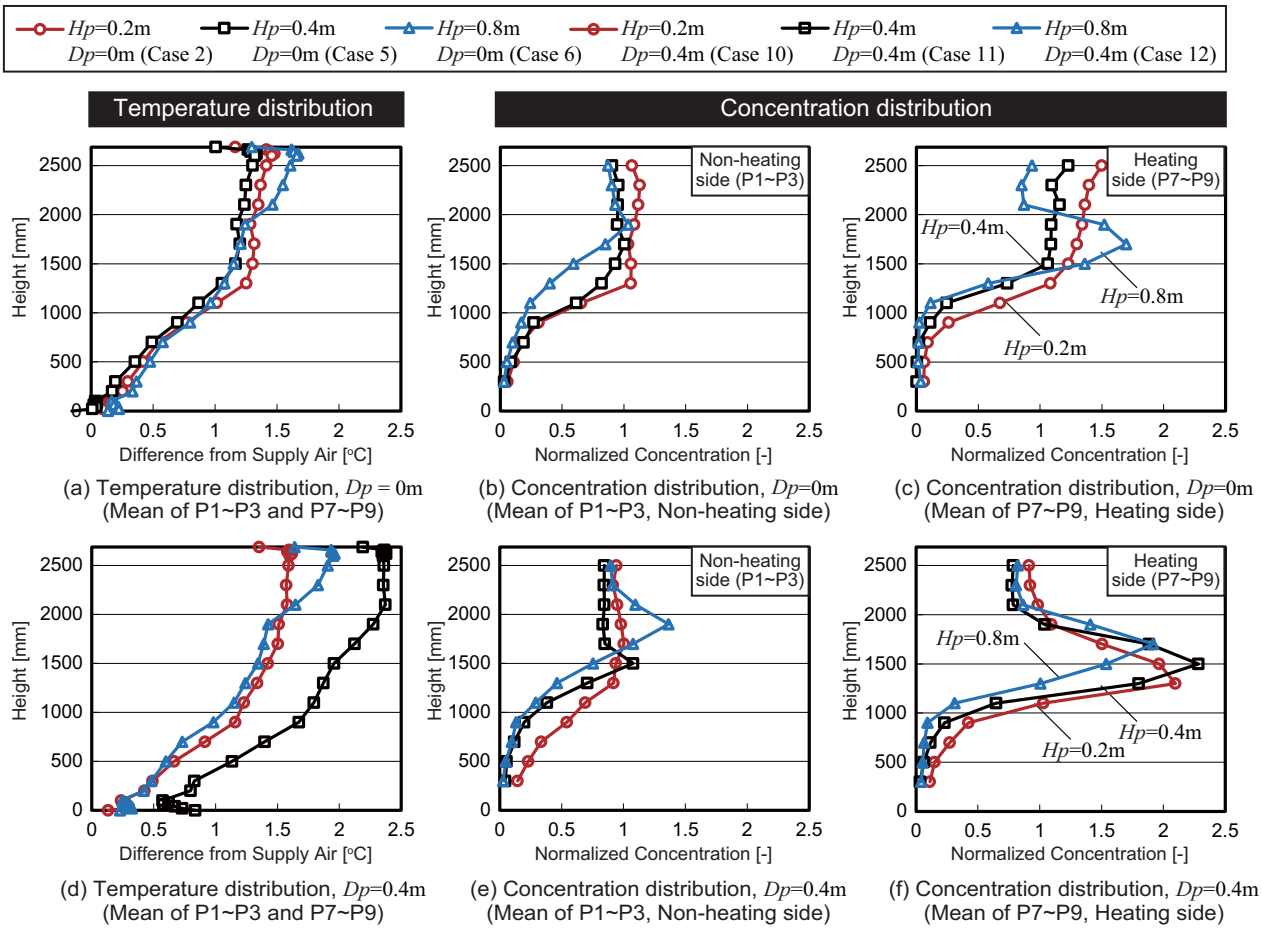


Figure 3.6 Measured temperature and concentration profiles (paratmeter: height of the panel H_p)

Influence of the distance between the panel and bed (D_p)

Figure 3.5 shows the influence of the horizontal distance between the panel and the bed (D_p). As shown in **Figure 3.5(a)**, temperature stratification formed in all cases. The temperature in the room increased with Dp. However, this is not because of D_p but because of the difference in heat loss through the envelopes of the chamber (**Table 3.2**). The vertical temperature differences and the temperature gradients were almost the same under the different Dp conditions. It indicates that D_p did not have much effect on the temperature distribution. There was no significant difference between cases in terms of the vertical concentration profile on the non-heating side of the panel. The contaminant interface height formed at the same level. On the other side, the contaminated air from manikin A was trapped in all cases on the heating side of the panel except for D_p = 0 m. When there was no space between the panel and bed, the plumes from the manikin A and panel merged into one plume and were efficiently exhausted. However, the locked-up phenomenon appeared when D_p was even only 0.05 m. It indicates that, when there was no space between the two heat sources, fresh air in the lower part of the room was entrained into the plume of the panel, and the two plumes rose separately. For this reason, the weaker plume from manikin A stagnated at a lower level and was unable to rise directly to the ceiling.

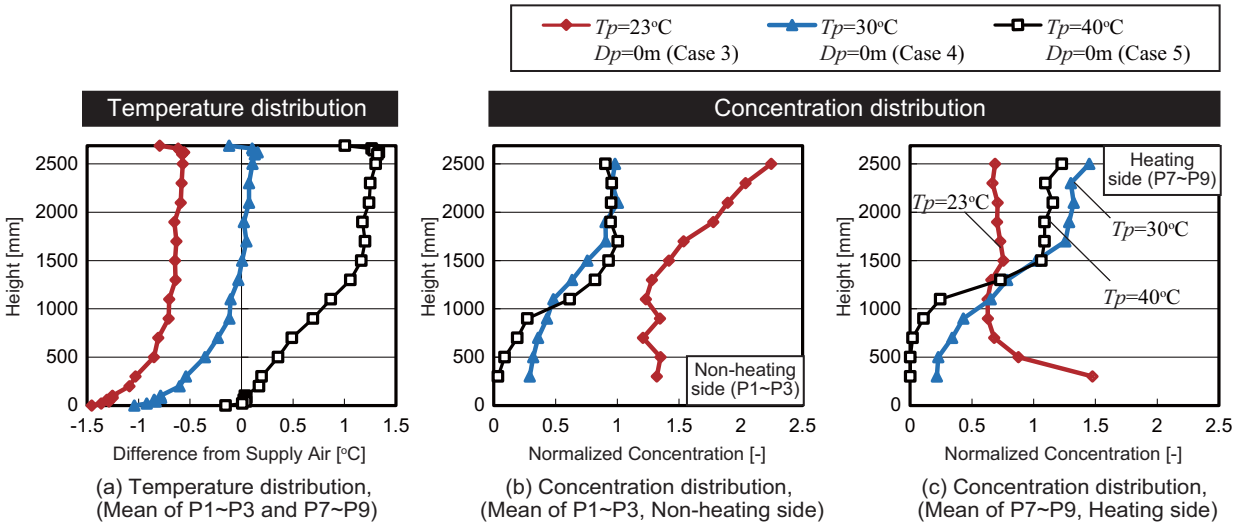


Figure 3.7 Measured temperature and concentration profiles (paratmeter: surface temperature of the panel T_p)

Influence of the height of the panel (H_p)

Figure 3.6 shows the influence of the height of the panel (H_p). As H_p increased, the temperature rose at a higher part of the room (**Figure 3.6(a)**). The concentration interface height formed at a higher level (**Figure 3.6(b), (c), (e), (f)**). The height where the contaminated air was locked-up also went up as the panel was located higher. When the height of the bottom end of the panel was higher than the bed, the contaminated air was locked on the heating side of the panel, even when D_p = 0 m (**Figure 3.6(c)**). Because the height of the bed was 0.4 m, there was space between the panel and bed in the vertical direction when the panel height was 0.8 m. The fresh air in the lower part was entrained through the space and went up to the ceiling without combining to the plume from the manikin A. When D_p = 0 m and H_p = 0.8 m, the contaminated air also trapped in non-heating side of the panel. It indicates that the contaminated air from the manikin passed under the panel and reached the non-heating side of the panel.

Influence of the surface temperature of the panel (T_p)

Figure 3.7 presents the influence of the surface temperature of the panel (T_p) on the room air temperature and concentration profiles. Temperature stratification was confirmed while the room temperature was lower than the supply air temperature when T_p was 23 and 30 °C (**Figure 3.7(a)**). Although the panel surface temperature was higher than the supply air temperature, the air temperature of the lower part had negative values in case of T_p = 30 °C. The heat loss was relatively large compared to heat generation in this case (**Table 3.2**, Case 4). The room air temperature must have been higher than the supply air if the room was completely insulated. As T_p increased, the heat load in the room became larger. This caused the vertical temperature gradient to increase. When T_p = 30 and 40 °C, the concentration in the lower part of the room was fresher than the upper part. However, when the surface temperature of the panel was lower than the supply air temperature (T_p = 23°C), the contaminated air from the manikin A was considered to be transported from the upper part back to the lower part by the downward flow of the panel. In this case, the contaminant concentration in the lower part was higher than the upper part and the contaminant concentration profile was unlike general DV.

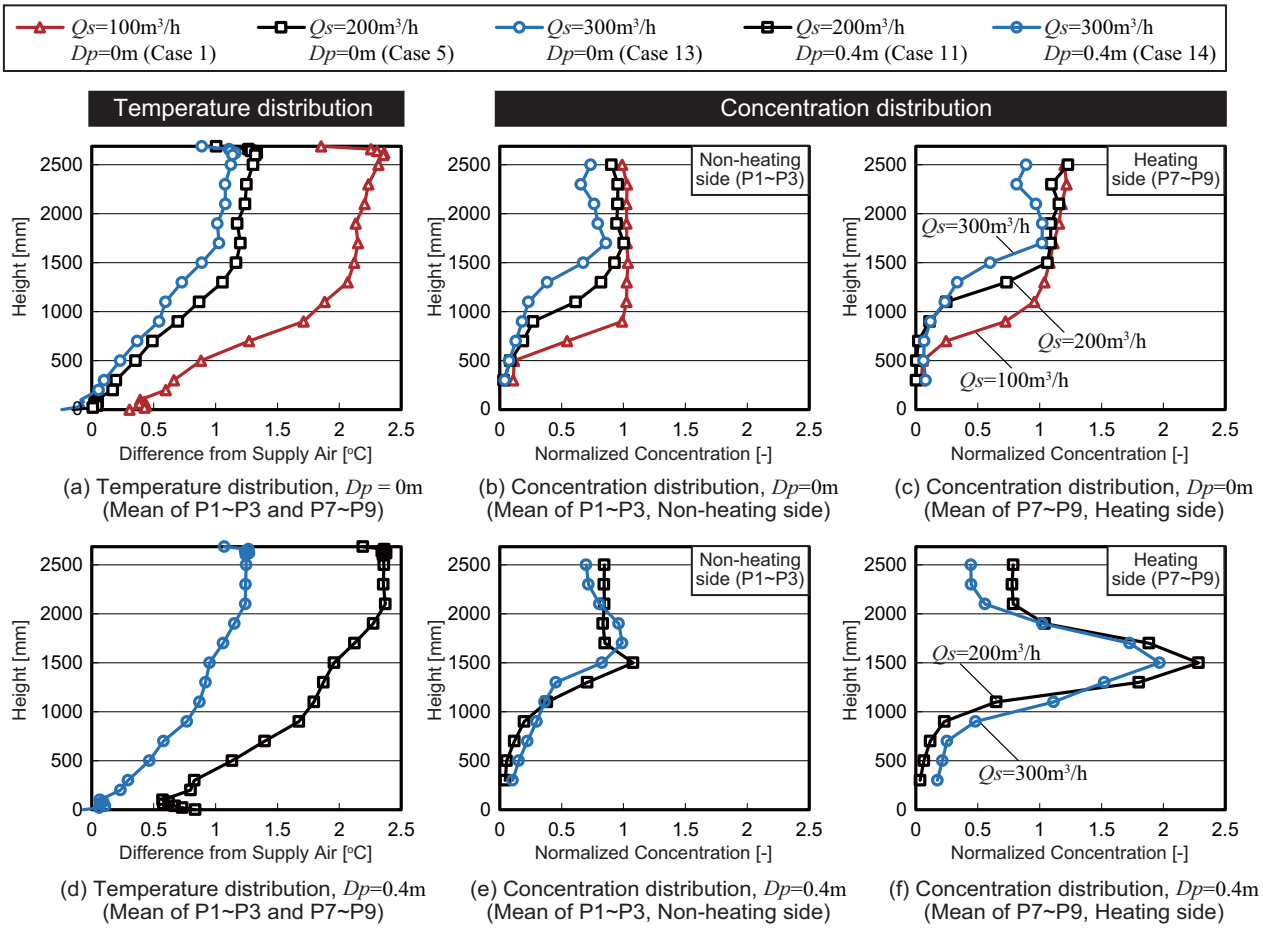
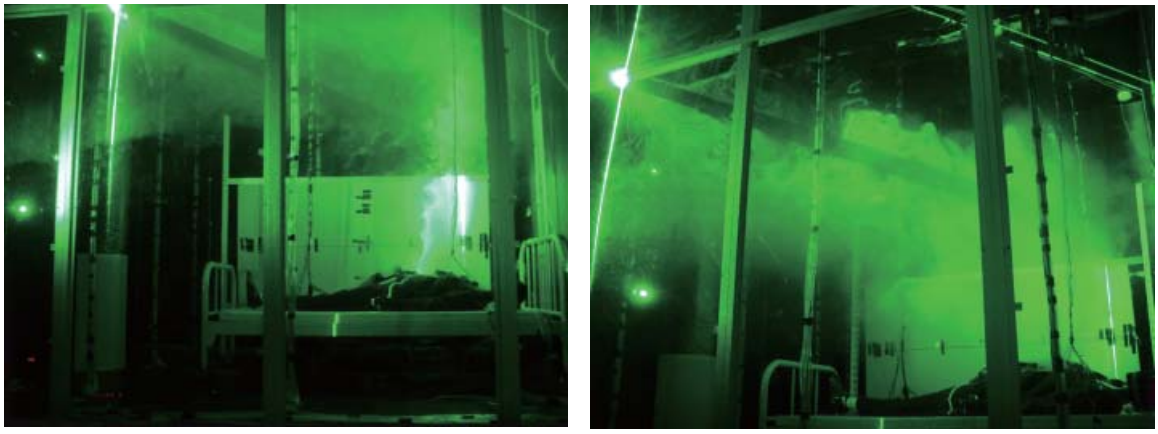


Figure 3.8 Measured temperature and concentration profiles (paratmeter: supply airflow rate Q_s)



(a) Case 5 (Q_s: 200m³/h, D_p: 0m, H_p: 0.4m) ***(b) Case 10 (Q_s: 200m³/h, D_p: 0.4m, H_p: 0.4m)***

Figure 3.9 Visualization of the contaminant plume from the lying manikin A

Influence of the supply airflow rate (Q_s)

The influence of the supply airflow rate (Q_s) is presented in **Figure 3.8**. As Q_s increased, the temperature difference between the supply and exhaust air became smaller and temperature stratification became weaker (**Figure 3.8(a), (d)**). When D_p = 0 m, the contaminant concentration interface was apparent in all cases, and the height of the contaminant interface formed higher as Q_s increased (**Figure 3.8(b), (e)**) in both sides of the radiant panel. However, when D_p = 0.4 m, the contaminated air was locked-up at the heating side of the panel, and no significant difference was evident between the neutral heights of Q_s = 200 and 300 m³/h and the

contaminant concentration distribution (**Figure 3.8(f)**). Although the contaminant concentration in the lower part was close to the supply air, the normalized concentration at the height of 1.5 m was higher than 2 and it indicates that the air quality at the breathing zone of the standing person was worse than the MV.

The plume from the lying manikin A is visualized using smoke in **Figure 3.9**. When the radiant panel and bed adjoined each other (Case 5, **Figure 3.9(a)**), the smoke from the lying manikin A merged with the convection flow along the panel and rose to the ceiling. The contaminant interface formed apparently and the air quality of the lower part of the room was kept fresh. However, although the contaminant interface formed and the lower part of the interface was cleanwhen there was space between the panel and bed, the smoke did not reach the ceiling and was locked-up. The clean air which was entrained into the plume of the panel was accumulated near the ceiling (Case 10, **Figure 3.9(b)**).

3.3 Personal Exposure

3.3.1 Experimental Setup

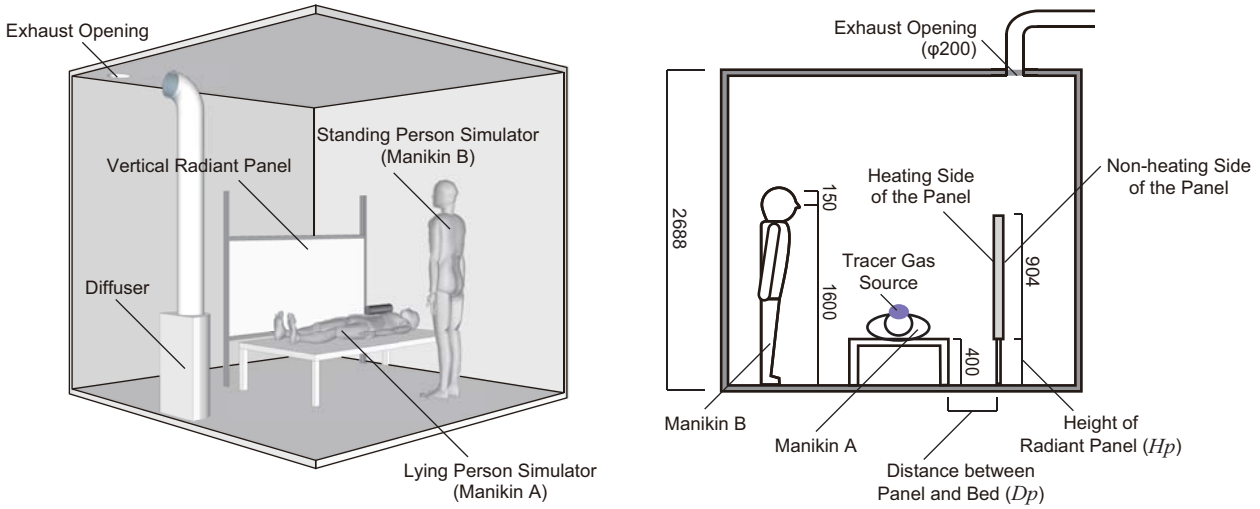
To investigate personal exposure of the standing person in the displacement-ventilated hospital ward with the radiant panel, the experiments were carried out in the experimental chamber mentioned in **Chapter 3.2**. The experimental set-up is shown in **Figure 3.10** and **3.11**. The standing manikin was placed near the bed (Manikin B). Manikin B was also wrapped in polyvinyl chloride (PVC) heating cable at equal intervals and put in sweat suits (**Figure 3.11(b)**). The heat generation from manikin B was controlled at 75W to represent the sensible heat load of the standing hospital staff. The tube for inhalation (**Figure 3.11(c)**) was placed on the face of manikin B. Inhalation was assumed to be steady, and the inhaled airflow rate was maintained at 14.4 L/min to represent the average amount of one breathing cycle[3-5].

3.3.2 Experimental Conditions

The measurement conditions are presented in **Table 3.3**. In order to examine personal exposure under different neutral heights, the experiments were performed with three different supply airflow rates; Q_s = 100, 200 and 300 m^3/h. In **Chapter 3.2**, it was found out that the contaminated air was locked-up when there was space between the radiant panel and bed. Hence, two different distances (D_p = 0 and 0.4 m) between the panel and bed were set up to compare personal exposures with and without contaminant stagnation. The unheated panel condition was added to change the heat load inside the chamber. If panel is not heated, Under the unheated panel condition, the panel was placed in the experimental chamber without heating or cooling.

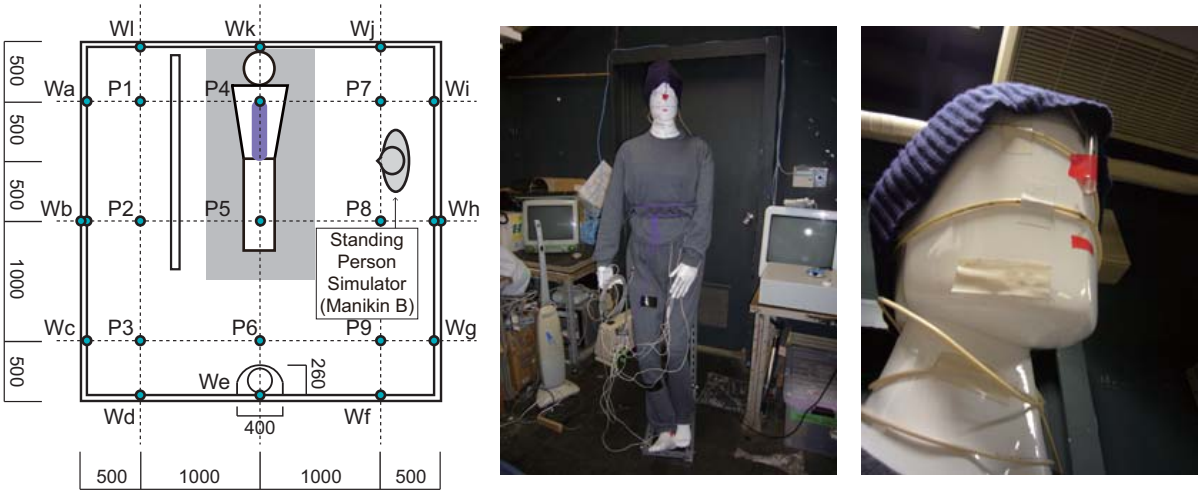
3.3.3 Measured and Predicted Results of Personal Exposure in a Displacement-ventilated with Radiant Panel

The measured personal exposures and concentration profiles of the surrounding air are shown in **Figure 3.12**. The minimum and maximum values of the measured exposures are also provided. As previously known, the inhaled air concentrations were less than the air concentration at the same height because of the entrainment



(a) Schematic view of the experimental room (b) Section view of the experimental room, [mm]

Figure 3.10 Schematic and section view of the experimental room



(a) Plan view of the experimental room and horizontal measurement points (b) Standing person simulator (c) Tube for the inhalation

Figure 3.11 Horizontal view of the experimental room and standing person simulator

Table 3.3 Experimental conditions to examine personal exposure

Cases	Supply airflow rate	Distance between the panel and bed	Height of the panel	Temperature of the panel surface
	Q_s [m^3/h]	D_p [m]	H_p [m]	T_p [°C]
Case 15	100	0	0.4	40
Case 16	100	0.3	0.4	40
Case 17	100	0.3	0.4	-
Case 18	200	0	0.4	40
Case 19	200	0.3	0.4	40
Case 20	200	0.3	0.4	-
Case 21	300	0	0.4	40
Case 22	300	0.3	0.4	40
Case 23	300	0.3	0.4	-

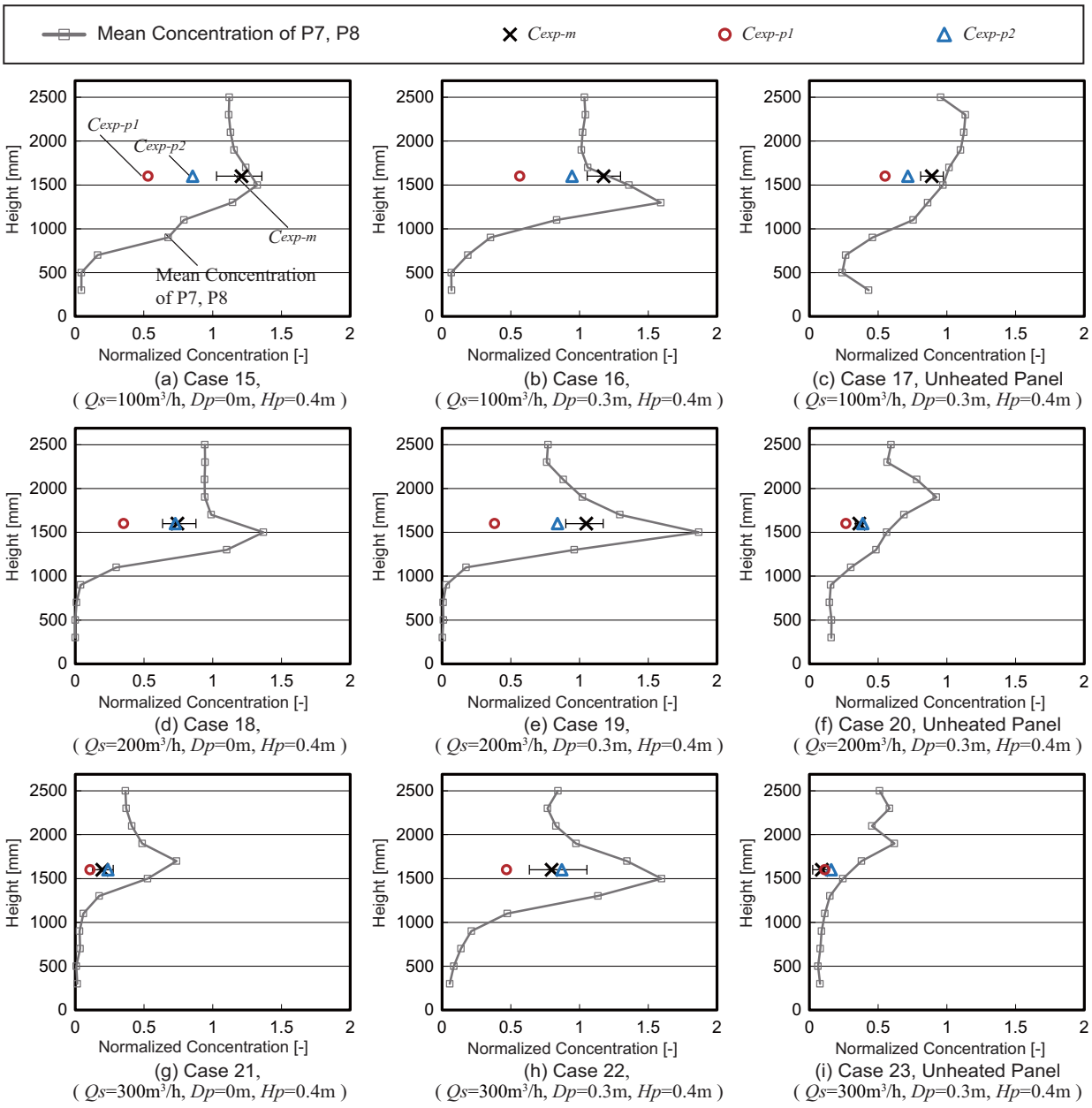


Figure 3.12 Measured and predicted personal exposures of a standing person with concentration profiles

effect of the plume around the body. The larger supply airflow rate created the higher neutral height. The inhaled air concentration decreased as the concentration interface height increased. When the supply rate was lower, the personal exposure was close to the concentration of the surrounding air at the breathing zone height. With contaminant stagnation, personal exposure increased.

The thermal plume around a standing person should be examined in order to accurately predict the personal exposure. If the convection flow along the body is known, personal exposure can be estimated as follows:

$$C_{exp} = \frac{\int_0^{y_{exp}} Q_h'(y)\, C(y) dy}{Q_h(y_{exp})} \quad \cdots(3\text{-}2)$$

$Q_h(y)$ is the plume airflow rate around the standing person and $Q_h'(y)$ is the entrained airflow rate to the plume at height y in the above equation.

Brohus and Nielsen[3-6] suggested a prediction model for the personal exposure in a displacement ventilated

room. They found a simple relation between the effectiveness of entrainment in the human boundary layer (η_e) and y_{st} / y_{exp} through experiments and several previous studies. η_e expresses the ability to supply air from the floor area to the breathing zone.

$$\eta_e = \frac{C_p - C_{exp}}{C_p - C_f} \quad \cdots(3\text{-}3)$$

Based on their measured results, personal exposure C_{exp} is defined as follows:

$$C_{exp} = C_b - \left(\frac{y_{st}}{y_{exp}}\right)(C_b - C_f) \quad \cdots(3\text{-}4)$$

However, the measured contaminant concentration profiles in this study indicated different properties from the experimental results of Brohus and Nielsen. The contaminant interface was not a flat line and yexp was sometimes located in the contaminant interface layer. C_b was greater than the concentration of exhausted air in some cases, especially when the contaminated air was locked up. Hence, their prediction model cannot be used as is. Based on their assumption that the entrained air flow rate is equal at every height, the personal exposure is given by

$$C_{exp-p1} = \frac{\int_0^{y_{exp}} C(y)dy}{y_{exp}} \quad \cdots(3\text{-}5)$$

The predicted personal exposures $C_{exp\text{-}p1}$ which are calculated from measured contaminant concentrations are also shown in Fig. 8.

Zhu et al.[3-7] studied the distribution of the inhalation region with experiments using a thermal manikin and computational fluid dynamics (CFD) analysis. Inhalation region means that the ratio of the air at any position to the total inhaled air. They measured the inhalation regions at the heights of the head, breast, waist, knee, and foot. Their results proved that the inhalation region was greater in the upper part than the lower part. They found the following instantaneous maximum shares of inhaled air from each body part[3-8] 100% at the head (1.5 m), 49.6% at the breast (1.25 m), 32.2% at the waist (0.95 m), and 16.3% at the knee (0.45m). $C_{exp\text{-}p2}$ is given as follows:

$$C_{exp-p2} = 0.5C_{head-breast} + 0.18C_{breast-waist} + 0.16C_{waist-knee} + 0.16C_{knee-foot} \quad \cdots(3\text{-}6)$$

In the present study, the inhalation shares were rounded, and the height of each body part was adjusted as follows: the head (mouth) at 1.6 m, breast at 1.3 m, waist at 1.0 m, and knee at 0.5 m. For the concentration value of each part (i.e., $C_{head\text{-}breast}$, $C_{breast\text{-}waist}$, $C_{waist\text{-}knee}$, $C_{knee\text{-}foot}$), measured contaminant concentrations between each part were averaged. For example, measured concentrations from the height of the breast to the height of the head are used for $C_{head\text{-}breast}$.

In most cases, $C_{exp\text{-}p1}$ was smaller than the measured $C_{exp\text{-}m}$. When the contaminant interface was near the breathing zone height, $C_{exp\text{-}p1}$ was close to the measured Cexp. Cexp-p2 was closer to the measured personal exposure than $C_{exp\text{-}p1}$. When

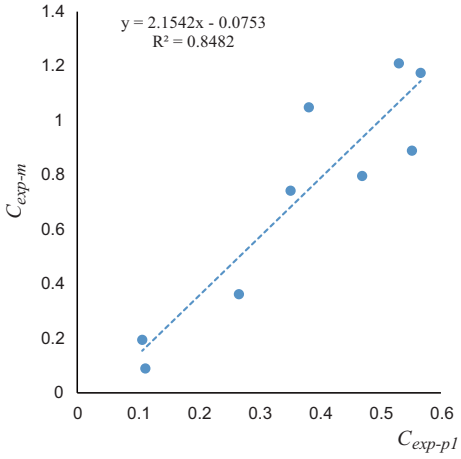


Figure 3.13 The relationship between measured $C_{exp\text{-}m}$ and $C_{exp\text{-}p1}$

the interface formed at a lower level or the contaminant was trapped, $C_{exp\text{-}p1}$ and $C_{exp\text{-}p2}$ were much smaller than $C_{exp\text{-}m}$. For reference, the relationship between $C_{exp\text{-}p1}$ and Cexp-m was examined. The linear function $C_{exp-m} = AC_{exp-p1} + B$ was used to approximate the relationship, and A = 2.154 and B = 0.075 were obtained with the coefficient of determination R^2 = 0.85 (**Figure 3.13**). Although $C_{exp\text{-}p1}$ did not match the measured result, a considerable correlation was confirmed in this study. $C_{exp\text{-}m}$ was approximately twice as large as $C_{exp\text{-}p1}$.

The entrained air was considered to be equal at every height in the prediction model for $C_{exp\text{-}p1}$. However, the upper part of the body may entrain a larger amount of air than the lower part of the body. If $C_{exp\text{-}p1}$ is used to predict all DV situations, the freshness of the inhaled air quality could be overestimated. Another reason for the lack of accuracy in $C_{exp\text{-}p1}$ may be the difference in measurement methods. Brohus and Nielsen[3-6] used a thermal manikin that could simulate actual respiration. In contrast, a simple manikin was used in this experiment, and the inhalation was regarded as steady. After all, in order to enhance the prediction accuracy, more measurements and CFD simulations are needed.

3.3.4 Personal Exposure of the Different Location in the room

The experimental results in **Chapter 3.3.3** were measured when the standing manikin was placed at the same location. However, the location of the standing person might also affect personal exposure. Brohus and Nielsen[3-6] also examined the influence of the height and location of a point contaminant source. They investigated personal exposure under two different conditions: the manikin standing facing the supply inlet and the manikin standing against the inlet. In addition, the measurements were carried out with the various height of a contaminant source. As a result, personal exposure varied with the height and location of a contaminant source. Although there were cases with the good air quality compared to the mixing ventilation; however personal exposure was worse than the mixing ventilation in many cases. Because the contaminant source was not a heat source in their research, the contaminant air might be entrained to the plume around the person simulator, especially when the contaminant source was located in the lower part. In this chapter,

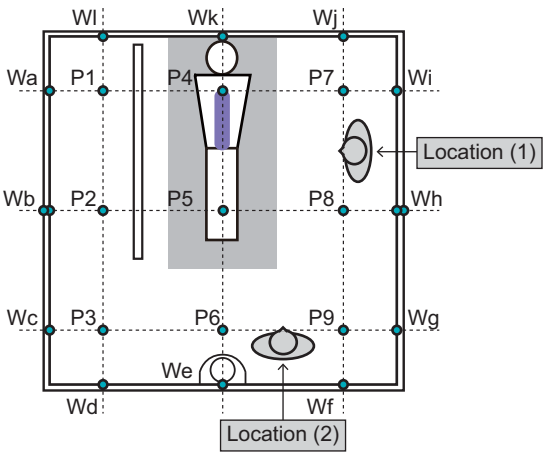
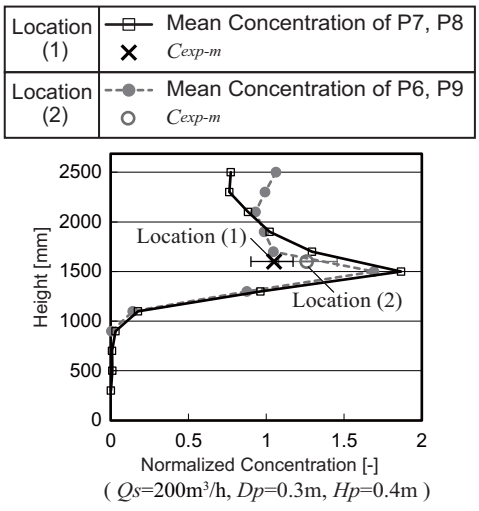


Figure 3.14 Location of standing manekin B



(Qs=200m³/h, Dp=0.3m, Hp=0.4m)

Figure 3.15 Measured personal exposures of a standing person with concentration profiles

one more measurement was carried out under different location of the standing manikin B (location (2)) to investigate the impact of the location of the supply inlet when the contaminant source is also a heat source. The original location of **Chapter 3.3.3** (location (1)) and location (2) are shown in **Figure 3.14**. The location (2) was closer to the supply inlet compared with the location (1), but the manikin B was standing with its back to the supply inlet. Case 19 (Q_s = 200 m^3/h, D_p = 0 .3 m, H_p = 0.4 m) was chosen to investigate the influence of the location because it has the highest contaminant concentration at the breathing zone.

Figure 3.15 presents the measured mean concentration near the standing person simulator (P7 and P8 for location (1), P6 and P9 for location (2)) and personal exposure. In both cases, the contaminated air was locked-up. The heights of the contaminant interface Personal exposure at the location (2) was higher than the location (1) even though it was close to the supply inlet. Personal exposure at the location (2) was as high as the contaminant concentration at the breathing height, while personal exposure at location (1) was lower than the contaminant concentration of the ambient air. The fresh supplied air could not reach to the front side probably because the supply inlet was located at the back side of the standing manikin. It indicates that where the medical staff mainly stand on when they are treating should be considered when deciding the location of the supply inlet.

3.4 Model Validation

Calculated and measured results of the cases of D_p = 0 m, H_p = 0.4 m with Q_s = 100, 200, 300 m^3/h are shown in **Figure 3.16**. Since D_p did not affect the temperature distribution significantly, the cases with different supply airflow rates were chosen to validate the prediction models for vertical temperature distribution. Xu and Yamanaka model (2001)[3-9] and Zonal model (Inagaki et al. (2012)[3-10] and Yamanaka et al. (2012)[3-11]) were used to forecast the temperature distribution, because Xu and Yamanaka model is the improved and detailed model of Mundt model; thus, it must have a better accuracy rather than Mundt model. Zonal model adopted the Mundt model's approach to the air temperature near the floor and ceiling, and the idea of mixed upper layer from Nielsen model. Hence, it would agree well with the measured results compared with the

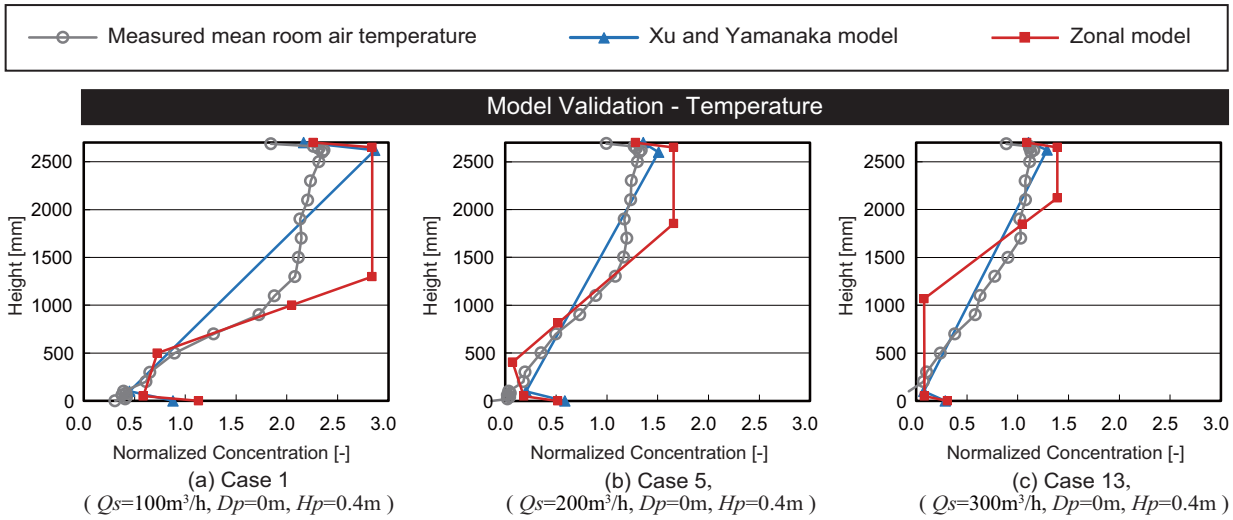


Figure 3.16 Calculated results with the zonal model (Contaminant concentration)

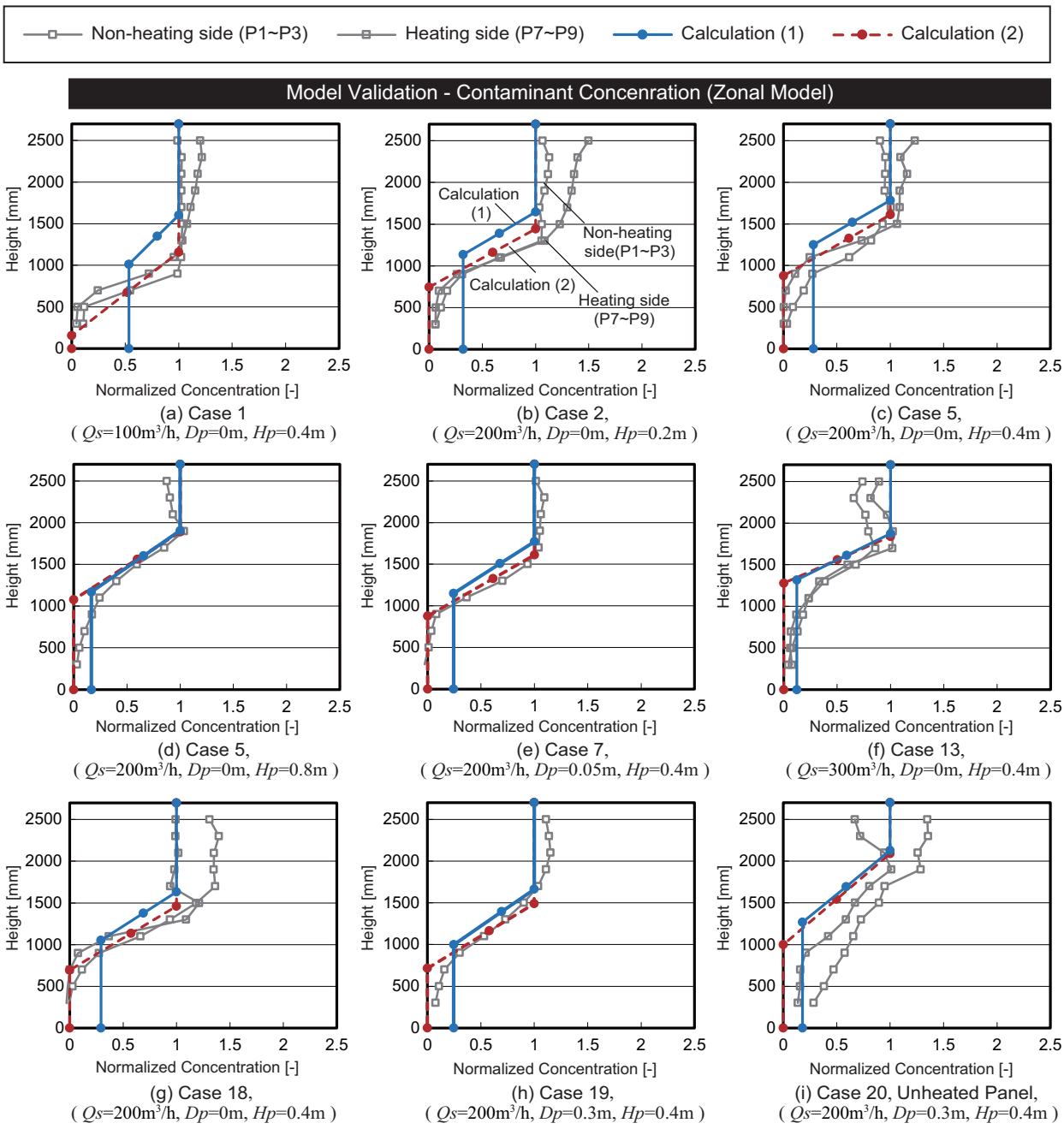


Figure 3.17 Calculated results with the zonal model (Contaminant concentration)

Nielsen model. When Q_s = 100 and 200 m^3/h, the zonal model corresponded with the measured results of the occupied zone. On the other hand, the calculated results of Xu and Yamanaka model was closer to the measured result than the zonal model. If supply airflow rate is large, the vertical temperature difference gets smaller and the temperature profile is nearly linear. On the other hand, both models did not match well with the air temperature of the upper part of the room. However, this disagreement might not be because of the calculation method of models. Calculated results overestimated the exhaust air temperature and it indicates that the heat loss through the envelopes was underestimated. Because the measurement points on the outer surfaces of the walls, floor and ceiling were limited, the actual heat loss or gain through envelopes may be different from the calculated results. The calculated panel surface temperature was also higher than the measured result. If the heat transfer through the envelopes are appropriately predicted, the calculated results

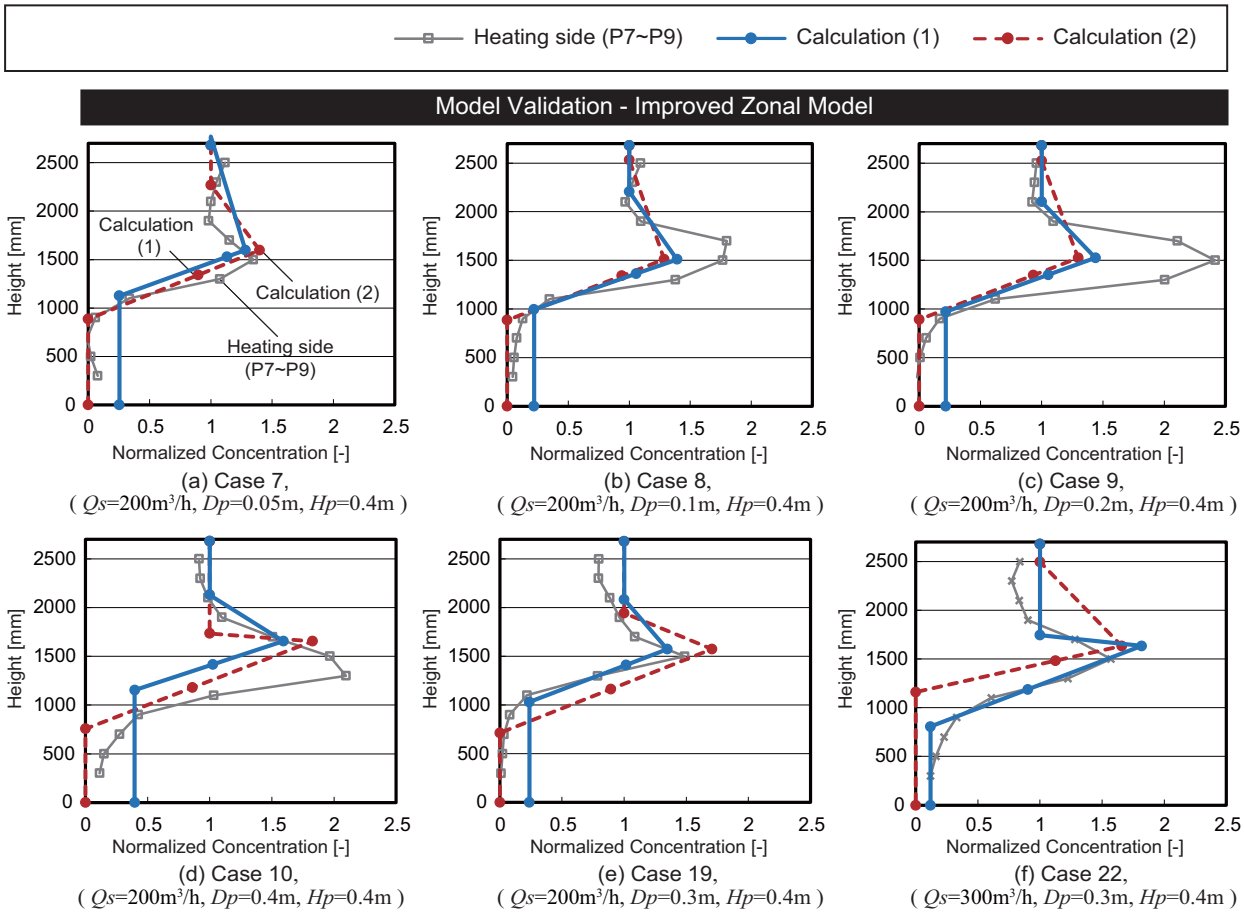


Figure 3.18 Calculated results with the improved zonal model (Contaminant concentration)

would get closer to the measured results.

Figure 3.17 presents the calculated concentration with the zonal model (Yamanaka et al. (2007)[3-12]) and the measured results. The averaged concentration profiles on both sides of the panel (P1–P3, P7–P9) are shown for cases when the contaminated air was not trapped. In the other cases, only the values of the non-heated side of the panel (P1–P3) are compared to the calculated results. The upward and downward flows along the walls were considered for calculation (1) with the above models. On the other hand, calculation (2) did not take into account convection flows on the walls at all.

The calculated results with the zonal model closely matched the measured contaminant profiles in most cases. When there was a considerable downward airflow in the room, the calculated height of the contaminant interface layer increased, and the contaminant concentration in the lower part also increased. In these cases, calculation (1) showed little correspondence with the measured results. One possible reason is that the measurement points of air temperature were not close enough to the walls. Calculated downward airflow rate using the measured room air temperatures and the wall surface temperatures might larger than the actual situation. The downward flow was proved to affect the stratification height and contaminant concentration of the lower zone in a previous study (Xu et al. (2002)[3-13]). However, the degree of effect is still unclear.

Figure 3.18 shows the results of the improved zonal model (Suzuki et al. (2008)[3-14] and Inagaki et al. (2011)[3-15] with the averaged concentration distribution of the heated side of the panel (P7–P9). The measured temperature values near floor (60mm) and near ceiling (2100mm) were applied to get the linear

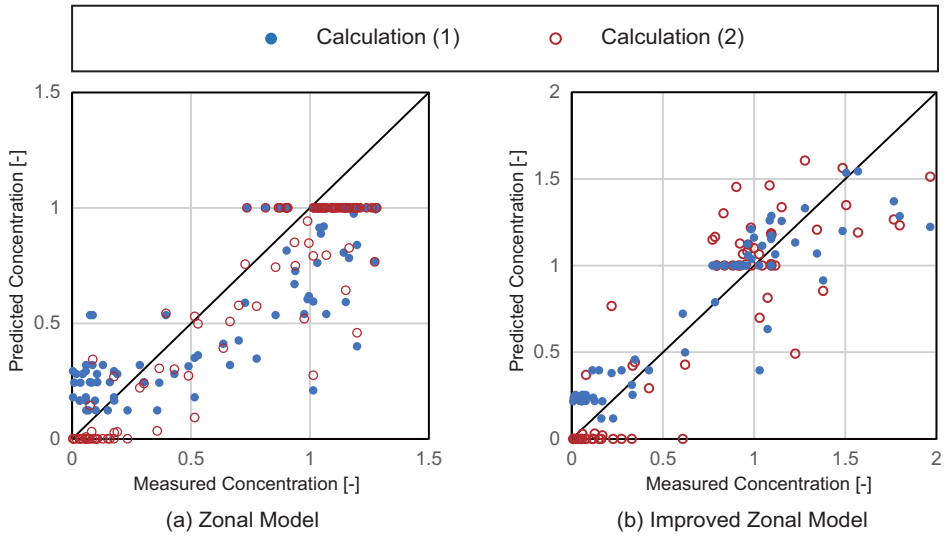


Figure 3.19 Comparison of predicted and measured concentration

temperature gradient ($\partial T/\partial y$) in this study. However, if the temperature values need to be calculated as well, the temperature model could be used. The calculated stagnation heights were close to the measured results. On the other hand, the concentration of the stagnation height did not correspond well with the measured results. However, whether the stagnation occurs and where it is located are more critical to predict rather than the contaminant concentration at the stagnation. As D_p gets larger, the concentration at the stagnation height becomes higher in the experiment results; nevertheless, there was no significant difference in the calculated results. When the radiant panel is close to the bed, the contaminant plume from the manikin would be entrained to the upward flow along the panel partially. If the panel is thoroughly far from the panel, two plumes would move individually. In this model, the change of the plume movement due to the distance between plumes was not reflected. Although the contaminated air was assumed to be equally divided among the upper and lower zones of the stagnation height, the actual situation may be different. The calculated stagnation height was higher than the measured results when the panel was located in the lower part (**Figure 3.18(d)**). The linearized temperature gradient between near the ceiling and floor was used to calculate the stagnation height. Accordingly, the calculated temperature gradient in the lower part was smaller than the actual temperature distribution, and the predicted stagnation height was higher than the measured results.

A comparison between the predicted and measured concentration is shown in **Figure 3.19**. For zonal model, the root mean square error (RMSE) of calculation (1) is 0.25 and 0.19 for calculation (2). Even though RMSE of calculation (2) is small, it tends to overestimate the air quality (**Figure 3.19(a)**). Calculation (1) is closer to the measured result with the improved zonal model (**Figure 3.19(b)**). RMSE of calculation (1) and (2) are 0.22 and 0.35. The convective airflow along the wall is not considered and the contaminant concentration below the interface layer is always ‘0’ with calculation (2). In order to avoid overrating the air freshness in the occupied zone, using calculation (1) might be better to predict the contaminant concentration profile of the room with DV.

3.5 Chapter Discussion and Conclusion

Measurements were conducted to evaluate the suitability of the vertical radiant panel with DV for hospital wards. Several panel conditions were changed to investigate their influence on the temperature and contaminant concentration distribution in a displacement ventilated room. Additionally, the zonal model and improved zonal model were applied to predict the contaminant concentration profiles. The following conclusions were obtained.

- When a vertical radiant panel is utilized for heating, it generates a stronger plume than the lying manikin, which diffuses contaminated air. For this reason, the contaminated air is trapped on its way to the ceiling, and the contaminant concentration of the stagnation level is higher than the concentration of the exhaust air. In contrast, if the radiant panel is utilized as a cooling system, the downward flow along the panel descends by entrainment near the contaminated air. Hence, the contaminant concentration at the lower level is higher than general DV. These results indicate that the location of the vertical radiant panel is important when it is used as a complementary heating or cooling system with DV. When it is heated, the radiant panel and contaminant source should be placed close together. The influence of convection flow from the heat source on the contaminant concentration distribution is profound; thus, an auxiliary heating or cooling system for DV should be examined thoroughly.
- If the supply airflow rate increases, the height of the interface layer and stagnation also go up. The height of the heat source influences the temperature and contaminant distributions.
- The personal exposure of a standing person is less than the contamination of the surrounding air at the breathing zone height because the person inhales the air inside the boundary layer around the person. When the contaminated air is locked up, the concentration of the inhaled air increases. Although personal exposure would become close to the concentration of the ambient air when a person is moving, a person who stays standing up for some time could benefit from this effect. In order to predict the personal exposure more accurately, it is essential to examine the plume around the body.
- The predicted vertical temperature profile using zonal model matched well with the measured air temperature in the lower part of the room. As the supply airflow rate gets larger, the temperature stratification becomes weaker. If the temperature distribution is linear, the calculated results of Xu and Yamanaka model was close to the measured results compared with the zonal model.
- The zonal model is valid for predicting the contaminant concentration profile when there is no stagnation. The calculated results were consistent with the experimental results in all cases. However, the downward flow along the wall affects the stratification height and contaminant concentration of the occupant zone, so its influence should be further studied. On the other hand, there is good correspondence between the measured concentration profiles and calculated results with the improved zonal model. The stagnation height is accurately predicted if the temperature gradient is properly applied. The movement mechanism of the trapped air should be investigated to increase the accuracy of the improved zonal model.

References

3-1) A. K. Melikov, J. B. Nielsen, Local thermal discomfort due to draft and vertical temperature difference in rooms with displacement ventilation, *ASHRAE Trans*. 96 (1989) 1050–1057

3-2) Q. Chen, L. Glicksman, System performance evaluation and design guidelines for displacement ventilation, American Society of Heating, Refrigerating and Air-Conditioning Engineers, Inc. 2003

3-3) R. Hwang, T. Lin, M. Cheng, J. Chien, Patient thermal comfort requirement for hospital environments in Taiwan, *Build. Enviro*. 42 (2007) 2980–2987.

3-4) J. Khodakarami, N. Nasrollahi, Thermal comfort in hospitals – A literature review, *Renewable and Sustainable Energy Reviews*, 16(6) (2012) 4071-4077

3-5) C. E. Hyldgård, Humans as a source of heat and air pollution, in: *Roomvent: 4th International Conference on Air Distribution in Rooms*, FINVAC, Helsinki, 1994.

3-6) H. Brohus, P. V. Nielsen, Personal exposure in displacement ventilated rooms, *Indoor Air* 6 (1996) 157–167.

3-7) S. Zhu, S. Kato, S. Murakami, T. Hayashi, Study on inhalation region by means of CFD analysis and experiment, *Build. Environ*. 40 (2005) 1329–1336.

3-8) S. Zhu et al., Numerical analysis on pollution of inhaled air with chemical contaminant in room (Part 6) Experimental study for pathway of inhaled air around a thermal manikin with a tracer gas method, in: *Proceedings of the Annual Meeting of the AIJ*, AIJ, Tokyo, 2000, pp. 893–894 (in Japanese).

3-9) M. Xu (2001) : Study on the prediction of contaminant concentration distribution in rooms with displacement ventilation, Doctoral Thesis, Osaka University.

3-10) T. Inagaki, T. Yamanaka, K. Sagara, H. Kotani, Y. Momoi, M. Shinozaki (2012) : Temperature and Contaminant Concentration Profiles in Four-Beds Sickroom with Displacement Ventilation (Part4) CFD Analysis of indoor airflow and application of zonal model, *Technical papers of annual meeting, the Society of Heating, Air-Conditioning and Sanitary Engineers of Japan*, pp.1751-1754 (In Japanese).

3-11) T. Yamanaka, K. Hisashi, S. Kazunobu, Y. Momoi, T. Inagaki, M. Shinozaki (2012) : Temperature and contaminant concentration in sick room with displacement ventilation, in: *Proceedings of the 9th International Forum and Workshop on Combined Heat, Air, Moisture and Pollutant Simulations* (CHAMPS 2012), IIS, Tokyo.

3-12) T. Yamanaka, H. Kotani, M. Xu (2007) : Zonal models to predict vertical contaminant distribution in room with displacement ventilation accounting for convection flows along walls, *Roomvent: 10th International Conference on Air Distribution in Rooms*, FINVAC, Helsinki.

3-13) M. Xu, T. Yamanaka, H. Kotani (2001) : Vertical profiles of temperature and contaminant concentration in rooms ventilated by displacement with heat loss through room envelopes, *Indoor Air*. 11, pp.111–119.

3-14) T. Suzuki, K. Sagara, T. Yamanaka, H. Kotani, A. Iwamura, T. Yamashita (2008) : Prediction of vertical profile of contaminant concentration in displacement-ventilated sickroom with radiant panel, *Transactions of the Society of Heating, Air-conditioning and Sanitary Engineers of Japan*, No. 141, pp.19-27 (In Japanese).

3-15)T. Inagaki, T. Yamanaka, K. Sagara, H. Kotani, Y. Momoi, T. Yamashita (2011) : Prediction of vertical profile of temperature and contaminant concentration in sickroom with displacement ventilation (Part 2) Prediction model of vertical profile of temperature and contaminant concentration, *Technical papers of annual meeting, the Society of Heating, Air-Conditioning and Sanitary Engineers of Japan*, pp. 2021–2024 (in Japanese).

Published Papers related to Chapter 3

Conference Papers

*International Conference

1) N. Choi, K. Sagara, T. Yamanaka, H. Kotani, T. Suzuki, T. Yamashita (2008) : Displacement Ventilation System with Radiation Panel for Sickroom - Influence of Radiation Panel on Contaminant Concentration Profile - , *Advanced building ventilation and environmental technology for addressing climate change issues,* Volume1, pp.141-146.

*Papers for Archtectural Institute of Japan (AIJ)

1) N. Choi, K. Sagara, T. Yamanaka, H. Kotani, T. Suzuki, T. Yamashita (2008) : Semi-personal air-conditioning system for sickroom by displacement ventilation with radiant panel (Part 9) Effect of radiant panel on temperature and contaminant concentration profile, *Proceedings of Technical Papers of Annual Meeting of AIJ Kinki branch*, pp.321-324. (In Japanese)

2) N. Choi, K. Sagara, T. Yamanaka, H. Kotani, T. Yamashita (2008) : Semi-personal air-conditioning system for sickroom by displacement ventilation with radiant panel (Part 11) Effect of radiant panel on temperature and contaminant concentration profile, *Summaries of Technical Papers of Annual Meeting of AIJ*, pp.665-666. (In Japanese)

3) N. Choi, T. Yamanaka, K. Sagara, H. Kotani, Y. Momoi, J. Yamada, T. Yamashita (2009) : Semi-personal air-conditioning system for sickroom by displacement ventilation with radiant panel (Part 14) Personal exposure of standing person in displacement-ventilated room, *Proceedings of Technical Papers of Annual Meeting of AIJ Kinki branch*, pp.129-132. (In Japanese)

4) N. Choi, T. Yamanaka, K. Sagara, H. Kotani, Y. Momoi, J. Yamada, T. Yamashita (2009) : Semi-personal air-conditioning system for sickroom by displacement ventilation with radiant panel (Part 16) Personal exposure of standing person in displacement-ventilated room, *Summaries of Technical Papers of Annual Meeting of AIJ*, pp.667-668. (In Japanese)

*Paper for The Society of Heating, Air-Conditioning and Sanitary Engineers of Japan (SHASE)

1) N. Choi, K. Sagara, T. Yamanaka, H. Kotani, T. Suzuki, T. Yamashita (2008) : Semi-personal air-conditioning system for sickroom by displacement ventilation with radiant panel (Part 8) Effect of radiant panel on temperature and contaminant concentration profile, *Proceedings of Technical Papers of Annual Meeting of SHASE Kinki chapter*, pp.41-44. (In Japanese)

2) N. Choi, K. Sagara, T. Yamanaka, H. Kotani, T. Suzuki, T. Yamashita (2008) :Semi-personal air-

conditioning system for sickroom by displacement ventilation with radiant panel (Part 10) Effect of radiant panel on temperature and contaminant concentration profile, *Proceedings of Technical Papers of Annual Meeting of SHASE*, pp.265-268. (In Japanese)

3) N. Choi, T. Yamanaka, K. Sagara, H. Kotani, Y. Momoi, J. Yamada, T. Yamashita (2009) : Semi-personal air-conditioning system for sickroom by displacement ventilation with radiant panel (Part 13) Personal exposure of standing person in displacement-ventilated room, *Proceedings of Technical Papers of Annual Meeting of SHASE Kinki chapter*, pp.103-106. (In Japanese)

4) N. Choi, T. Yamanaka, K. Sagara, H. Kotani, Y. Momoi, J. Yamada, T. Yamashita (2009) : Semi-personal air-conditioning system for sickroom by displacement ventilation with radiant panel (Part 15) Personal exposure of standing person and contaminant concentration distribution in displacement-ventilated room, *Proceedings of Technical Papers of Annual Meeting of SHASE*, pp.221-224. (In Japanese)

Original Papers

1) N. Choi, T. Yamanaka, K. Sagara, Y. Momoi, T. Suzuki (2019) : Displacement ventilation with radiant panel for hospital wards: Measurement and prediction of the temperature and contaminant concentration profiles, *Building and Environment*, Volume 160, 106197.

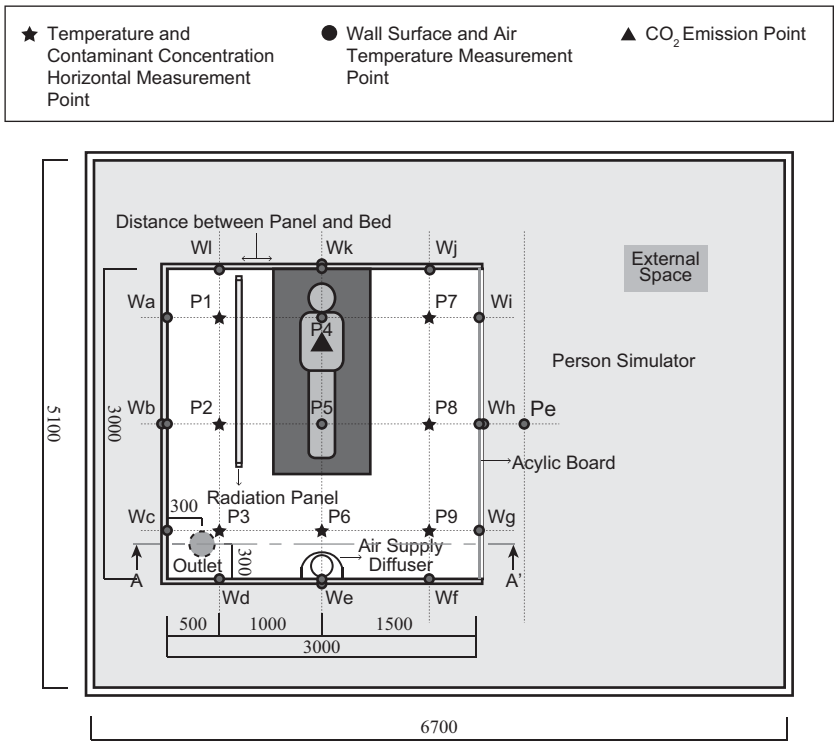
Chapter 4.
Influence of Vertical Convection Airflow along a Vertical Surface

4 Influence of Vertical Convection Airflow along a Vertical Surface

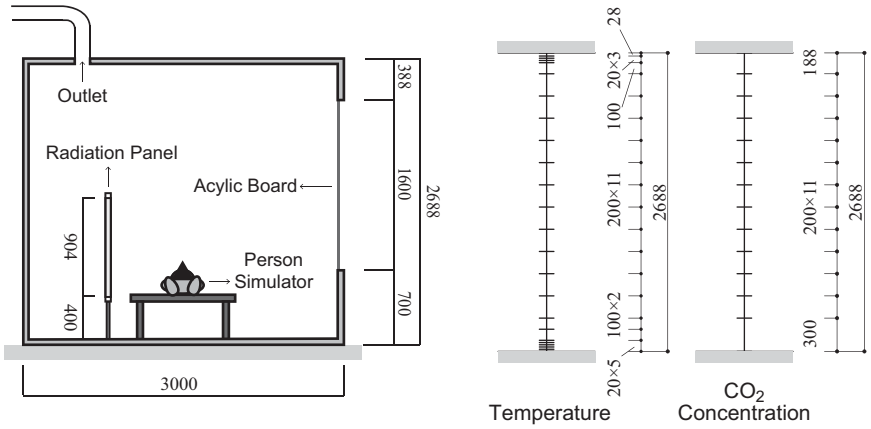
4.1 Purpose

The contaminant concentration in the displacement-ventilated room is sensitive to disturbances, whereas the temperature distribution is nearly impervious because of the stable temperature gradient. The vertical airflow along a wall or a window is also may have a significant effect on the contaminant concentration distribution in a room with DV (Kosonen et al. (2017)[4-1)], Zheng et al. (2019)[4-2)]). In a room with DV, the contaminant interface between the lower clean zone and upper mixing zone is formed at the neutral height. Hence, the height of the contaminant interface is affected by convection airflow. When there is temperature difference between the inner wall surface and the room air, downward or upward airflow is generated along the wall and it will influence the contaminant concentration distribution in the room. Especially during cold seasons, if the thermal insulation of walls or windows is poor, downward airflow occurs along the inner surface and would transport contaminated air from the upper part of the room to the occupied zone. Xu et al. (2001) [4-3)] examined the influence of the heat loss thruogh envelopes in a room with DV and it was revealed that the downward airflow along the cold wall considerably affects the indoor environment. Higashimoto et al. (2003)[4-4)] studied about the pradiction of the contaminant concentration in a displacement-ventilated room with cold wall and suggested the model that took account of the downward airflow along the wall. Furthermore, because DV is ideal for cooling, it should be used carefully when rooms must be heated. However, there are few studies focused on DV with a small cooling load or during the heating season (Fang et al. (2014) [4-5)]). If the supply air temperature is higher than the room air temperature, the supplied air will go directly to the ceiling because of buoyancy. For this reason, DV cannot be used for heating and a separate heating system, such as radiators or convectors, is recommended for the perimeter zone during cold seasons (Kosonen et al. (2017)[4-1)], Chen and Glicksman (2003)[4-6)]). However, to take appropriate measures for the perimeter zone, we must fully understand the influence of convective airflow along walls or windows on the temperature and contaminant concentration in a displacementventilated room.

This study suggests using DV to solve the unpleasant odor problem in a ward. Because a general ward has a window, the influence of convection airflow along the window in a displacementventilated room should be revealed before applying DV to a ward. In this chapter, the full-scale experiments were performed to investigate the influence of the convection airflow along the wall on an indoor environment in a ward with DV. The air temperature in the outer chamber was varied to generate different amounts of downward or upward airflow along the wall. The vertical and horizontal temperature and contaminant concentration distributions were measured under various conditions.



(a) Plan view of experimental room and horizontal measurement points



(b) Section view of experimental room (c) Vertical measurement points

Figure 4.1 Experimental room and measurement points

4.2 Experimental Investigation in Single-bed Ward

4.2.1 Experimental Setup

Measurements were performed in a full-scale displacement ventilated room (3,000 mm long, 3,000 mm wide, and 2,688 mm high) setup as a single-bed hospital ward. Experimental setup is shown in **Figure 4.1**. The displacement ventilated room was built in the test room and the walls and ceiling were insulated with a 50 mm thick polystyrene foam. In order to simulate the window, 5 mm thick acrylic board was installed at the height of 700 – 2300 mm on one wall. The heated lying mannequin which was made of wood with heating-cable was used as a person simulator. Heat generation of the person simulator was controlled at 40W as sensible heat load of slumbering human. Radiant panel was installed as a complementary heating system. The one side face to the person simulator was only heated and the other side of the panel was not heated (insulated).

The temperature of the test room (external space) was altered to investigate the temperature and contaminant concentration distribution in the displacement-ventilated ward under different outdoor temperatures (T_{oc}). T_{oc} was monitored at Pe. Fresh air was supplied from half-cylinder displacement-type diffuser (D: 400 mm, H: 750 mm, T: 260 mm). The exhaust opening (ϕ = 200 mm) was on the ceiling. CO_2 was used as tracer gas to simulate the odor frome the body and emitted from the tubed located on the human simulator. CO_2 airflow rate was controlled at 0.5 L/min by mass flow controller.

Measurement point of air temperatures were 9 points (P1-P9) in horizontal plane and 22 points in vertical direction, 198 points in total. Wall surface temperatures (Wa-Wl) were measured at 6 points vertically (i.e. 72 points for all). Virtual air temperature was measured at PO and 5 points in vertical direction. CO_2 concentrations (P1~P3, P6~P9) were measured at 12 points vertically (i.e. 72 points for all). T-type thermocouples (f = 0.32 mm, ASTM E230 Standard class (Tolerance : ± 1.0 °C or ± 0.75 %)) were used to measure air and surface temperatures. CO_2 concentration was measured using non-dispersive infrared (NDIR) gas analysers. The gas analysers were calibrated before the measurement every time.

4.2.2 Experimental Conditions

Table 4.1 shows the experimental conditions. Supply air temperature T_s was controlled at approximately 25 °C and supply airflow rate was 200 m^3/h. The surface temperature of the radiant panel (T_p) was maintained at approximately 40 °C when the panel is heated. External temperature (T_{oc}) means the air temperature outside the chamber (ambient space around the experimental chamber) and it was changed to examine the indoor environment with different amount of downward and upward convection airflow rate along the window (acrylic board in thie experiment). The case without heating radiant panel was also adopted to investigate the influence of the radiant panel. Additionally, distance between the radiant panel and bed (D_p) was altered

Table 4.1 Experimental conditions

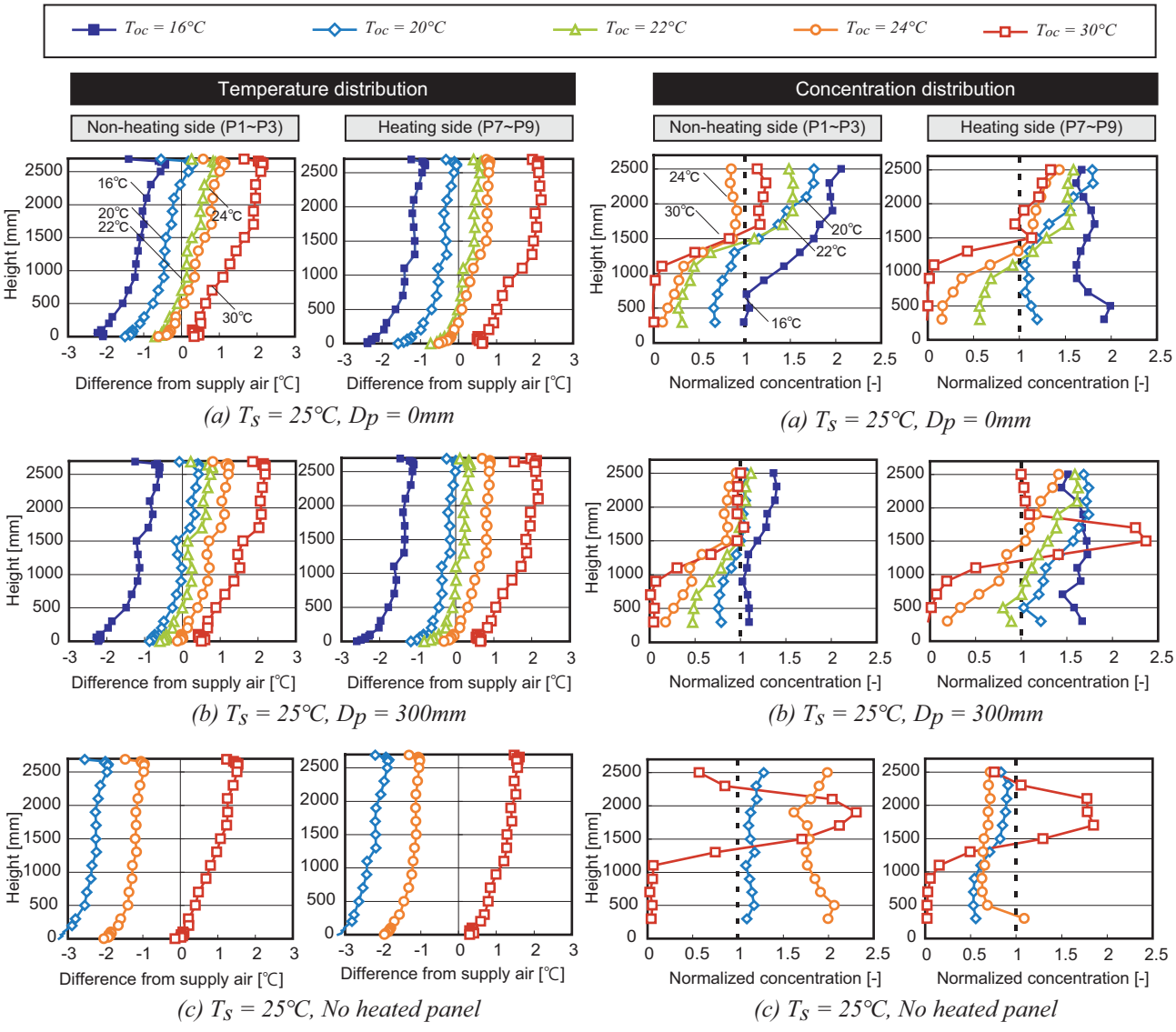
Cases	Supply airflow rate	Supply air temperature	External temperature	Distance between the panel and bed	Temperature difference between the supply and exhaust air
	Q_s [m^3/h]	T_s [°C]	T_{oc} [°C]	D_p [mm]	T_e - T_s [°C]
Case 1	200	25	16	0	−0.725
Case 2	200	25	16	300	−0.834
Case 3	200	25	20	0	0.063
Case 4	200	25	20	300	0.236
Case 5	200	25	20	No heated panel	−1.830
Case 6	200	25	16.74	0	0.776
Case 7	200	25	17.55	300	0.540
Case 8	200	25	17.67	0	1.242
Case 9	200	25	18.22	300	1.010
Case 10	200	25	18.26	No heated panel	-0.970
Case 11	200	25	17.84	0	2.160
Case 12	200	25	18.39	300	2.188
Case 13	200	25	18.73	No heated panel	1.246

because it was found out that D_p affect on the contaminant concentration distribution in the previous study (in Chapter 3).

The temperature difference between the supply and exhaust air of each case is also presented in **Table 4.1**. As the air temperature outside the chamber (T_{oc}) got higher, the temperature difference between T_e and T_s also became larger. When the panel was not heated, the temperature difference was small because the total heat gain in the room was small.

4.2.3 Experimental results

Figure 4.2 shows the measured results of vertical profile of temperature. The horizontal axis of graph means the temperature difference from supply air temperature. As graphs indicate, the air temperature gradient was positive in all cases. The air temperature got higher as T_{oc} rose. In cases of using heated radiation panel, indoor air temperature of displacement ventilated room is lower than supply air temperature 25 °C when



(a) T_S = 25℃, Dp = 0mm

(b) T_S = 25℃, Dp = 300mm

(c) T_S = 25℃, No heated panel

Figure 4.2 Vertical temperature profile (parameter : External space temperature T_{oc})

Figure 4.3 Vertical contaminant concentration profile (parameter : External space temperature T_{oc})

T_{oc} was 16, 20 and 22 °C. In conditions without heated radiation panel, excepting the case that T_{oc} was 30 °C, supply air temperature was higher than indoor air temperature in all cases. When panel was not heated, thermal stratification was weaker than other case, because the total heat generation was low. Because the total heat generation in the room was almost same, there was not a large difference between conditions of D_p = 0 mm and 300 mm. However, in the condition without the heated panel, the room air temperature was lower than other conditions, because panel was not heated and the total heat gain of the room was small. Hence, When T_{oc} = 30 °C, the temperature difference between the measured temperature results with and without panel was smaller than other conditions.

Figure 4.3 shows the measured results of vertical profile of CO_2 concentration. When D_p is 0 mm, the impact of T_{oc} is shown in **Figure 4.3 (a)**. When T_{oc} was low (T_{oc} : 16, 20, 22 °C), the CO_2 concentration was high in any height of the room and interface of the concentration was not confirmed. As T_{oc} became higher, contaminant concentration of lower zone decreased. The contaminant interface formed apparently in the case of T_{oc} = 30 °C.

Figure 4.3 (b) shows the impact of T_{oc} when D_p was 300 mm. Contaminant concentration profile was similar to the results of D_p = 0 mm. In the previous study, when there was a space between panel and bed, contaminated air was locked-up in the front side of the panel (in Chapter 3, Suzuki et al. (2008)[4-7]). Because fresh air in the lower level of the room was entrained to strong thermal plume along the panel and rose directly to the ceiling, the weaker plume with contaminated air from human body could not reach the ceiling. However, in this experiment, the stagnation of contaminant concentration was not seen in all cases except for the case of T_{oc} = 30 °C. It can be said that pollutant air descended with downward airflow along the window.

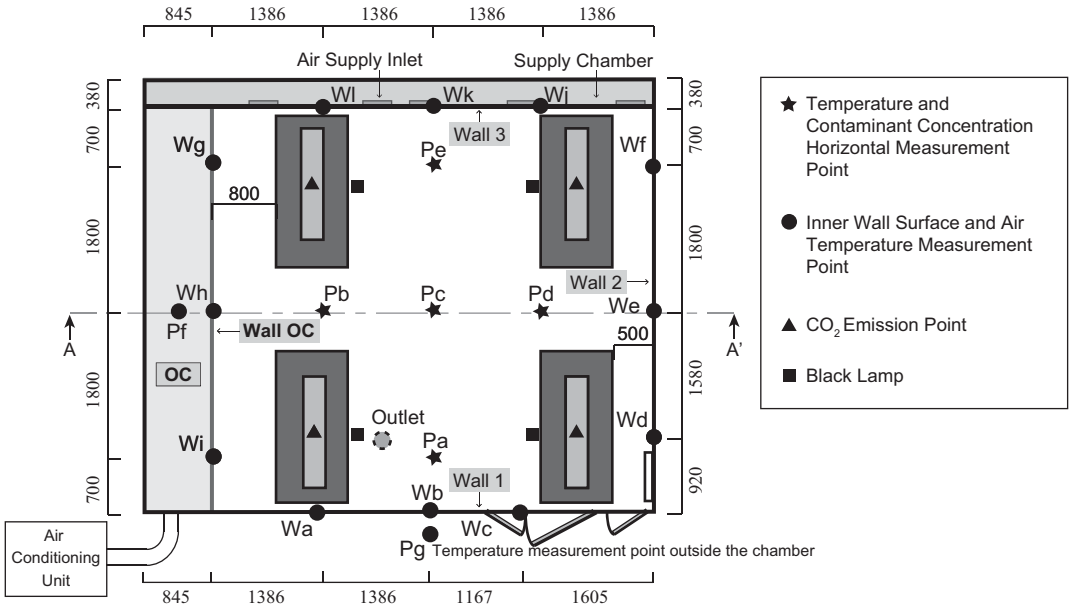
Figure 4.3 (c) presents the measured results when the radiant panel was not heated. The contaminant concentration of lower zone was high, even in the case of T_{oc} = 24 °C. When T_{oc} was 30 °C, the stagnation of contaminant concentration is seen in both sides of the panel. Because T_{oc} was higher than indoor air temperature, the temperature of window surface was also high and the upward airflow was generated along the window. The contaminant interface was more apparent when the radiation panel was heated. The distance from panel to bed had no significant influence on the contaminant concentration, except for the cases of T_{oc} = 30 °C.

When supply air temperature was higher than indoor air temperature, supply fresh air did not spread along the floor, and went up right after being supplied from the diffuser. Hence, the supplied fresh air might be exhausted directly and the contaminant concentration of all room was high.

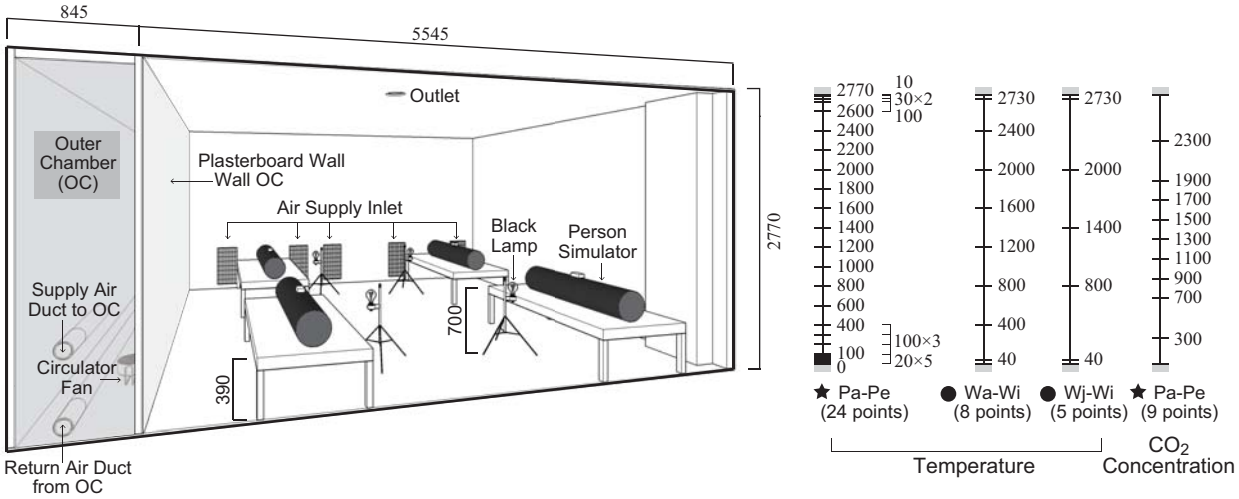
4.3 Experimental Investigation in Four-bed Ward

4.3.1 Experimental Setup

Measurements were conducted in a full-scale environmental chamber that was 5,000 mm long, 5,545 mm wide, and 2,770 mm high. **Figure 4.4** shows the experimental setup. The experimental room was set up as a four-bed hospital ward. According to the hospital facility standard of the Ministry of Health, Labor and Welfare, the floor area of a hospital ward in Japan should be 6.4 m^2 or more per patient. The floor area of the experimental room met this standard (6.8 m^2 per bed). The height of the room also satisfied the Building Standards Law in Japan (higher than 2.1 m). The locations of the beds were based on the general layout of four-bed hospital rooms in Japan. A 12.5 mm plasterboard was installed and assumed to be adjacent to the outdoor air (Wall OC). The space between the Wall OC and Wall 4, which was called the outer chamber (OC), simulated the outdoors or a non-air-conditioned room. The temperature inside the OC was changed by controlling the supply air temperature from the air conditioner. The air in the OC was fully mixed by circulators. Clean air was supplied through five supply inlets (320 mm wide by 620 mm high) which were placed on Wall 3. High-efficiency particulate air (HEPA) filters were installed in each supply inlet. The supply air temperature (T_s) was controlled at 15 °C and 20 °C. The exhaust opening (ϕ = 130 mm) was in the ceiling. The extract airflow rate (391 m^3/h) was measured using an airflow meter with a capture hood. Four person simulators were placed on each bed to simulate a person lying down. Each person simulator was made of a metal cylinder (ϕ = 300 mm, H = 1500 mm) wound in a polyvinyl chloride heating cable at equal intervals and wrapped in fabric. The heat generation of each person simulator was maintained at 40 W to represent a sensible heat load for a person lying down. Black lamps (light bulbs with dark violet glass) were placed near each bed to simulate electrical devices, such as televisions. The heat emission of each black lamp was maintained at approximately 60 W. Thus, the total heat generation in the experimental room was 400 W. CO_2 was used to simulate body odor and was distributed from the tube, which was placed in a sponge on each person simulator and diffused gradually. Because CO_2 was used as the tracer gas to simulate the passive contaminant (odors), the flow rate could not be large. Regarding the accuracy of the measurement equipment for CO_2 concentration, the CO_2 flow rate was maintained at 0.5 L/min from each emission point being 2 L/min in total. The temperature and CO_2 concentration measurement points are shown in **Figure 4.4 (a), (c)**. Pc was located at the center of the room. Pb and Pd had different horizontal distances from the Wall OC, and were added to examine the horizontal temperature and contaminant distribution. Pa and Pe were chosen to investigate the differences depending on the distance from the supply inlet. T-type thermocouples (f = 0.32 mm, ASTM E230 Standard class (Tolerance : ± 1.0 °C or ± 0.75 %)) were used to measure air and surface temperatures. Vertical temperature distributions were measured from five locations (Pa-Pe) at 24 heights, including the floor and ceiling surface. Because temperature gradients change near the floor and ceiling in the room with DV, the measurement points were placed tightly. The inner wall surface temperatures were measured from twelve locations (Wa-Wl) around the room, at six heights (Wa-Wi) and five heights (Wj-Wl). The air temperatures in the OC were measured from Pf at eight heights. The air temperature outside the experimental chamber (To) was also measured at Pg. Vertical CO_2 concentration distributions were measured from five locations (Pa-Pe) at nine heights with CO_2 recorders with nondispersive infrared (NDIR)



(a) Plan view of experimental chamber and horizontal measurement points



(b) Schematic view of experimental chamber (c) Vertical measurement points

Figure 4.4 Experimental setup and the measurement points

sensors (Accuracy : ± 50 ppm or ± 5 % RD). To observe the contaminant interface layer, the measurement points were placed primarily at mid-room height. To minimize the error of measured concentration results, all CO_2 recorders (48 in total) were calibrated using three or four different concentrations of the calibration gas. Temperature and concentration data recorded after reaching a steady-state were used for the analyses. Temperature results were averaged over 20 minutes, and CO_2 concentration results were averaged over 10 minutes.

4.3.2 Experimental Condition

Table 2 shows the experimental conditions. Supply air temperature T_s was controlled at approximately 15 °C in Cases 1–13 and 20 °C in Cases 14–19. Regarding thermal comfort, 15 °C is rather low for the supply air temperature in the room. However, because the experiments were conducted during the cold season, T_s was

Table 4.2 Experimental conditions

Cases	Supply airflow rate	Supply air temperature	Exhaust air temperature	Temperature difference between the OC and supply air	Temperature difference between outside the chamber and supply air
	Q_s [m^3/h]	T_s [°C]	T_e [°C]	T_{oc} - T_s [°C]	T_o - T_s [°C]
Case 1	391	14.77	15.68	−4.60	−4.03
Case 2	391	14.74	15.8	−4.35	−4.60
Case 3	391	14.77	16.75	−3.10	0.54
Case 4	391	14.74	16.66	−2.99	−0.03
Case 5	391	14.78	16.71	−2.04	−1.33
Case 6	391	14.74	16.74	−0.69	−0.60
Case 7	391	14.77	17.55	0.71	0.51
Case 8	391	14.67	17.67	2.39	0.04
Case 9	391	14.78	18.22	3.42	1.47
Case 10	391	14.83	18.26	4.37	0.55
Case 11	391	14.82	17.84	4.52	−2.90
Case 12	391	14.84	18.39	6.32	−1.83
Case 13	391	14.83	18.73	8.64	−3.79
Case 14	391	19.94	20.11	−6.40	−8.53
Case 15	391	19.92	20.06	−5.22	−9.76
Case 16	391	19.86	20.72	−4.74	−3.80
Case 17	391	19.99	20.77	−3.64	−8.16
Case 18	391	19.93	20.99	−2.38	−5.95
Case 19	391	19.97	21.24	−0.14	−7.06

set lower than usual to minimize heat loss through envelopes other than the Wall OC. Case 8 was selected as the reference condition because there was very little heat or and gain through the envelopes, including the Wall OC. In Case 8, $T_{Wall\ OC}$ and $T_{ave\text{-}r}$ were nearly equal, and T_o was also close to T_s. To examine the indoor environment with different amounts of downward airflow along the Wall OC, the gap between the outer chamber temperature (T_{oc}) and Ts was gradually widened from Case 8 to Case 1. Because the cooling capacity of the air conditioning unit for OC was limited, the T_s = 20 °C condition was added to further widen the gap between T_{oc} and T_s until the vertical temperature and concentration distribution were no longer stratified (Case 14, 15). For a reference, the maximum difference between the average inner wall surface temperature of the Wall OC ($T_{Wall\ OC}$) and the mean room air temperature of the displacement-ventilated chamber was approximately 3 °C (Case 14). The cases where T_{oc} was higher than the experimental room air temperature (Case 9–13) were also adopted to investigate the influence of upward airflow along the wall.

4.3.3 Experimental Results

Although the experimental chamber was insulated, there were heat losses and gains through the walls, ceiling, and floor depending on the ambient temperature at the time of measurement. **Figure 4.5** shows the difference between the average inner wall surface temperature and the air temperature measured at the nearest

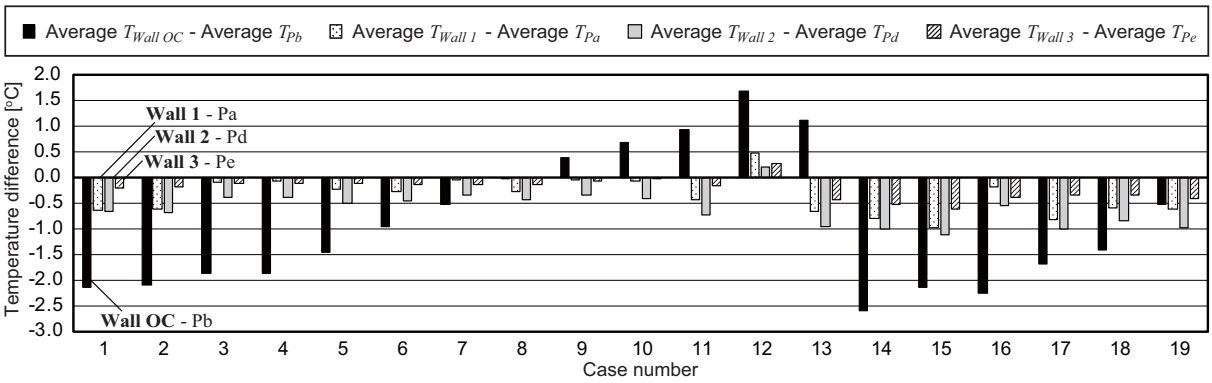


Figure 4.5 Experimental conditions

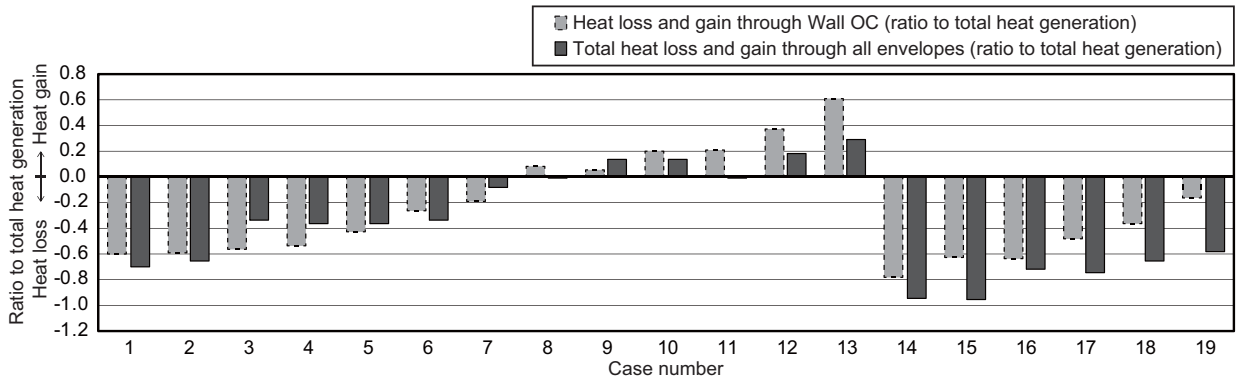


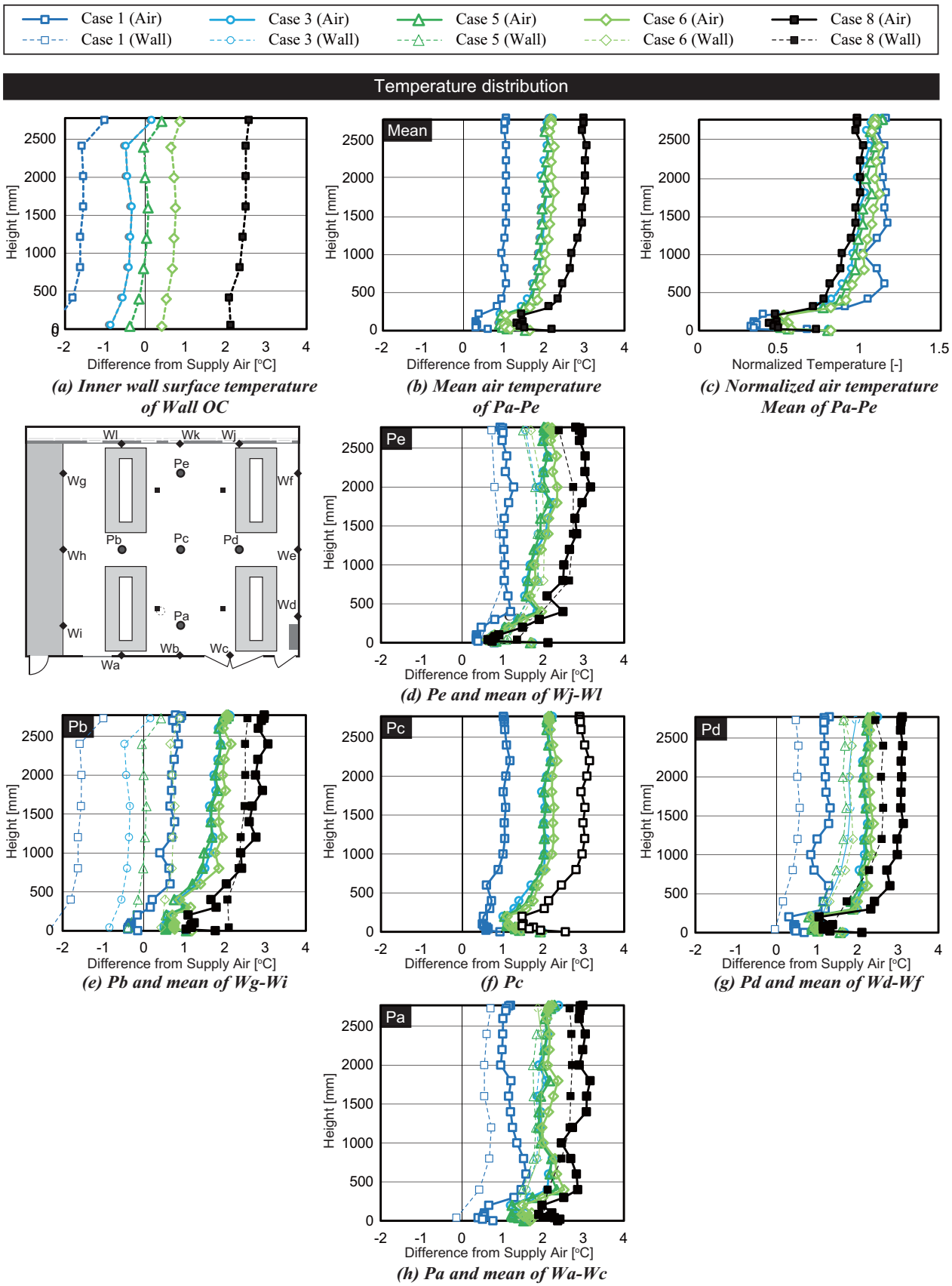
Figure 4.6 Experimental conditions

point to the wall in each case. Because the nearest point was not close enough to measure the air temperature near the wall, the actual temperature difference would be smaller than the values in **Figure 4.5**. The Wall OC was the target wall, the surface temperature of which was altered to induce downward or upward convection flow along the wall. As shown in **Figure 4.5**, the surface temperature of Wall OC changed as intended. However, the surface temperatures of other walls were also changed because of heat loss. Because the temperature difference between the outside and inside of the chamber was larger when T_s = 20 °C, all walls in the chamber were cooler than the air. The heat loss and gain through Wall OC and all envelopes in each case are shown in **Figure 4.6**. The heat loss and gain through Wall OC were calculated using the outer and inner surface temperatures and the thermal conductivity of the plasterboard (0.2 W/(mK)). Heat loss and gain through all envelopes were calculated using the following equation.

If the heat loss through Wall OC was greater than the total heat loss, it indicated there was heat gain through the ceiling and floor (Cases 3–5, 7, 9). On the contrary, if total heat loss was larger than the heat loss through Wall OC or the total heat gain was smaller than the heat gain through Wall OC, it indicated there was heat loss through other walls or the ceiling or floor (Cases 1, 2, 6, 10, 12–19).

4.3.3.1 Influence of downward convection flow along the cold wall

Figure 4.7 presents the measured vertical air temperature profiles of the four conditions for the cold wall (T_s = 15 °C, Cases 1, 3, 5, 6). The inner wall surface temperature profiles are also shown with the measured results of the closest measurement of the air temperature. For comparison, the results of Case 8 are also shown because heat loss and gain through all envelopes was almost zero in Case 8. As T_{oc} decreased,



(a) Inner wall surface temperature of Wall OC

(b) Mean air temperature of Pa-Pe

(c) Normalized air temperature Mean of Pa-Pe

(d) Pe and mean of Wj-Wl

(e) Pb and mean of Wg-Wi

(f) Pc

(g) Pd and mean of Wd-Wf

(h) Pa and mean of Wa-Wc

Figure 4.7 Measured temperature distribution (T_s = 15 °C, with cold wall)

the room air temperature lowered noticeably and the temperature gradient weakened. Comparisons of the normalized temperature distribution for each condition are shown in **Figure 4.7 (c)**. The normalized temperature near the floor was approximately 0.5. The inner wall surface temperature of Wall OC ($T_{Wall\ OC}$) was close to the air temperature in Case 8. In this case, the $T_{Wall\ OC}$ of the upper part was lower than the air temperature, and $T_{Wall\ OC}$ of the lower part was higher than that of the air. In other cases, the entire surface of Wall OC was cooler than the air; thus, downward convective airflow might be generated across its entire height. In Case 1, the vertical temperature difference was small and it was hardly stratified. The temperature difference between the inner wall surface and the room air was big at Pb, because Wall OC was cooled. The inner wall surface temperature near Pa and Pe (Wa-Wc, Wj-Wl) is close to the room air temperature, while there was a temperature difference between Wd-Wf and Pd. The room air temperature was low near the Wall OC and the temperature got higher as it became further from the Wall OC.

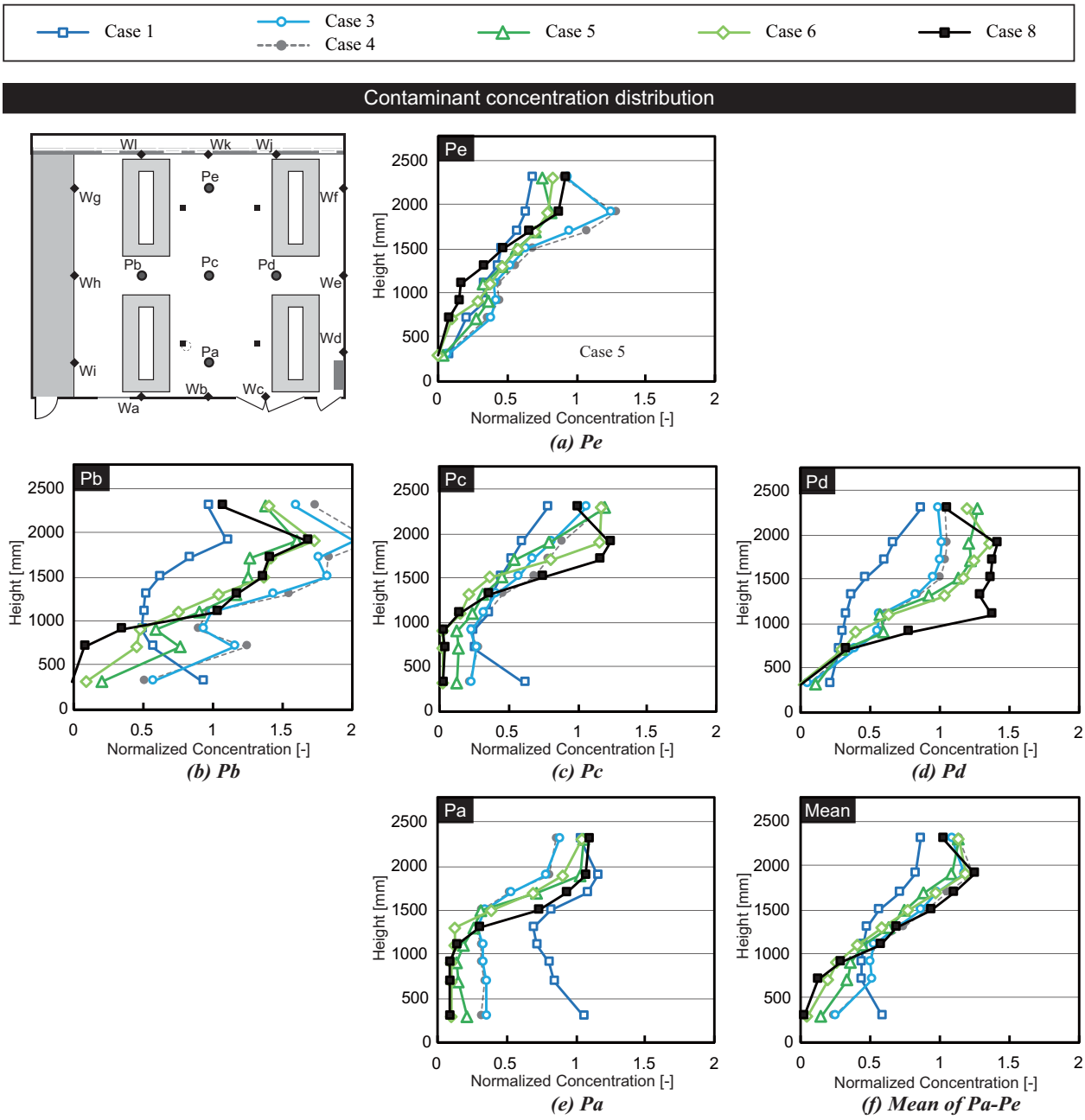
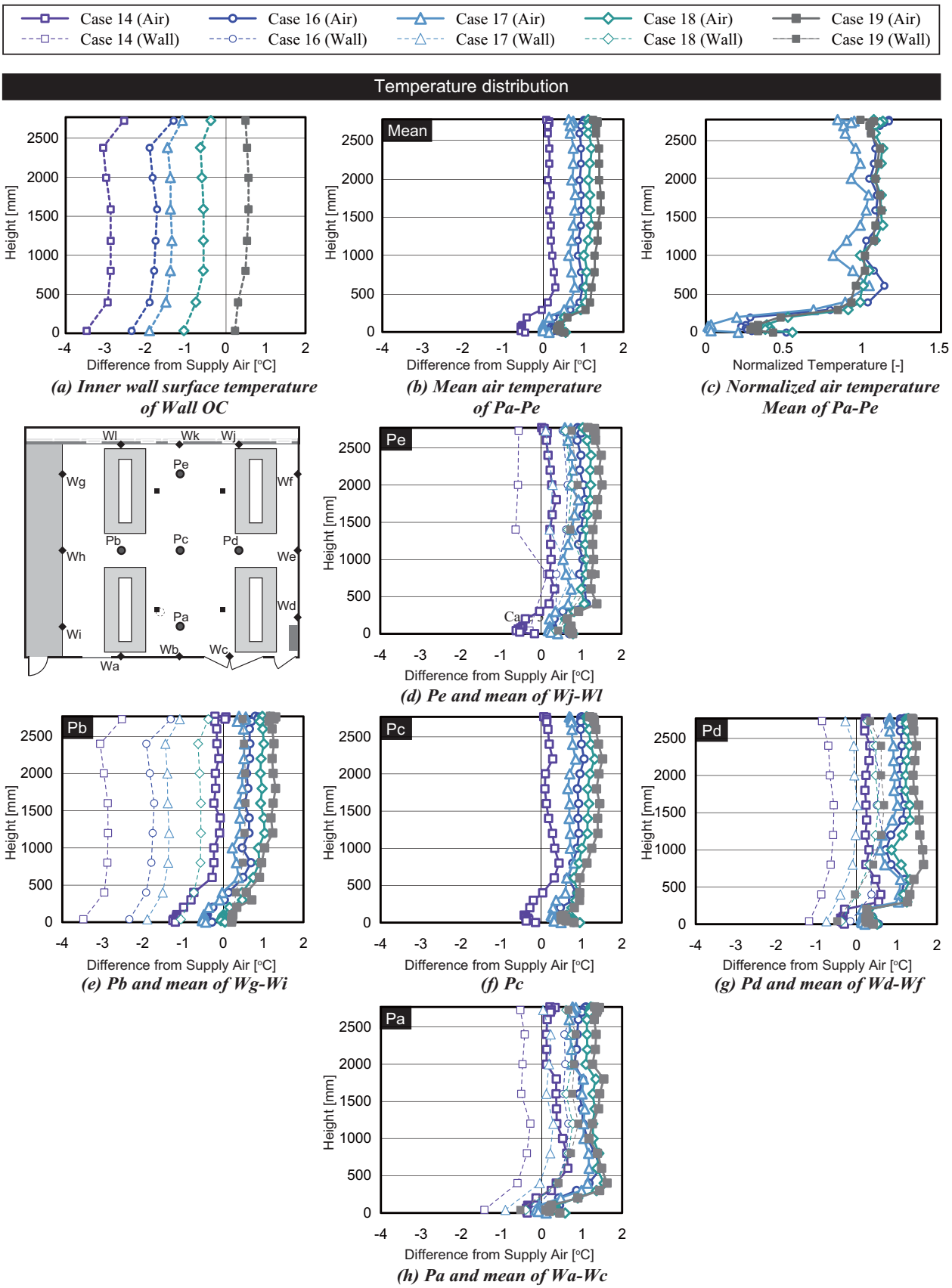


Figure 4.8 Measured contaminant concentration distribution (T_s = 15 °C, with cold wall)

The contaminant concentration profiles of each measurement point (Pa-Pe) and the mean contaminant concentration profile are shown in **Figure 4.8**. Case 3 and Case 4 were conducted under similar conditions (**Table 2**, **Figure 4.5** and **Figure 4.6**), and the results of Case 4 are presented for reference to show the validity of the measured results. In this experiment, the contaminant interface layer tended to be located higher, as $T_{Wall\ OC}$ was lowered (Pa, Pc, Pd). The contaminant interface is known to be formed over the neutral height where the supply airflow rate and the total upward airflow rate are equal (Sandberg and Blomqvist (1989)[4-8] and Nielsen (1993)[4-9]). Hence, if the downward airflow increased, the neutral height would go up. However, the contaminant concentration in the lower part also increased, because the larger the downward airflow generated, the more contaminant air in the upper part would be transferred to the lower part. Furthermore, the contaminant interface became indistinct, owing to the weak stratification. Case 1 was conducted under the lowest T_{oc} among the T_s = 15 °C conditions, and the contaminant concentration of the lower part was nearly equal to the exhaust air at Pa and Pb. The vertical contaminant concentrations were distributed differently depending on the location of the measurement point. Pa was the farthest measurement point from the supply inlet and the contaminant concentration interface formed higher and more distinctly there than at other points, except for Case 1. Pb was the point nearest to the Wall OC, hence the contaminant concentration at Pb was most influenced by Wall OC. The contaminant concentration near the floor rose as Wall OC became cooler. Pc was located at the center of the room and was also affected by the downward convection airflow of Wall OC. Pd was at the farthest point from Wall OC and the downward airflow along Wall OC had relatively less of an effect on the contaminant concentration at Pd. Since Pe was located close to the supply inlet, the air near the floor was as fresh as the supply air.

The measured temperature distributions for cases in which T_s = 20 °C with the cold wall (Cases 14–19) are shown in **Figure 4.9**. The measured results generally showed a similar trend as the cases in which T_s = 15 °C (**Figure 4.7**). However, the temperature difference between the inner wall surface and room air was larger than the cases with T_s = 15 °C, because the supply air temperature was high and it was considerably higher than the ambient temperature (outside the experimental chamber). The surface temperature at Wa-Wc and Wj-Wl was also lower than the room air, while it was close the room air temperature when T_s was 15 °C. DV could be applied properly only when the supply air temperature (T_s) is lower than the room air temperature; however, the air temperature near the floor was lower than T_s in Case 14. The normalized air temperature near the floor was nearly 0 in Case 16 and it was lower than 0 in Case 14 (**Figure 4.9 (c)**). The air temperature is nearly constant except for the lower part of the room.

The measured contaminant concentration distributions for cases in which T_s = 20 °C are presented in **Figure 4.10**. In this case, the contaminant concentration in the lower part of the room was as high as that of the exhaust air at all measurement points. Compared to the cases with T_s = 15 °C, the gap between T_{oc} and T_s was further widened, and the heat loss through other envelopes was larger because the supply air temperature was much higher than the outside air temperature. Hence, the stability of stratification became weaker, and the contaminant interface was indistinguishable in many cases, except for Case 19. Even though the contaminant interface was confirmed, because the contaminated air was entrained by the downward airflow of the wall and fell into the lower part of the room, the contaminant concentration near the floor was high. At



(a) Inner wall surface temperature of Wall OC

(b) Mean air temperature of Pa-Pe

(c) Normalized air temperature Mean of Pa-Pe

(d) Pe and mean of Wj-Wl

(e) Pb and mean of Wg-Wi

(f) Pc

(g) Pd and mean of Wd-Wf

(h) Pa and mean of Wa-Wc

Figure 4.9 Measured temperature distribution (T_s = 20 °C, with cold wall)

the measurement point near Wall OC (Pb), the contaminant concentration adjacent to the floor was close to 1, except in Case 19. It was clear that the greater the downward convection flow along the walls, the worse the air quality in the lower part of the room became, especially at Pc. On the other hand, the contaminant concentration in the lower part was as low as that of the supply air, and a contaminant interface was formed in Case 19.

4.3.2 Influence of upward convection flow along the warm wall

Figure 4.11 shows the measured temperature distribution of the cases in which Wall OC was warm (T_s = 15 °C). As the surface of Wall OC became warmer, the air temperature in the room increased. The vertical temperature difference was significantly larger than the cases with cold wall. The temperature gradient was

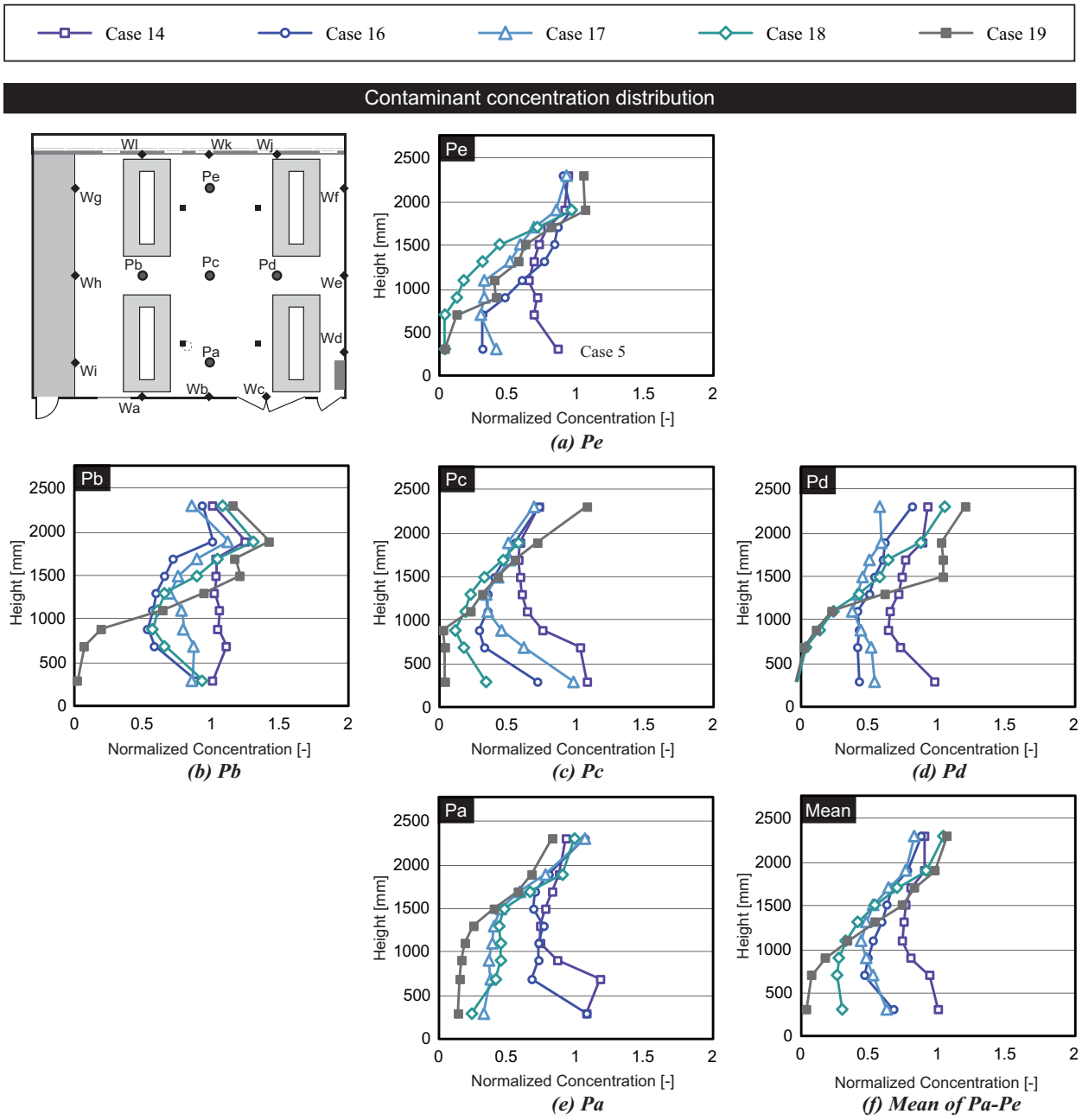
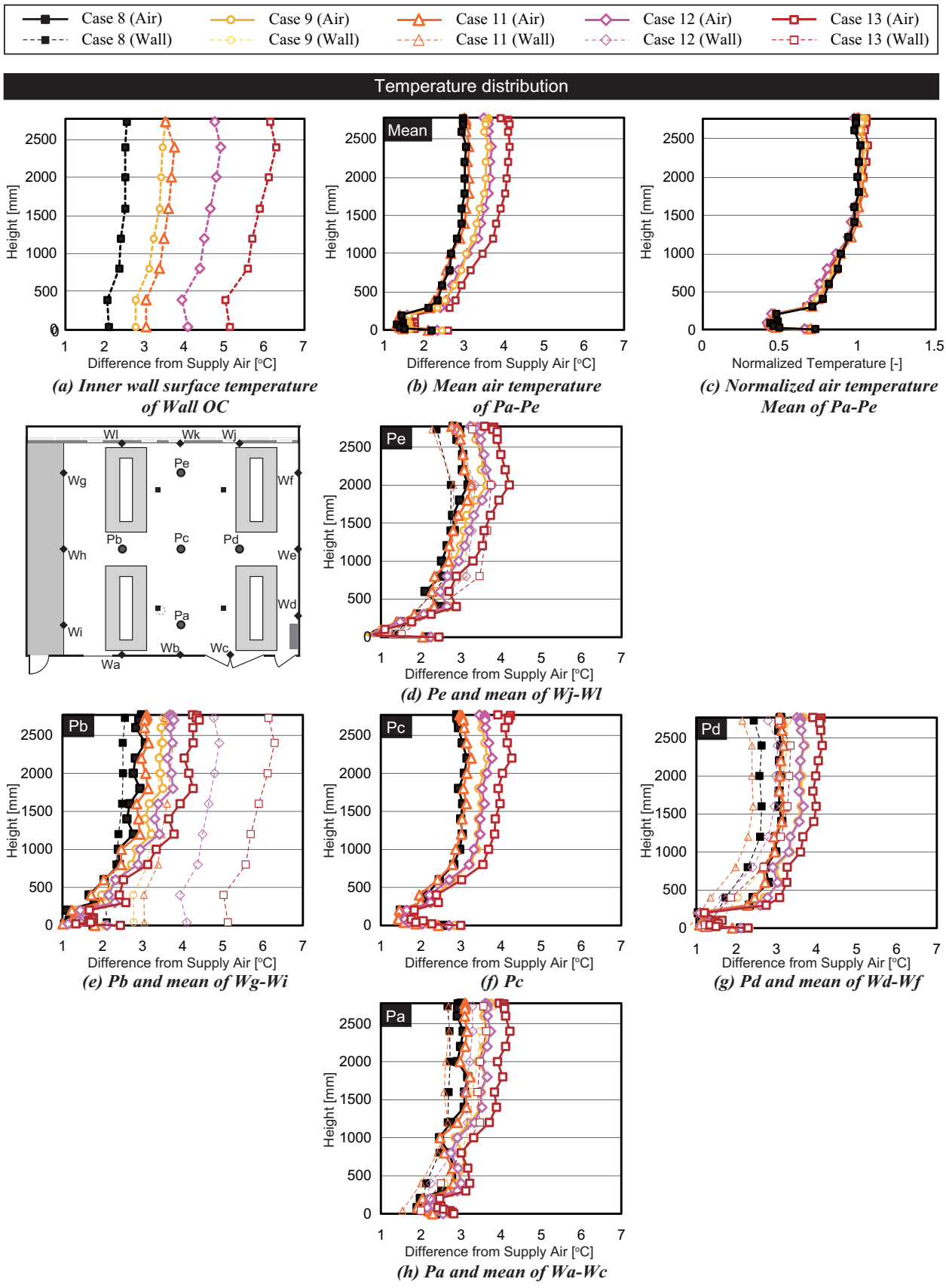


Figure 4.10 Measured contaminant concentration distribution (T_s = 20 °C, with cold wall)



(a) Inner wall surface temperature of Wall OC

(b) Mean air temperature of Pa-Pe

(c) Normalized air temperature Mean of Pa-Pe

(d) Pe and mean of Wj-Wl

(e) Pb and mean of Wg-Wi

(f) Pc

(g) Pd and mean of Wd-Wf

(h) Pa and mean of Wa-Wc

Figure 4.11 Measured temperature distribution (T_s = 15 °C, with warm wall)

also apparently positive. The normalized temperature near the floor was 0.5 in all cases (**Figure 4.11(c)**). Previous studies (Nielsen (1996)[4-10] and Brohus and Ryberg (1999)[4-11]) have shown that the relative temperature at the floor κ in a displacement-ventilated room with a point heat source was roughly 0.3 and κ was 0.6 when the heat sources were sedentary persons. In this experiment, four cylinders, each simulating lying person (line heat sources) and the black lamps (point heat sources) were used. As a result, κ was approximately 0.5 if there was a positive concentration gradient. The air temperature increased in the lower part of the room; however, the vertical temperature distribution in the upper part of the room was nearly consistent. The inner wall surface temperature of Wa-Wc was close to the room air temperature, because the wall Wa-Wc was more insulated rather than other walls and there was a supply air chamber behind the wall. Since the Wall OC was heated, the wall surface temperature at Wg-Wi was higher than the measured results at Pb. However, the wall temperature at Wa-Wf tended to be lower than the room air, because of the low

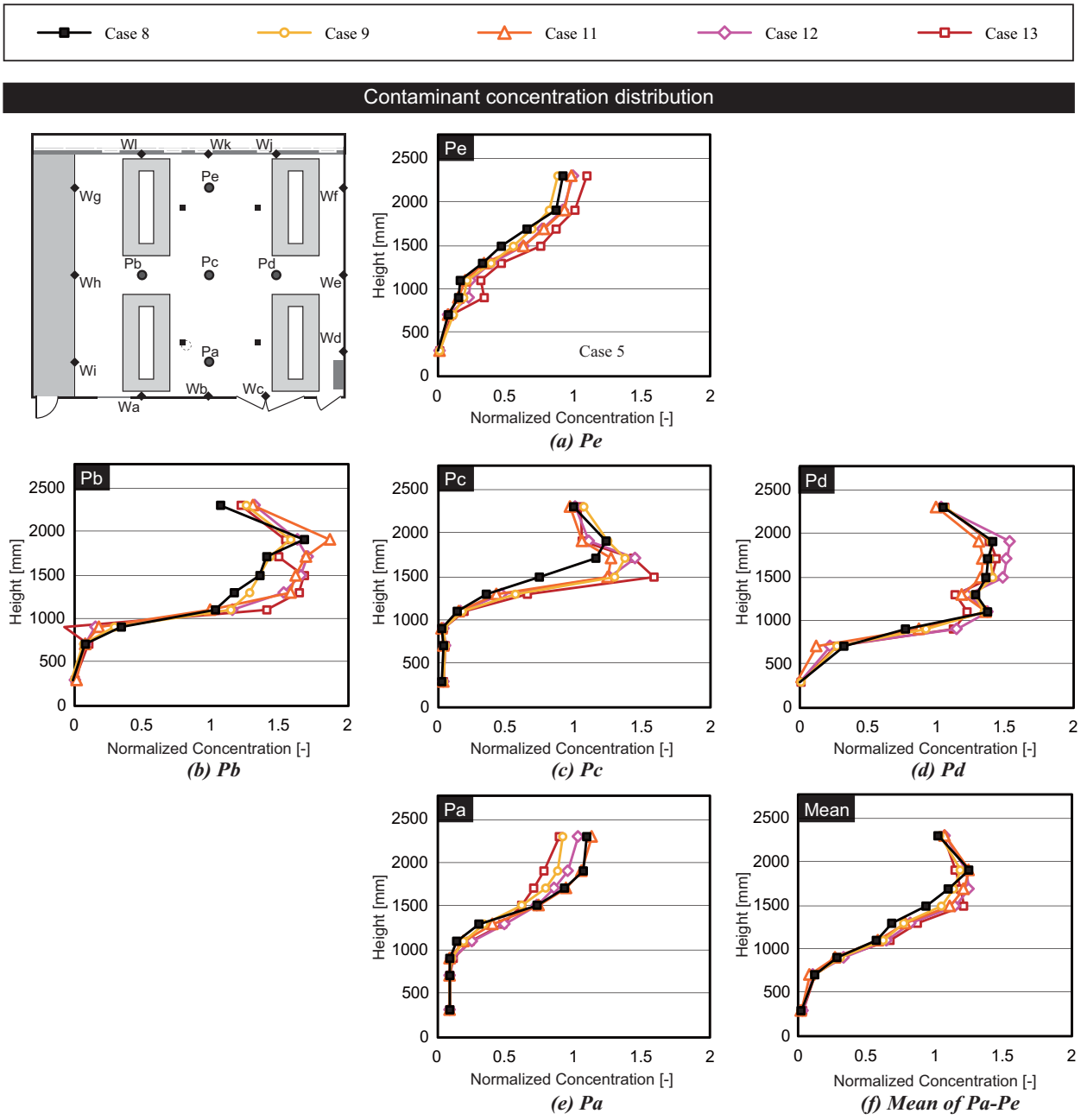


Figure 4.12 Measured contaminant concentration distribution (T_s = 15 °C, with warm wall)

ambient temperature.

The measured vertical contaminant concentrations are presented in **Figure 4.12**. As the surface temperature of the Wall OC increased, the height of the contaminant interface lowered slightly because the plume rate in the room increased. However, there was no appreciable difference between the cases compared with the results when the wall was cold. Because the heat gain in the room was large, the stratification was stable and the contaminant interface was distinctly formed. The upward airflow along the wall went up while entraining the air around the wall like other plumes, and it did not affect the concentration in the lower part. However, it influenced the contaminant concentration distribution in the upper part of the room. In the displacementventilated room, the contaminated air is locked up when there are other plumes with a higher temperature than the plume from the contaminant source (Kosonen et al. (2017)[4-1)], Gao et al. (2012)[4-12)]). Hence, if the upward convection flow along the wall is stronger than the contaminated plume, the plume would be locked up at a height where the room air and the plume air temperatures are equal. Contaminant stagnation was occurred near Wall OC (Pb, Pc), especially in Case 13, which had the highest Wall OC surface temperature.

4.4 Influence of downward convective airflow along the wall on the contaminant concentration in the lower part of the room

The simplifed model for predicting vertical contaminant concentration in a room with DV (**Figure 4.12**, Section 2.2.1) is validated in this section. In this experiment, Q_p is the sum of the plume rates from the lying cylinders and black lamps. Because the black lamp was considered a point heat source.

A comparison of the measured and predicted C_d is presented in **Figure 4.13 (a)**. Additionally, the relationship between the $T_{oc} - T_s$ and C_d for each case is also shown in **Figure 4.13 (b)** for a reference. As the OC cooled, the C_d increased, drastically so in Cases 14 and 15. The measured $C_{d\text{-}n}$ indicates the average of the measured contaminant concentration under the neutral height in all measurement points. The convection heat generation by the black lamp was assumed to be half of the total heat generation. The interval of vertical direction (Δy) to calculate the vertical convection airflow along a vertical surface (Equation) was set to 10 cm, and the measured wall surface temperature and air temperature measured at the nearest measurement point corresponding to each wall (W1 and Pa, W2 and Pd, W3 and Pe, and Wall OC and Pb) were used for ΔT. When the measured $C_{d\text{-}n}$ was between 0 and 0.4, the calculated and measured C_d were close, but the

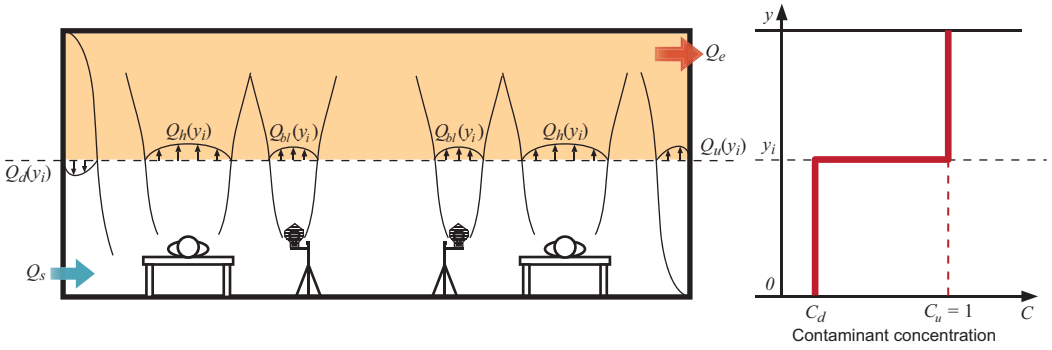
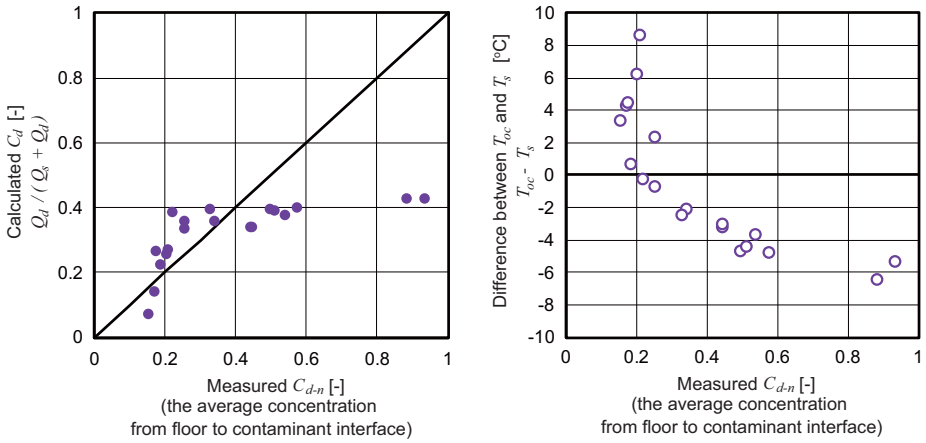


Figure 4.12 Simplifed model for vertical contaminant concentration distribution

calculated C_d tended to be larger. Because the measurement points from the walls were not close enough to the wall, the temperature difference between the wall and the air might be overestimated and the predicted convection airflow rate could be greater than its actual volume. To validate this simple method for predicting C_d, more cases should be examined. On the other hand, when the measured $C_{d\text{-}n}$ was larger than 0.4, the calculated C_d was smaller than the measured result. As the measured $C_{d\text{-}n}$ increased, this gap widened, because the concentration distribution was close to the mixing ventilation. If the heat loss in the room is substantial, the temperature and the contaminants stratification weaken, and it causes poor air quality in the lower part of the room. In these cases, the predicted C_d does not correspond with the measured value, because the equation in this model only takes account of the influence of the downward airflow.



(a) Comparison of measured and calculated C_d (b) Measured C_d and T_{oc} - T_s

Figure 4.13 Comparison of measured and calculated C_d

4.5 Heat loss and the contaminant concentration in the lower part of the room

Figure 4.14 presents the relationship between the proportion of heat loss to total heat generation and the predicted downward airflow rate along the walls at neutral height $Q_d(y_i)$ for each case. The neutral height (the height of contaminant interface) was calculated by Eq. (1). As heat loss through the wall increased, the inner wall surface became cooler and more downward flow was generated along the wall. Hence, the downward flow rate along the wall is relative to heat loss through the wall. However, as it was mentioned in Section (2.4), the predicted $Q_d(y_i)$ tends to be larger than the measured value. **Figure 4.14** shows that downward airflow exists even in the case with no heat loss. Hence, the relationship between heat loss and contaminant concentration was examined (**Figure 4.15**), because heat loss can be calculated accurately. **Figure 4.15 (a)** shows the relationship between the heat loss through the Wall OC and the contaminant concentration in the lower part of the room ($C_{ave\text{-}1.1m}$). $C_{ave\text{-}1.1m}$ is the average contaminant concentration to a height of 1.1 m, which represents the personal exposure of a sedentary person. The case numbers are also presented in the figure. As heat loss through the wall increased, $C_{ave\text{-}1.1m}$ became proportionally higher; further heat loss, the gentle slope changes into a steep incline and $C_{ave\text{-}1.1m}$ becomes close to the concentration of the exhaust air. The cases on the sharp incline matched the cases in which the calculated results were smaller than the measured values in Section (2.4). This supports that the contaminant concentration was affected by the weak stratification in

these cases, and it could not be regarded as ideally displacement-ventilated. The relationship between the total heat loss through all envelopes in the room and $C_{ave\text{-}1.1m}$ is presented in **Figure 4.15 (b)**. Although $C_{ave\text{-}1.1m}$ increased with total heat loss, the relationship was not significant compared with the heat loss through Wall OC. This difference occurred because the heat loss and gain through the ceiling and floor were also included in the total heat loss, although they influence the contaminant concentration differently. For example, the $C_{ave\text{-}1.1m}$ in Case 19 appeared low, although the heat loss was relatively large. However, the heat loss through the wall was small, whereas the heat loss through the ceiling or floor was large. On the contrary, the values of $C_{ave\text{-}1.1m}$ in Cases 3 and 4 were high compared to their total heat loss. Although the heat loss through Wall OC was large in these cases, the apparent total heat loss was small because of the heat gain through the ceiling or floor. The heat loss through horizontal surfaces did not have much effect on the contaminant concentration, compared with that of the heat loss through vertical surfaces. In conclusion, C_d increased with the downward airflow rate proportionally when the heat gain in the room is enough to form a positive temperature and concentration gradient. On the other hand, if the heat loss was large and the temperature stratification was weak, C_d increased sharply. However, it is unclear how much heat gain is required for DV. **Figure 4.16** shows the relationship of the C_d and the temperature difference between the exhaust and supply air included in the measured results in Chapter 2 and Section 4.2 for reference. The C_d was low when the temperature difference between exhaust and supply air was greater than 1 °C. To examine the minimal heat gain to form the positive concentration gradient, more cases should be conducted under different room and heat generation conditions.

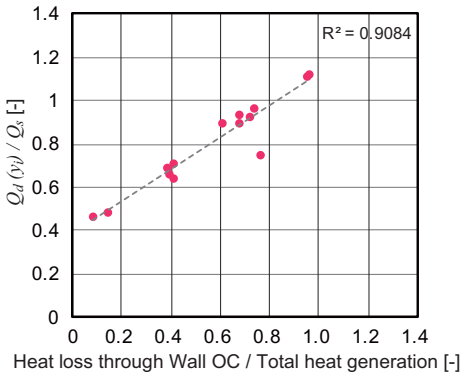
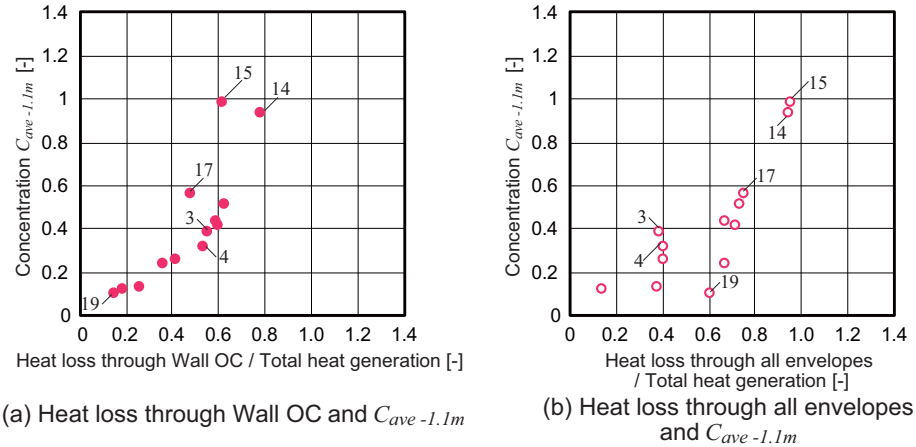


Figure 4.14 Heat loss and downward convection airflow along the walls



(a) Heat loss through Wall OC and $C_{ave\text{-}1.1m}$

(b) Heat loss through all envelopes and $C_{ave\text{-}1.1m}$

Figure 4.15 Heat loss and contaminant concentration in the lower part of the room

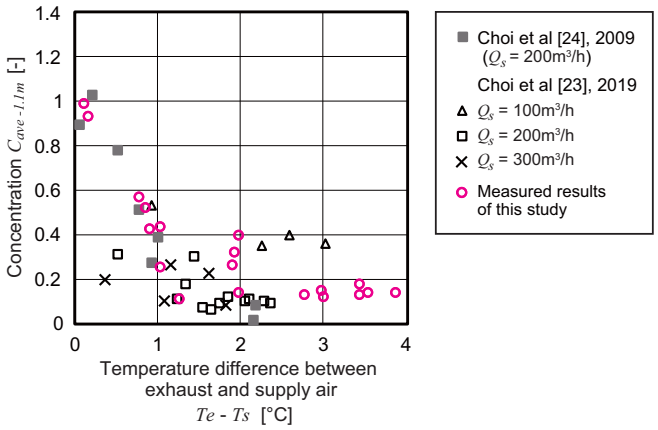


Figure 4.16 Heat loss and contaminant concentration in the lower part of the room

4.6 Model Validation

In this section, zonal model for the temperature and contaminant concentration (**Figure 4.17**) is validated. **Figure 4.18** shows the calculated vertical temperature profiles and the measured results for each measurement point. The Mundt and Nielsen models were also used to predict the vertical temperature profiles, to compare with the results of the zonal model. In the Nielsen model, the neutral height can be obtained by the equation for forecasting the mixing height. Nevertheless, as the calculated neutral height tends to be higher than its actual situation (Kosonen et al. (2017)[4-13], Latrovet et al. (2020)[4-14]), we used Eq. (4) to predict it more precisely. Furthermore, there was no results for the relationship between Archimedes number and the normalized air temperature near the floor when the heat sources are the lying person. Hence, the air temperature near the floor from the Mundt model. As a result, the calculated temperatures near the floor and ceiling were close to the measured results. The Mundt model assumes that the temperature profile near the floor and ceiling is linear, and it is considered to work well with a warm window or ceiling (Kosonen et al. (2017)[4-1]). However, if there are other main heat sources (occupants) in the occupied zone beside a warm window, the temperature distribution is layered (Kosonen et al. (2017)[4-13]). The temperature distribution was stratified in this experiment; thus, the results from the Mundt model did not match well with the measured results. The predicted temperature in the upper part of the room with the Nielsen and zonal models corresponded with the measured temperatures. However, the temperature below the neutral height, as calculated with the zonal model, was low and had little correspondence with the measured result.

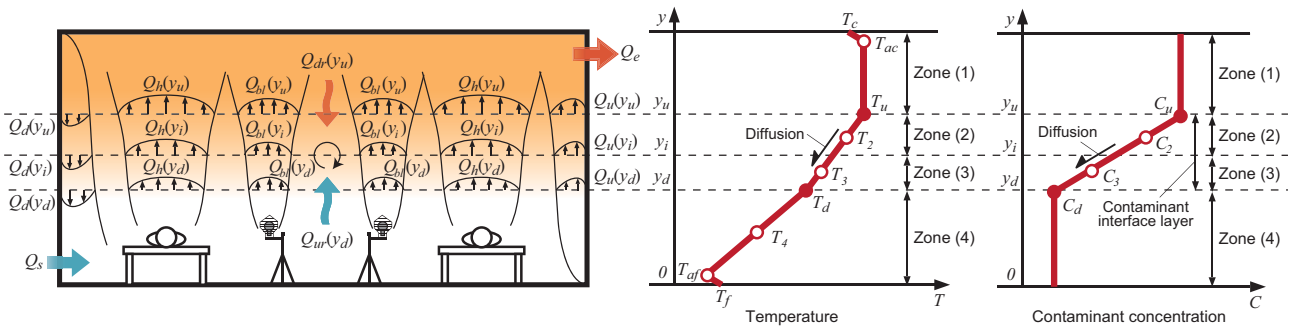


Figure 4.17 Coupled zonal model
(Zonal model for predicting vertical temperature and contaminant concentration profiles)

Although the surface temperature is not uniform and temperature stratification also formed on the vertical surface, the mean temperature of the surface was applied. For this reason, the temperature difference was magnified in the upper part of the room and might cause a decrease in the temperature in the lower part of the room. Another possible reason is the inaccurate prediction of radiation and convection heat transfer because the outer surface temperatures of the envelopes were not observed in this experiment. On the other hand, the results calculated using the Nielsen model with the revised neutral height also tended to be lower in the occupied zone, but were still close to the experimental results. However, the vertical temperature distribution could not be correctly predicted when the inner wall surface temperature was too low to form the temperature stratification, because it was different from the general temperature distribution in the displacement-ventilated room.

The predicted contaminant concentration profiles are shown in **Figure 4.19**. The convection airflow along the wall was calculated using three air temperature values: the measured temperature distribution (calculation (1)), the calculated results with the zonal model (calculation (2)), and the Nielsen model (calculation (3)). The zonal model is for predicting the contaminant distribution in a room with DV. Hence, it cannot be used when the distribution is not stratified. The calculated height of the contaminant interface layer matched well with the actual neutral height, except in the cases with no apparent contaminant interface. In these cases, the calculated contaminant concentration in the lower part tended to be less than the measured results (in Fig. 15, Case 2 and 4). As discussed in Section 4.4 and 4.5, the reason for the high contaminant concentration

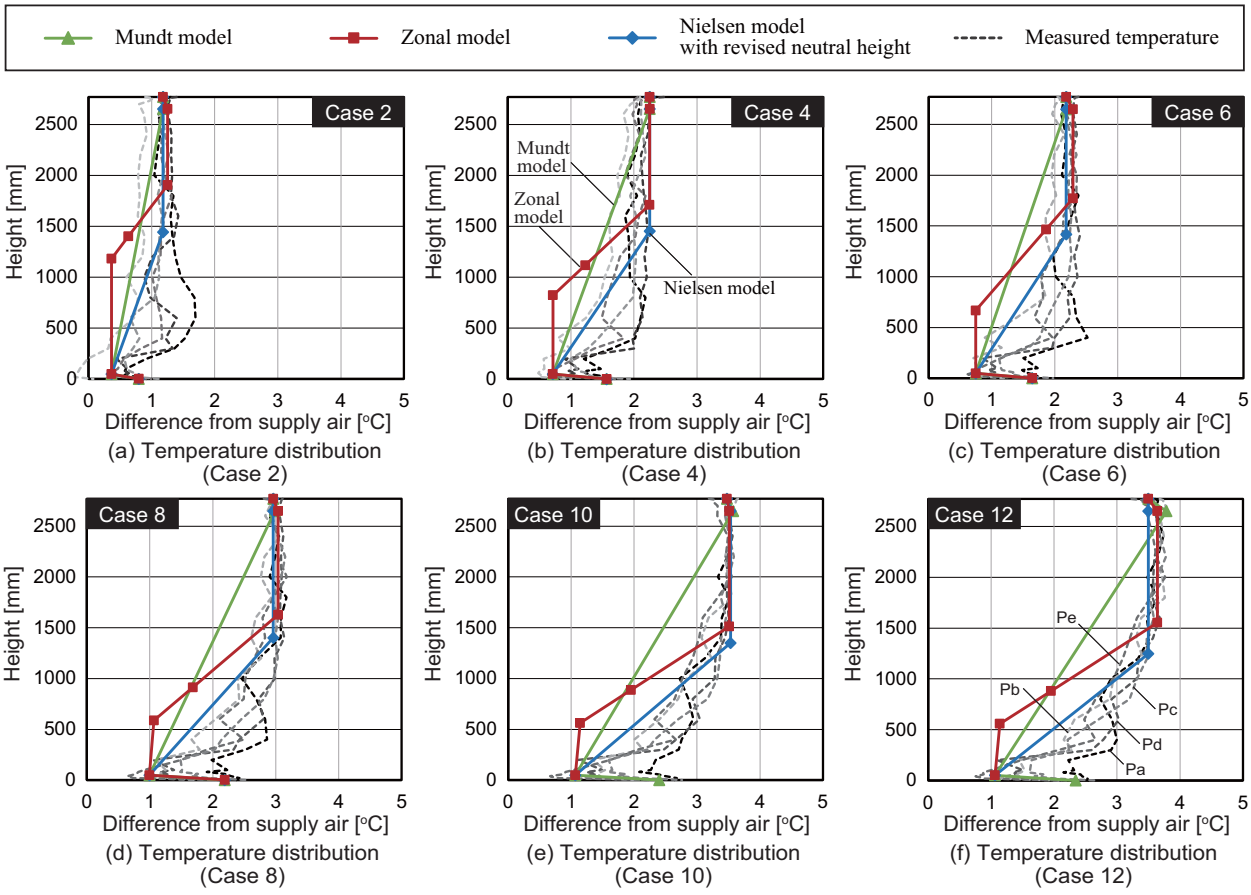


Figure 4.18 Comparison of calculated and measured temperature distributions

in the lower part might be the unstable stratification. The predicted contaminant concentration in the lower part of the room using the results of the two models (calculations (2) and (3)), which were lower than the measured air temperature, were closer to the measured contaminant concentration compared with calculation (1). The contaminant concentration with calculation (1) tended to be higher than the measured concentration. As stated in Section (2.4), this finding indicated that the downward airflow was overestimated in calculation (1), because the measurement point was not close enough to calculate the convection airflow along the wall. The temperatures predicted with the zonal and Nielsen models might be closer to the air temperature near the wall.

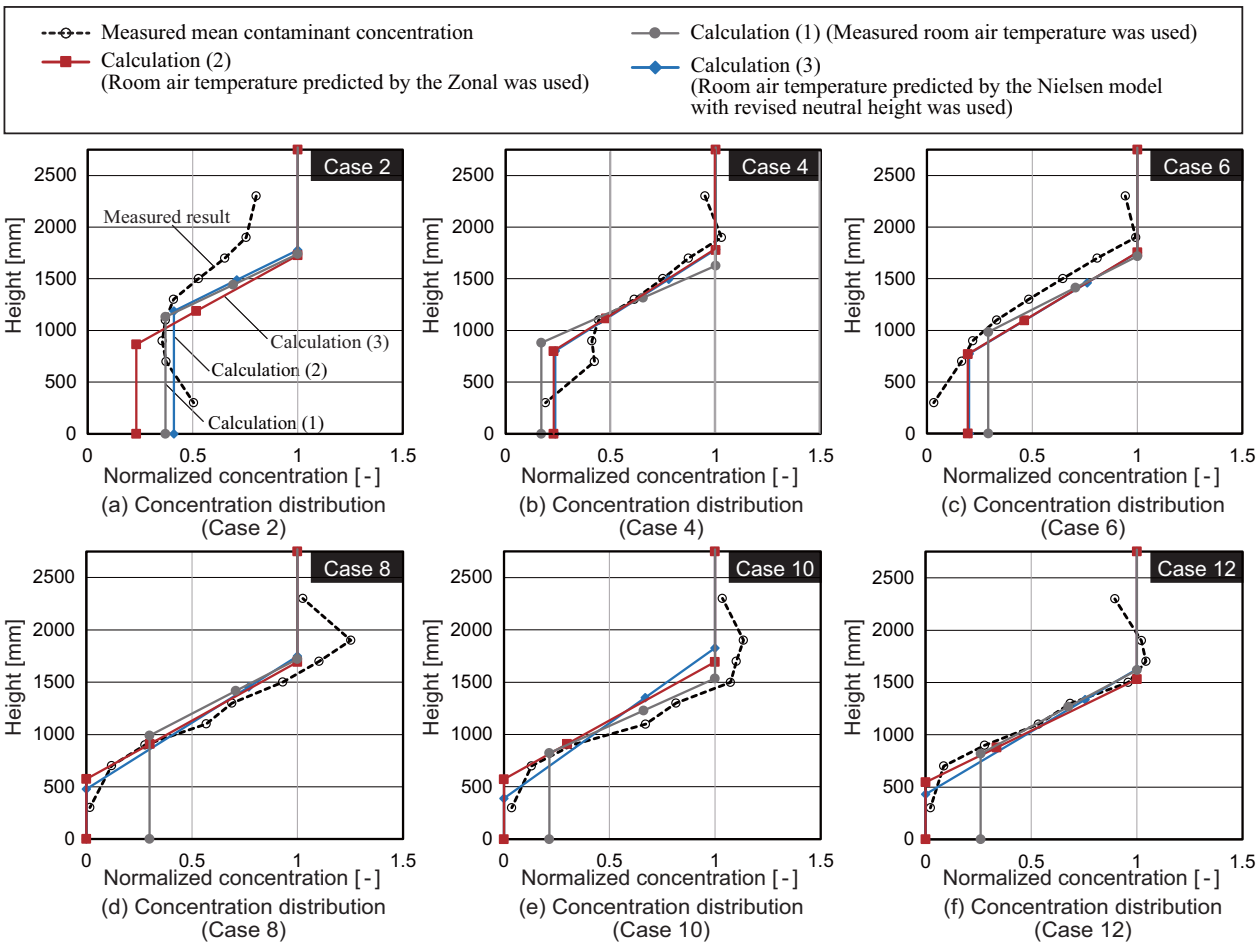


Figure 4.19 Comparison of calculated and measured concentration distributions

4.5 Chapter Discussion and Conclusion

Experiments were conducted to investigate the influence of the downward and upward convection airflows along a vertical surface on the thermal environment and indoor air quality in a hospital ward. The surface temperature of one inner wall was changed to generate different amounts of downward and upward airflow. From the measured results of this experiment, the following conclusions can be drawn..

- When outdoor temperature is low and heat loss through the window is large, it coul be said that the distance from panel to bed has no influence on contaminant concentration profile. Because of downward airflow along window, pollutant air descends to the floor and contaminant stagnation is not formed.
- When there is downward convective airflow along a vertical surface in a room with DV, the contaminated air in the upper zone will be transported back to the occupied zone. As the wall surface temperature lowers, the downward airflow rate and heat loss increase, and the contaminant concentration in the lower part of the room increases. In the cases with significant heat loss through the wall, the positive concentration gradient disappeared, and the concentration distribution was similar to that of mixing ventilation.
- If the upward convection airflow along the wall is stronger than the contaminated plume, the contaminant air will stagnate before reaching the ceiling. However, because the contaminant is locked-up near the wall in the upper area, it will not influence the contaminant concentration in the lower part of the room, though the upward airflow along the wall slightly lowers the height of the contaminant interface layer.
- In the horizontal distribution, the contaminant concentration of areas far from the wall is not considerably influenced by convection airflow along the wall, as long as the air distribution is stratified.
- Although the calculated results tended to be higher than the actual concentration, the C_d could be roughly predicted by this method, only when the temperature and contaminants stratification was not weak.
- To predict the vertical contaminant concentration more precisely, the zonal model can be used. The zonal model agrees well with the measured values of the contaminant concentration if the convection airflow rate can be estimated precisely. Because the air temperature of the upper part tends to be constant, the temperature distribution can be simply predicted by the Nielsen model if the neutral height is properly predicted. The prediction models cannot be used when the air distribution is close to the mixing ventilation, because the models were made under the assumption that the temperature and concentration distributions are stratified.
- The supply airflow rate and the heat generation in the room also influenced the thermal stratification and the contaminant concentration distribution in a room with DV. Additionally, the convection airflow rate along the wall was not only related to the temperature difference between the wall and air, but also the height and width of the wall. Because the experiments in this study were performed in one type of room under one supply airflow rate and heat generation condition, further study involving various conditions of supply airflow rate, heat generation, and area ratio of the wall is needed.

References

4-1) R. Kosonen, A. Melikov, E. Mundt, P. Mustakallio, P. V. Nielsen (2017) : REHVA Guidebook No. 23: Displacement Ventilation, REHVA, Brussels.

4-2) G. Zheng, C. Shen, A. Melikov, X. Li (2019) : Improved performance of displacement ventilation by a pipe-embedded window, *Building and Environment*. 147, pp.1–10.

4-3) M. Xu, T. Yamanaka, H. Kotani (2001) : Vertical profiles of temperature and contaminant concentration in rooms ventilated by displacement with heat loss through room envelopes, *Indoor Air*. 11, pp.111–119.

4-4) Higashimoto. H, Yamanaka. T, Kotani. H (2003) : Profile of temperature and contaminant concentration in displacement ventilated room with cold wall – application of block-model with plume from heat source–, *Journal of Environmental Engineering (Transaction of AIJ)*, No.571, pp.47-53. (In Japanese)

4-5) L. Fang, B. W. Olesen, X. Wu, F. Wang, J. Zhao (2014) : Comparison of mixing and displacement ventilation in a low energy office building during heating season, *Proceedings of Indoor Air 2014, 13th International Conference on Indoor Air Quality and Climate* - University of Hong Kong, Hong Kong.

4-6) Q. Chen, L. Glicksman (2003) : System performance evaluation and design guidelines for displacement ventilation, American Society of Heating, Refrigerating and Air-Conditioning Engineers, Inc., Atlanta, GA.

4-7) T. Suzuki, K. Sagara, T. Yamanaka, H. Kotani, A. Iwamura, T. Yamashita (2008) : Prediction of vertical profile of contaminant concentration in displacement-ventilated sickroom with radiant panel, *Transactions of the Society of Heating, Air-conditioning and Sanitary Engineers of Japan*, No. 141, pp.19-27

4-8) M. Sandberg, C. Blomqvist, Displacement ventilation in office rooms, *ASHRAE Trans*. 95(2) (1989) 1041-1049.3

4-9) P. V. Nielsen, Displacement ventilation: Theory and design, Aalborg University, Aalborg, 1993.

4-10) P. V. Nielsen, Temperature distribution in a displacment-ventilated room, *In Roomvent '96: Proceedings of the 5th International Conference on Air Distribution in room*, Yokohama, Japan (1996) Vol.3 232-330.

4-11) H. Brohus, H. Ryberg, The kappa model - a simple model for the approximate determination of vertical temperature distribution in rooms, Department of Building Technology and Structural Engineering, Aalborg University (1999)

4-12) N. Gao, Q. He, J. Niu, Numerical study of the lock-up phenomenon of human exhaled droplets under a displacement ventilated room, *Building Simulation*. 5 (2012) 51-60

4-13) R. Kosonen, N. Lastovets, P. Mustakallio, G. C. da Graça, N. M. Mateus, M. Rosenqvist (2016) : The effect of typical buoyant flow elements and heat load combinations on room air temperature profile with displacement ventilation, *Building and Environment*. 108, pp.207–219.

4-14) N. Lastovets, R. Kosonen, P. Mustakllio, J. Jokisalo, A. Li (2020) : Modelling of room air temperature profile with displacement ventilation, *Internation Journal of Ventilation*, 19:2, pp.112-126.

Published Papers related to Chapter 4

Conference Papers

*Papers for Archtectural Institute of Japan (AIJ)

1) T. Ihama, T. Yamanaka, T. Kobayashi, N. Choi, M. Wakasa (2019) : Ventilation performance in four-bed sickroom with displacement ventilation (Part 3) Influence of temperature difference between indoor and outdoor on temperature distribution, *Proceedings of Technical Papers of Annual Meeting of AIJ Kinki branch*, pp.65-68. (In Japanese)
2) M. Wakasa, T. Yamanaka, T. Kobayashi, N. Choi, T. Ihama (2019) : Ventilation performance in four-bed sickroom with displacement ventilation (Part 4) Influence of temperature difference between indoor and outdoor on contaminant concentration distribution, *Proceedings of Technical Papers of Annual Meeting of AIJ Kinki branch*, pp.69-72. (In Japanese)
3) T. Ihama, T. Yamanaka, T. Kobayashi, N. Choi, M. Wakasa (2019) : Ventilation performance in four-bed sickroom with displacement ventilation (Part 5) Influence of wall surface temperature on indoor temperature distribution, *Summaries of Technical Papers of Annual Meeting of AIJ*, pp.809-810. (In Japanese)
4) M. Wakasa, T. Yamanaka, T. Kobayashi, N. Choi, T. Ihama (2019) : Ventilation performance in four-bed sickroom with displacement ventilation (Part 6) Influence of wall surface temperature on indoor contaminant concentration distribution, *Summaries of Technical Papers of Annual Meeting of AIJ*, pp.69-72. (In Japanese)

*Paper for The Society of Heating, Air-Conditioning and Sanitary Engineers of Japan (SHASE)

1) M. Wakasa, T. Yamanaka, T. Kobayashi, N. Choi, T. Ihama (2019) : Displacement ventilation for a four-bed hospital ward (Part 1) Influence of cooled and heated walls on temperature distribution, *Proceedings of Technical Papers of Annual Meeting of SHASE Kinki chapter*, A-26. (In Japanese)
2) T. Ihama, T. Yamanaka, T. Kobayashi, N. Choi, M. Wakasa (2019) : Semi-personal air-conditioning system for sickroom by displacement ventilation with radiant panel (Part 2) Influence of cooled and heated walls on contaminant concentration distribution, *Proceedings of Technical Papers of Annual Meeting of SHASE Kinki chapter*, A-27. (In Japanese)
3) T. Ihama, T. Yamanaka, T. Kobayashi, N. Choi, M. Wakasa (2019) : Temperature and contaminant concentration profiles in four-bed sickroom with displacement ventilation (Part 5) Influence of upward airflow along the walls, *Technical papers of annual meeting, the Society of Heating, Air-Conditioning and Sanitary Engineers of Japan*, pp. 429-432
4) M. Wakasa, T. Yamanaka, T. Kobayashi, N. Choi, T. Ihama (2019) : Temperature and contaminant concentration profiles in four-bed sickroom with displacement ventilation (Part 6) Influence of downward airflow along the walls, *Technical papers of annual meeting, the Society of Heating, Air-Conditioning and Sanitary Engineers of Japan,* pp.433-436 (In Japanese).
5) N. Choi, T. Yamanaka, T. Kobayashi, T. Ihama, M. Wakasa (2019) : Temperature and contaminant

concentration profiles in four-bed sickroom with displacement ventilation (Part 7) Prediction of temperature and contaminant concentration profiles with considering upward and downward airflow along the walls, *Technical papers of annual meeting, the Society of Heating, Air-Conditioning and Sanitary Engineers of Japan,* pp. 437-440 (In Japanese).

Original Papers

1) N. Choi, T. Yamanaka, T. Kobayashi (2020) : Influence of vertical airflow along walls on temperature and contaminant concentration distributions in a displacement-ventilated four-bed hospital ward, *Building and Environment*, Volume 183, 107181.

Chapter 5.
Influence of Internal Partition Curtains

5 Influence of Internal Partition Curtains

5.1 Purpose

Inpatients spend most of their day in the hospital ward. Because a patient shares a ward with other patients, it is important to protect their privacy, especially in multiple-bed hospital wards. Since most hospital wards in Japan are multiple-bed wards, the internal partition curtains are installed for privacy. Individual curtains generally stretch from near the floor to the ceiling. Noh et al. (2018)[5-1)] has found that the curtains interfere with air movement, which could reduce the ventilation efficiency of the room with mixing ventilation. Hanada et al. (2014)[5-2)] examined the influence of the partition curtain in a multiple-bed ward with low velocity fabric air diffuser on the ceiling. When the curtains were used, the contaminant concentration outside the curtain where the contaminant source was located was lower than without the curtain.

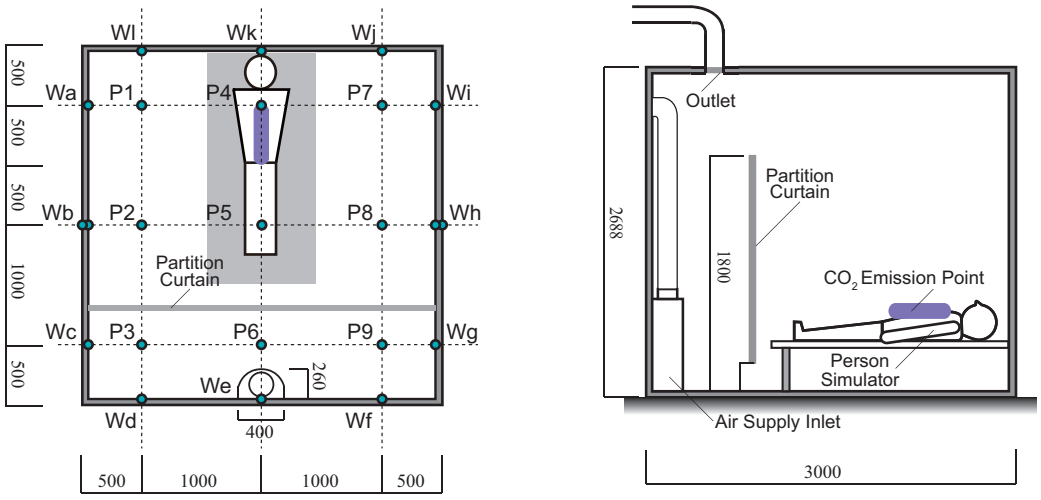
Displacement ventilation (DV) is particularly known to be affected by layout or partitions (Kosonen et al. (2017)[5-3)]), because the supplied air spreads along the floor and the room air is not circulating. In order to take advantage of DV properly, the influence of partition curtains on the ventilation performance of the room with DV should be investigated in advance. Since the airflow in the room with DV is similar to the piston flow, it is expected that the contaminated air can be exhausted more efficiently if the partition curtain is installed appropriately. In this chapter, the impact of internal partition curtains was examined by full-scale experiments to find the best curtain condition for the DV. The temperature and contaminant concentration were measured under the conditions with/without the internal partition curtain.

5.2 Experimental Investigation in a Single-bed Ward

In this section, the influence of the internal partition curtain on the temperature and contaminant concentration distribution of a single-bed ward with DV was examined. Generally, the partition curtain is not required in a single-ward. However, as a primary step for investigating the influence in the multiple-bed ward, the basic behavior of the supplied air and contaminated air in a single-ward with the partition curtain was studied.

5.2.1 Experimental Setup

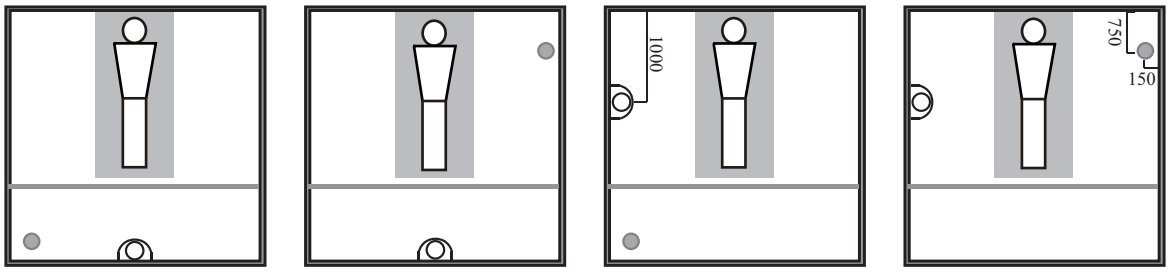
Experiments were performed in a full-scale experimental room (3,000 mm long, 3,000 mm wide, and 2,688 mm high) setup as a single-bed hospital ward with DV (mentioned in **Chapter 3.2.1** and **4.2.1**). Experimental setup is shown in **Figure 5.1**. All envelopes of the experimental room were insulated with a 50 mm thick polystyrene foam and the internal wall surfaces were colored with mat black. Fresh air was supplied from



(a) Plan view of the experimental room and horizontal measurement points

(b) Section view of the experimental room

Figure 5.1 Horizontal and section view of the experimental room



(a) S1, E1 *(b) S1, E2* *(c) S2, E1* *(d) S2, E2*

Figure 5.2 Locations of the inlet and outlet

half-cylinder displacement-type diffuser (D: 400 mm, H: 750 mm, T: 260 mm). The exhaust opening (ϕ = 200 mm) was on the ceiling. A Lying manikin was used as person simulator and heat generation was controlled at 40W. CO_2 was used as tracer gas to simulate the odor from the patient and emitted from the tubed located on the center of the human simulator's chest. CO_2 airflow rate was controlled at 0.5 L/min by mass flow controller. 100% polyester fabric was installed to simulate the partitione curtain. The top (upper end) of the curtain was located at a height of 1,800 mm. The curtain was fixed to the side walls and there is no space between the curtain and wall.

Measurement point of air temperatures were 9 points (P1~P9) in horizontal plane and 22 points in vertical direction, 198 points in total (See Chapter **Chapter 3.2.1**). Wall surface temperatures (Wa~Wl) were measured at 6 points vertically (i.e. 72 points for all). T-type thermocouples (f = 0.32 mm) were used to measure air and surface temperatures. CO_2 concentration was measured using three non-dispersive infrared (NDIR) gas analysers. The temperature was measured every 1 minute. The concentration was measured every 10 seconds for 2 minutes at each measurement point. All gas analysers were calibrated before the measurement. The measured data was acquired after the temperature and contaminant concentration reached a steady state.

Table 5.1 Experimental conditions

Cases	Location of supply inlet	Location of outlet	Supply airflow rate	Bottom height of partition curtain
			Q_s [m^3/h]	h_c [mm]
Case 1	S1	E1	100	250
Case 2	S1	E1	200	125
Case 3	S1	E1	200	250
Case 4	S1	E1	200	400
Case 5	S1	E1	300	250
Case 6	S1	E2	100	250
Case 7	S1	E2	200	250
Case 8	S1	E2	300	250
Case 9	S2	E1	100	250
Case 10	S2	E1	200	250
Case 11	S2	E1	300	250
Case 12	S2	E2	100	250
Case 13	S2	E2	200	250
Case 14	S2	E2	300	250
Reference case[5-4)]	S1	E1	200	without curtain

5.2.2 Experimental Conditions

Table 5.1 shows the experimental conditions. The supply air temperature T_s was 22 °C and the ambient temperature of the experimental room was also maintained at 22 °C. The inlet and outlet were placed on two different locations to examine whether the inlet and outlet being located inside or outside of the curtain affects the indoor environment. **Figure 5.2** presents the locations of the inlet and outlet of the experiment. As the supply airflow rate increases, the height of the contaminant interface gets higher. To investigate the influence of the partition curtain under different interface heights, the supply airflow rate was varied between three values; 100, 200 and 300 m^3/h. The height of the bottom end of the curtain (the length of the curtain) was also altered because it was expected that the airflow rate passing under the curtain would be affected by the space between the floor and curtain. Additionally, the reference case (Iwamura et al. (2007)[5-4)]) from the previous study was adopted to compared with the measured results without curtain.

5.2.3 Experimental results

Influence of the bottom height of the partition curtain

Figure 5.3 shows the measured results of vertical temperature and contaminant concentration profiles under the different bottom height of the curtain. (the inlet location S1, the outlet location E1, and Q_s = 200 m^3/h (Case 2, 3, 4 and reference case)). The measured results inside the curtain means the average value of the results of the measurement points inside the curtain (P1, P2, P7, P8). The results outside the curtain indicates the average of the measured results of measurement point P3, P6 and P9.

There was a positive temperature gradient inside the curtain, while the temperature outside curtain was

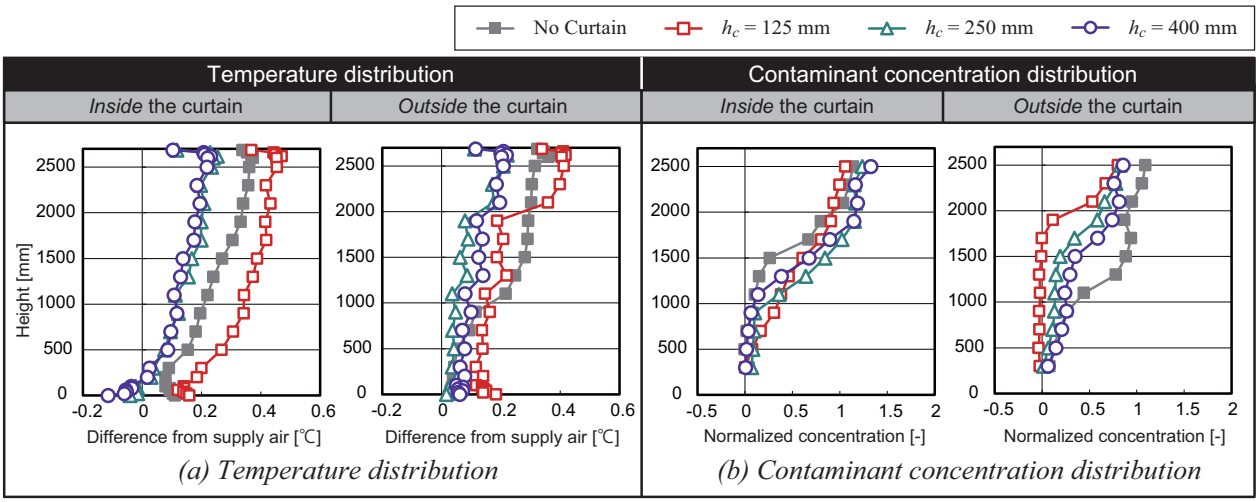


Figure 5.3 Temperature and contaminant concentration distributions inside and outside the curtain (Influence of the bottom height of the curtain)

nearly consistent compared to the case without curtain. Outside the curtain, the temperature increase occured in the upper part of the curtain. In Case 2 (h_c = 250 mm), the air temperature inside the curtain was higher than other cases, possibly because the supplied airflow rate into the curtain was small.

The contaminant interface layer of the cases with partition curtain forms lower than without curtain. Some of supplied air could not go into the curtain and exhausted directly. The bottom height of the curtain gets lower, the height of the contaminant interface outside the curtain becomes higher, while the interface inside the curtain gets lower. As the bottom height goes up, the contaminant concentration profile becomes close to the results of reference case. When the space between the floor and curtain is small, the supplied air would be accumulated outside the curtain. In case with the lowest bottom height of the curtain (Case 2, h_c = 250 mm), the contaminant interface inside the curtain was not apparent. The supplied air piled up outside the curtain might flow into the curtain passing the upper space of the curtain.

Influence of the locations of the inlet and outlet

Figure 5.4 presents the results of vertical temperature and contaminant concentration profiles under the different inlet and outlet locations. (Q_s = 100, 200 and 300 m^3/h, h_c = 250 mm).

In all cases, the air temperature was stratified inside the curtain, while the temperature outside the curtain was nearly constant except for the upper part of the room. When Q_s = 100 m^3/h, the air temperature of the case with S2, El was higher than other inlet and outlet locations (**Figure 5.4 (a)**). The case with S2, E2 had the highest air temperature profiles when Q_s = 200 m^3/h (**Figure 5.4 (c)**). This is probably because the heat loss and gain through the envelopes were different in each case. The vertical air temperature differences in all cases were not much different. Hence, there seemed to be less impact of the locations of inlet and outlet on the vertical temperature in the displacement-ventilated single-bed ward with partition curtain.

When both inlet and outlet were located outside the curtain, the height of the contamiant interface layer was relatively lower than other cases. It indicates that the supplied airflow rate into the curtain might be small in this case. The interface layer tended to form higher if inlet was placed inside the curtain.

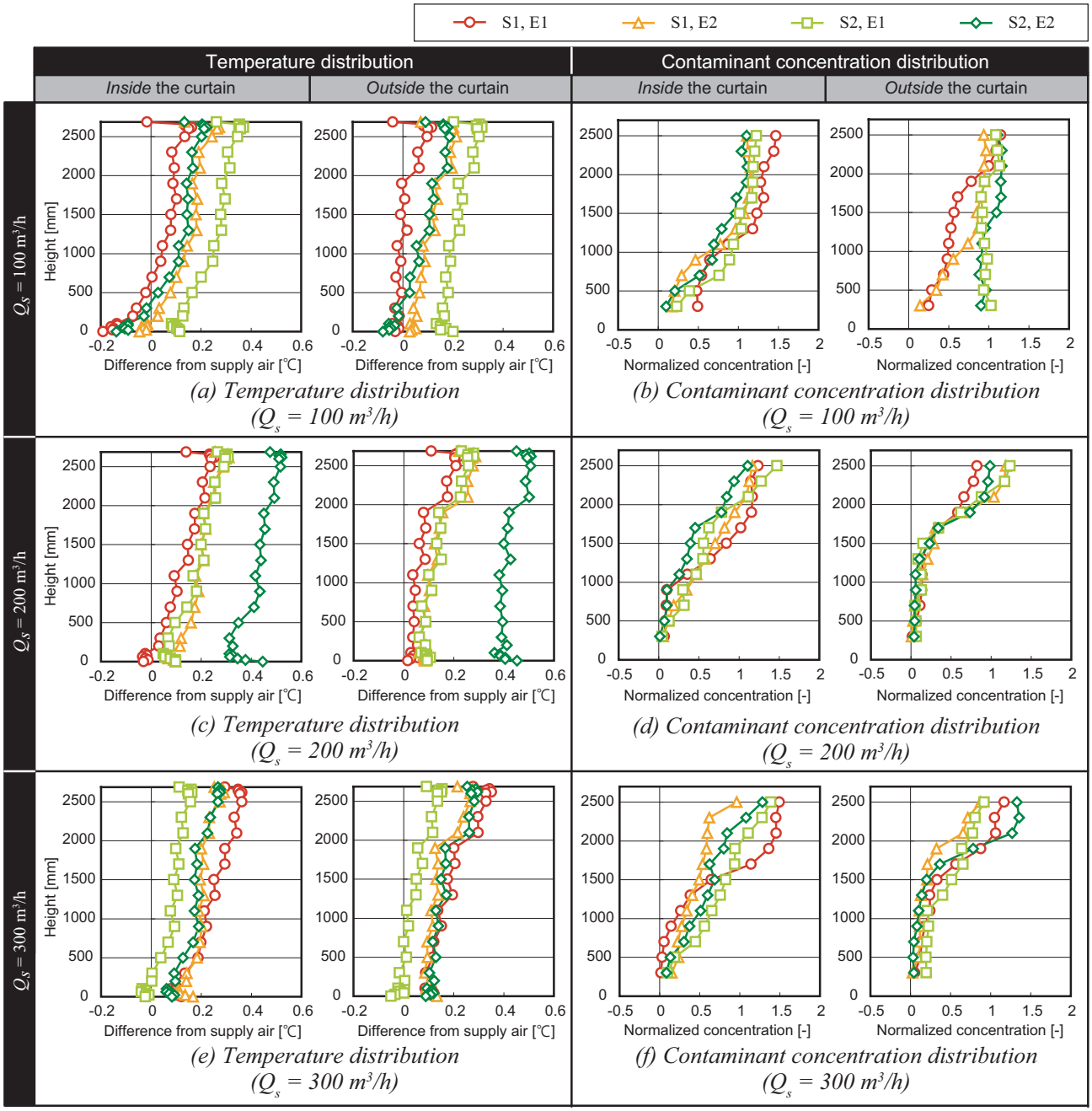


Figure 5.4 Temperature and contaminant concentration distributions inside and outside the curtain (Influence of the location of the inlet and outlet)

Influence of the supply airflow rate

The measured temperature and contaminant concentration profiles when supply airflow rate was a parameter are shown in **Figure 5.5**. If supply airflow rate increases, the temperature stratification becomes weak in a general displacement-ventilated room. However, the temperature gradient did not change in some cases, even though the supply airflow rates were altered because of the heat loss and gain through the envelopes.

The contaminant interface obviously went up as supply airflow rate increased, especially inside the curtain. When the supply inlet was located inside the curtain, the contaminant concentration outside the curtain was not stratified and was close to the mixing ventilation in the case of Q_s = 100 m^3/h. The downward airflow might be generated along the wall in the cases with high contaminant concentration in the lower part of the room.

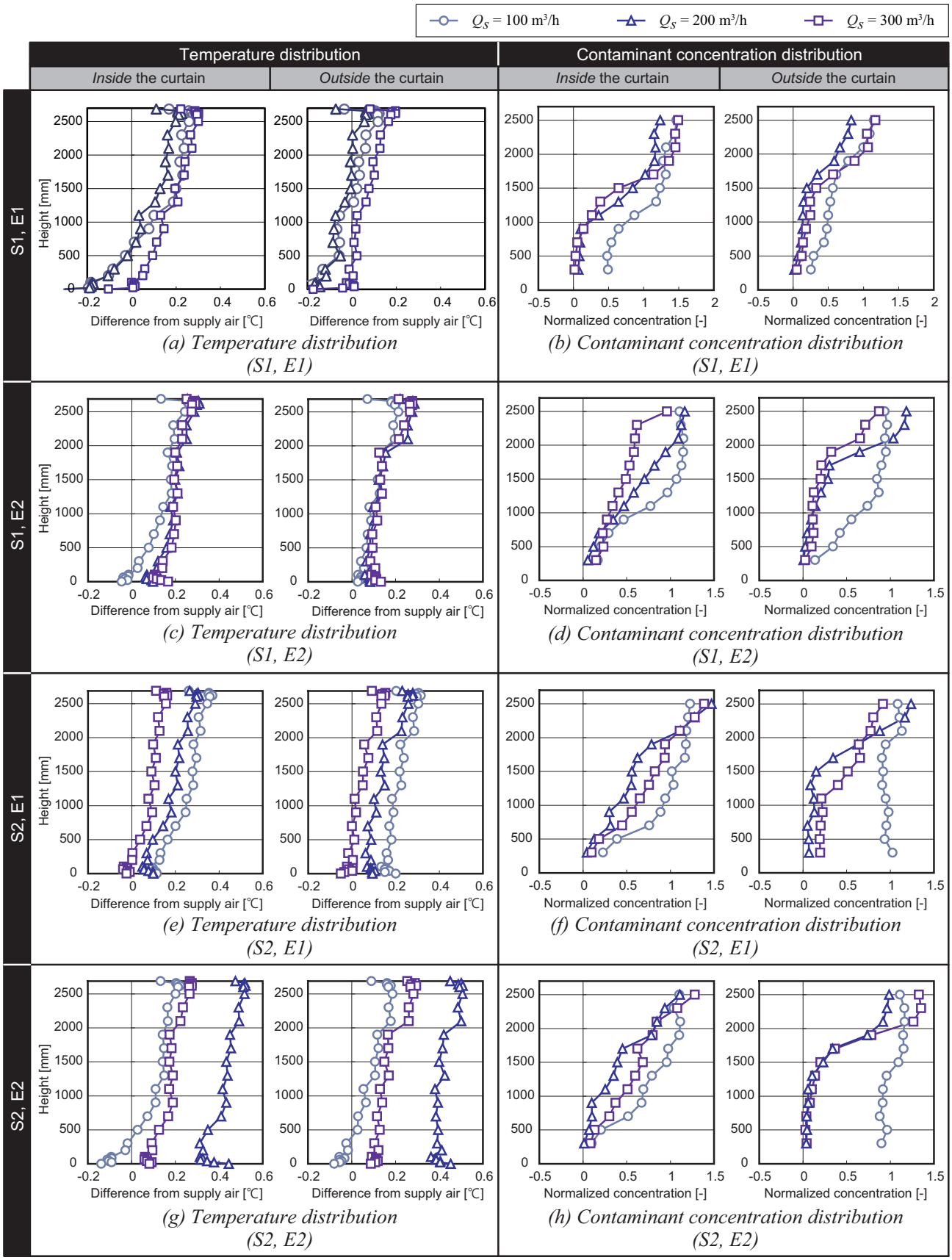


Figure 5.5 Temperature and contaminant concentration distributions inside and outside the curtain (Influence of the supply airflow rate)

5.3 Experimental Investigation in a Four-bed Ward

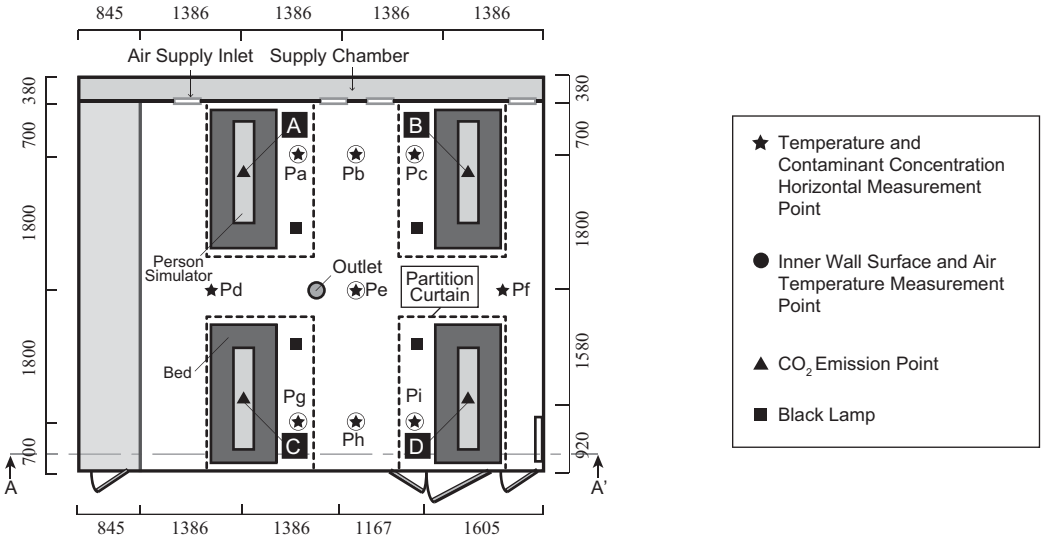
5.3.1 Experimental Setup

Experiments were conducted in a full-scale experimental chamber set up as a four-bed hospital ward, with a length of 5,545mm, a width of 5,450mm, and a height of 2,770mm (mentioned in **Chapter 4.3**). **Figure 5.6 and 5.7** show the experimental arrangement and measured points. Supply air was provided through four supply inlets on the wall. The outlet was positioned on the ceiling. The total extract airflow rate was measured by airflow meter with a capture hood and it was approximately 395 m^3/h. The supplied airflow velocity was about 0.16 m/s at the inlet surface. Four person simulators (galvanized iron cylinder wrapped with polyester fabric, ϕ = 300 mm, H = 1500 mm) were placed on the beds, and four black lamps were located near each bed to simulate the heat sources in the hospital wards such as television. The heat generations of each person simulator and black lamp were controlled at approximately 40W and 60W (400W in total). Inner partition curtains manufactured for hospital wards (100% polyetser) were installed for each bed. The upper part of the curtain was mesh. CO_2 was used to simulate the unpleasant odor in the hospital ward and was emitted from a tube sticking in a sponge on the person simulator. CO_2 flow rate was maintained at 1 L/min, and it was emitted from one person simulator (A, B, C, D).

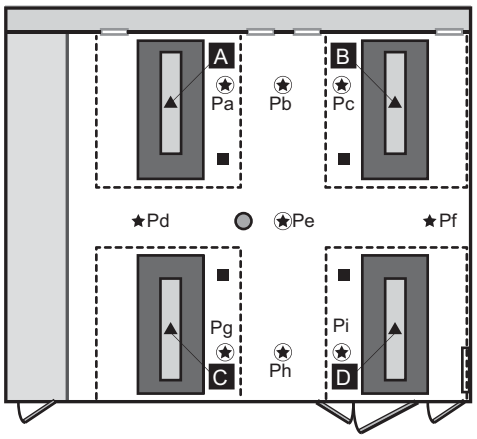
Measurement points Pa, Pc, Pg, Pi were located inside the curtain. Indoor environment outside the curtain (passageway) was also measured from Pb, Pd, Pe, Pf and Ph. Three different curtain settings (S0, S1, S2, (**Figure 5.6 (a), (b), (c)**)). Vertical temperature distributions were measured from seven locations (Pa-Pc, Pe, Pg-Pi) at 24 heights, including the floor and ceiling surface. Temperature distribution was measured with T-type thermocouples (f = 0.32 mm, ASTM E230 Standard class, Tolerance : ± 1.0 °C or ± 0.75 %). CO_2 concentration was measured using nondispersive infrared (NDIR) sensors and all sensors were calibrated. Vertical CO_2 concentration distributions were measured from nine locations (Pa-Pi) at nine heights and concentrations of the supply and exhaust air were also measured. The data for analysing was taken after the temperature and contaminant concentration reached a steady state. Temperature and concentration were measured every one minute. The temperature results were averaged for twenty minutes and the concentration results were averaged for ten minutes.



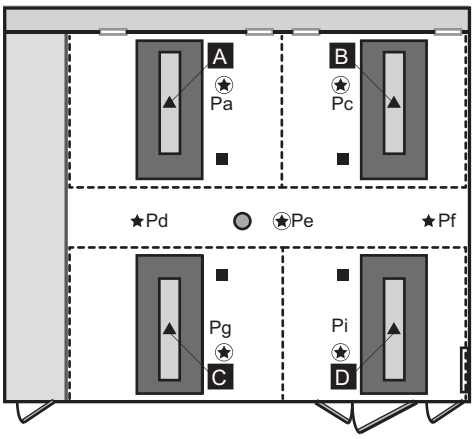
Figure 5.6 Experimental arrangement



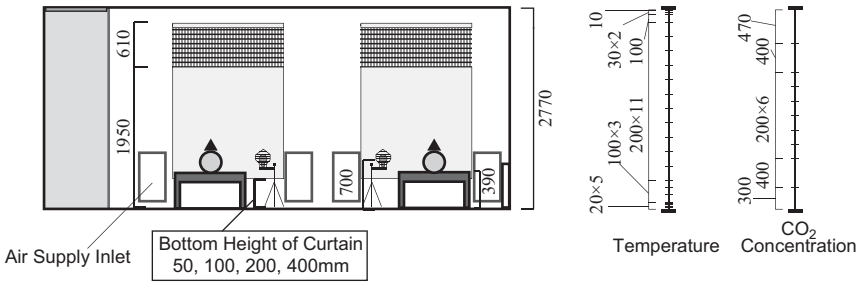
(a) Horizontal view and measurement points (Curtain setting S0)



(b) Horizontal view and measurement points (Curtain setting S1)



(c) Horizontal view and measurement points (Curtain setting S2)



(d) Section view and vertical measurement points

Figure 5.7 Horizontal and section view of the experimental room, measurement points and curtain setting

Table 5.2 Experimental conditions

Cases	Curtain Setting	Bottom height of curtain *hc* [mm]	CO_2 emission point				Temperature difference between supply and exhaust air *Te* - *Ts* [°C]
A, B, C, D	No curtain		A	B	C	D	4.29
S0-50-A, B, C, D	S0	50	A	B	C	D	4.63
S0-100-A, C		100	A		C		4.36
S0-200-A, B, C, D		200	A	B	C	D	4.49
S0-400-A, B, C, D		400	A	B	C	D	4.48
S1-50-A, B, C, D	S1	50	A	B	C	D	5.19
S1-100-A, C		100	A			D	4.33
S1-200-A, C		200	A			D	4.34
S1-400-A, B, C, D		400	A	B	C	D	4.40
S2-50-A, B, C, D	S2	50	A	B	C	D	4.04
S2-100-A, C		100	A			D	4.12
S2-200-A, C		200	A			D	4.40
S2-400-A, B, C, D		400	A	B	C	D	4.25

5.3.2 Experimental Condition

Experimental conditions were presented in **Table 5.2**. Since it was expected that whether the supply inlet is located inside or outside curtain would affect the contaminant concentration, three different arrangements of partition curtains and supply inlets were adopted: no inlet inside the curtain (S0, All inlets were outside the curtain), one inlet inside curtain A and B (S1, Two inlets were outside the curtain), and two inlets inside curtain A and B (S2, No inlet was outside the curtain). In **Section 5.2.3**, it was probed that the supply airflow rate arrived inside the curtain changed depending on the length between the floor and bottom end of the curtain. Hence, the bottom height of the partition curtain was also altered: 50, 100, 200, and 400 mm. Tracer gas (CO_2) was emitted from one of the bed A, B, C and D. In some cases, CO_2 was only emitted from bed A or C because it was assumed that the air distributions in curtain A and B, as well as curtain C and D, were not much different.

Although the experimental room was insulated, there was heat loss and gain through the walls, ceiling and floor because of the temperature difference between the experimental room and ambient air. In order to minimize the difference in heat loss or gain through envelopes in all cases, the supply air temeprature was altered depending on the outdoor temperature. The supply air temperature was set 2 °C lower than daily mean outdoor temperature, which was forecasted by the Japan Weather Association. The temperature differences between the supply and exhaust air in all cases are presented in **Table 5.2**. If there was no heat loss or gain through envelopes, the temperature difference would have been 3 °C. However, the values of temperature difference were larger than 3 °C in all cases, which means there was heat gain through envelopes. The great difference of heat gain was not confirmed between each case, except for Case S1-50. The heat gain in Case S1-50 was larger than other cases.

5.3.3 Temperature Distribution

Figure 5.7 shows the comparison of the measured vertical temperature profiles at Pa, Pe and Pg when the bottom height of the curtain h_c was 50 mm and 400 mm. Pa was the measurement location inside the curtain, and it was close to the supply inlet. Pg was also positioned inside the curtain, but it was far from the inlet. Pe was placed outside the curtain, and it was located in the center of the floor. The air temperature near the floor at Pg tended to be higher than Pa and Pe. As it gets far from the inlet, the air temperature near the floor becomes higher because of the heat transmission from the floor. Especially in Case of the curtain setting S2 and h_c = 50 mm, the temperature difference between Pg and other two points was large. In this case, it might take longer time the supplied air to reach inside the curtain C and D, because all of inlets were located inside the curtain A and B, and the space between the curtain and floor was smaller than other cases.

Figure 5.8 presents the vertical normalized temperature profiles under the different curtain settings. The temperature was normalized because the temperature differences between the supply and extract were different in each case. The temperature profiles without curtains were also shown to examine the influence of the partition curtain on the temperature distribution. When the curtain was set as S2 and h_c = 50 mm, the air temperature near the inlet (Pa) was lower than the case without curtain, while the temperature at Pg was higher. However, if the length between the bottom end of the curtain and floor was large (h_c = 400 mm), the partition curtain did not have a considerable impact on the vertical temperature profile in the room. Enough space between the curtain and floorwould be desirable in a ward with DV. A normalized air temperature near floor (κ) was approximately 0.2 at Pa, 0.5 at Pe and 0.6 at Pg. Because the air temperature profiles in

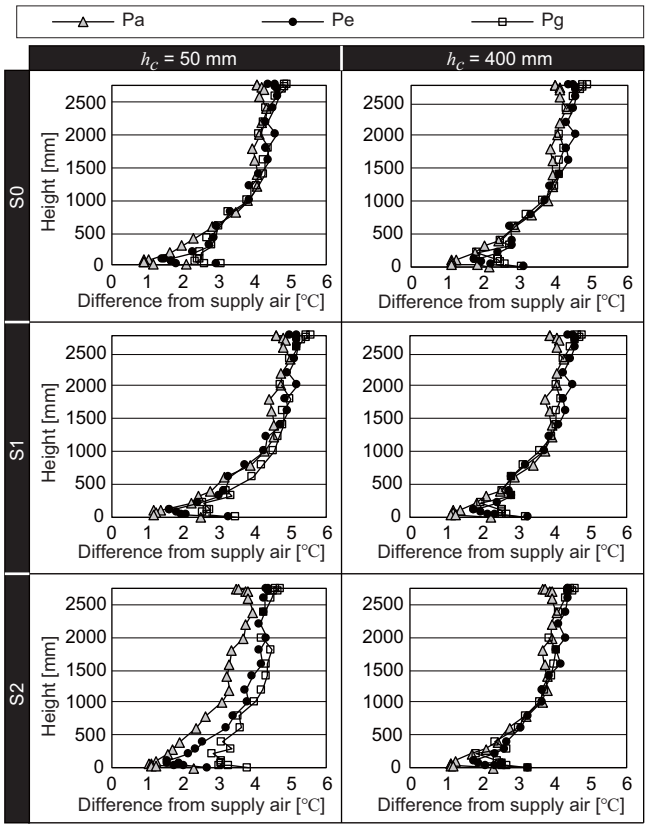


Figure 5.8 Vertical temperature profiles (hc = 50, 400 mm)

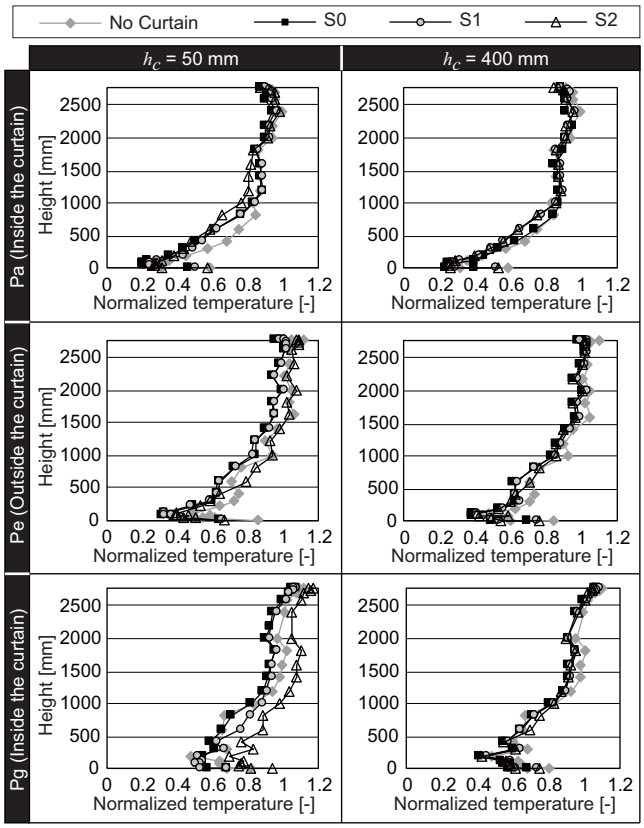
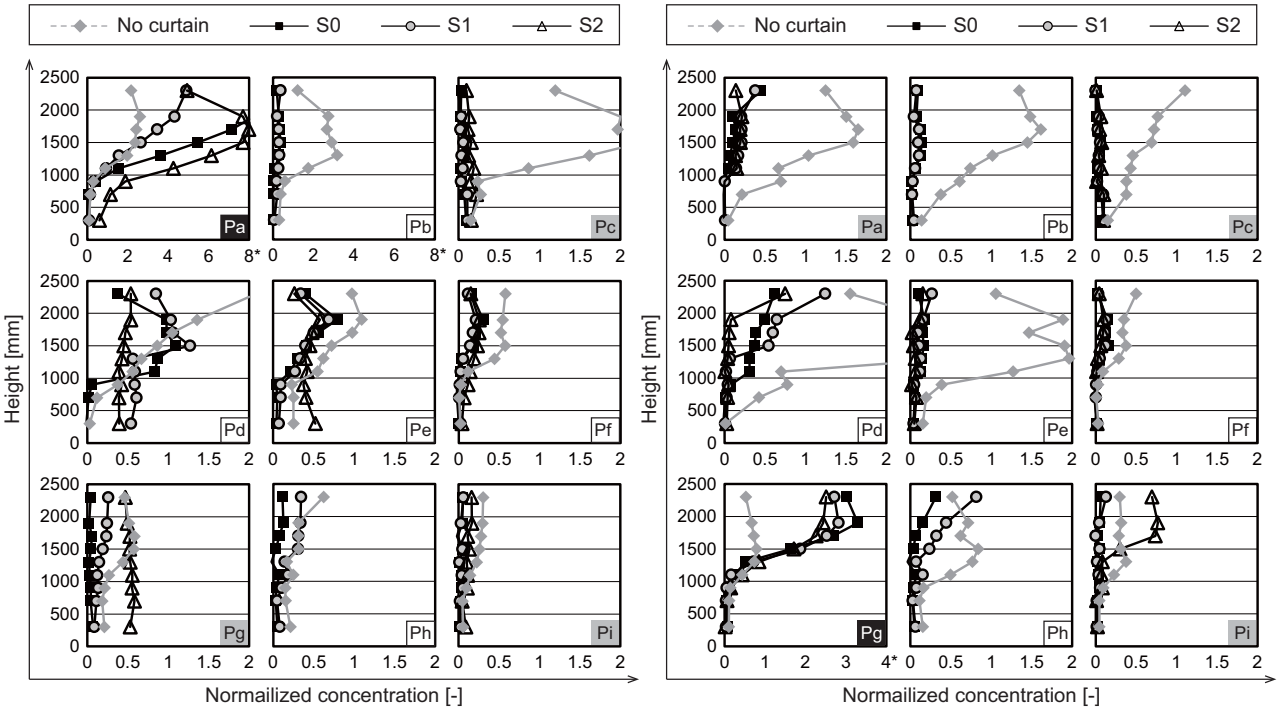


Figure 5.9 Vertical normalized temperature profiles (hc = 50, 400 mm)

the upper part of the room were not much different except for the case of S2-50, the vertical temeperature difference was large near the inlet.

5.3.4 Contaminant Concentration Distribution

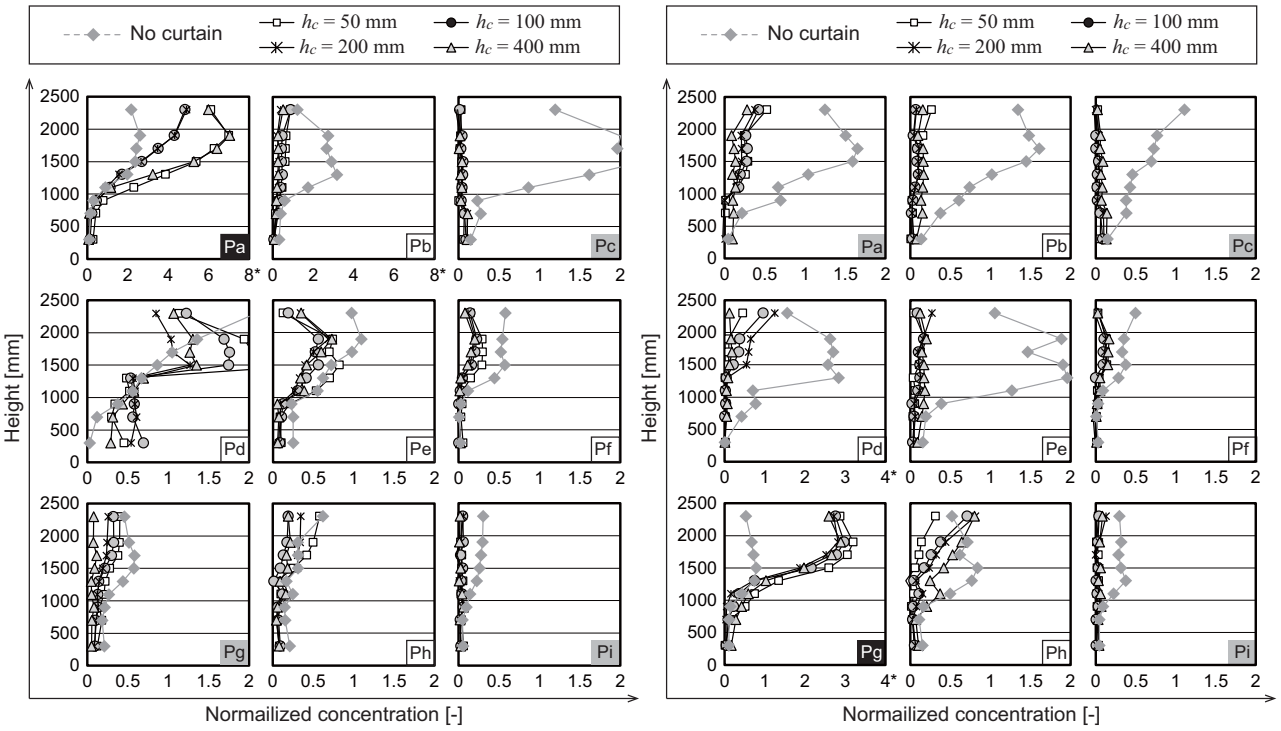
The concentration profiles under different curtain settings when h_c was 200 mm are shown in **Figure 5.10**. When contaminated air was emitted from curtain A (**Figure 5.10 (a)**), the air quality inside the partition curtain where a contaminant source did not exist (Pc, Pg, Pi) was as fresh as supply air except in the case of S2. The concentration distributions in the space outside the partition curtains (Pb, Pd, Pe, Pf, Ph) were relatively low compared with the case without curtains. Although the concentration of the upper part in the curtain with CO_2 emission was significantly high, the contaminant interface apparently formed and the lower part could be kept clean. If all supply inlets were inside the curtain A and C (S2), the concentration at Pd, Pg tended to be high, presumably because the supplied air had to pass the curtain with CO_2 emission, and contaminant air came out from the curtain. When the contaminant source was located in curtain C (**Figure 5.10 (b)**), the contaminant concentration in the upper part of the curtain C (Pg) was also higher than the results without curtain; however it was lower than the case with emission point in curtain A. It indicates that the larger amount of fresh air was supplied inside the curtain C than curtain A. The contamiant interface was also confimed obviously in curtain C. At almost all measurement points, the contamiant concentration was lower than the case without curtain except for Case S2 at Pi. In this case, the contaminated air from curtain C might flow to the upper part of curtain D. However, there was no significant difference regard curtain setting



(a) CO_2 emission point in curtain A (Case A, S0-200-A, S1-200-A, S2-200-A)

(b) CO_2 emission point in curtain C (Case C, S0-200-C, S1-200-C, S2-200-C)

Figure 5.10 Vertical contaminant concentration profiles (h_c = 200 mm)
****** *maximum value of x-axis is larger than other graphs because the concentration was higher than other measurement points*



(a) CO_2 emission point in curtain A (Case A, S1-50-A, S1-100-A, S1-200-A, S1-400-A)

(b) CO_2 emission point in curtain C (Case C, S1-50-C, S1-100-C, S1-200-C, S1-400-C)

Figure 5.11 Vertical contaminant concentration profiles (Curtain setting S1)
****** *maximum value of x-axis is larger than other graphs because the concentration was higher than other measurement points*

at other measurement points, when the emission point was in curtain C. It was found that the contaminated air was more efficiently exhausted owing to the partition curtain.

Figure 5.11 shows the measured contaminant concentration profiles under different bottom height of the curtain when the curtain setting was S1. Except for the measurement point Pa (inside the curtain with CO_2 emission) and Pd (in passageway), the air quality with partition curtain was better than the results without the curtain in cases with CO_2 emission point in curtain A (**Figure 5.11 (a)**). Even though Pb, Pd, Pe, Pf, Ph were located in the same space, the concentration profile at Pd tended to be higher than other measurement points. It may be because Pd was the closest measurement point to the exhaust outlet. In curtain A (Pa), the contaminant concentration of the upper part in case of h_c = 100 and 200 mm was lower than the case of h_c = 50 and 400 mm. In section 5.2, it was found out that the larger space between the curtain and floor exists, the more airflow could supplied into the curtain. However, if it is a multiple-bed ward and the supply inlets are placed only one side, the supplied air would pass through the curtain near inletnd go into other curtain easily. It indicates that too much space between the curtain and floor is also undesirable. When h_c was 50mm, the contaminant concentration at Pd was significantly higher than other conditions. Because the air temperature inside curtain A was lower than outside the curtain, the contaminated air rose the upper part inside the curtain might descend outside the curtain. On the other hand, when the contaminant source was located in curtain C (**Figure 5.11 (b)**), the bottom height of the curtain (h_c) did not considerably affect the contaminant concentration. Since the supply inlets were placed on one wall in this experiment, the measured contaminant concentration results were different between the curtains near the inlet (A, B) and far from the inlet (C, D).

The further study is needed to examine the impact of partition curtain on the contaminant concentration when the curtains were located impartially from the supply inlets.

5.3.5 Personal Exposure of Lying, Sitting and Standing Person

The contaminant concentrations at the height of the breathing zone (personal exposure) of all cases are presented in **Figure 5.12, 5.13 and 5.14**. **Figure 5.12** shows the results of curtain setting S0, and **Figure 5.13** and **Figure 5.14** present the results of S1 and S2. Personal exposure in the figure indicates the normalized contaminant concentration at the height of 1,500 mm (for standing person), 1,100 mm (for sitting person), and 700 mm (for lying person). Although it is known that the actual personal exposure is lower than the contaminant concentration of ambient air (Brohus and Nielsen (1996)[5-5]), the measured contaminant concentration at the breathing height was examined as personal exposure in this study, to avoid overestimating air quality. The measured results were sorted by the locations; inside the curtain with CO_2 emission point, inside other curtains, and outside the curtain (passageway). The measured result inside other curtains is average of the measured results inside three curtain. Personal exposure outside curtain is average concentration of five measurement points (three measurement points for S2 conditions) located outside the curtain.

As it was expected, personal exposure inside the curtain with CO_2 emission was higher than the concentration of exhaust air. However, the air quality at a height of 700 mm was still acceptable, becausre the contaminant concentration was stratified. As the bottom height of the curtain went up, personal exposure tended to decrease. However, when the curtain setting was S1, personal exposure was relatively lower in

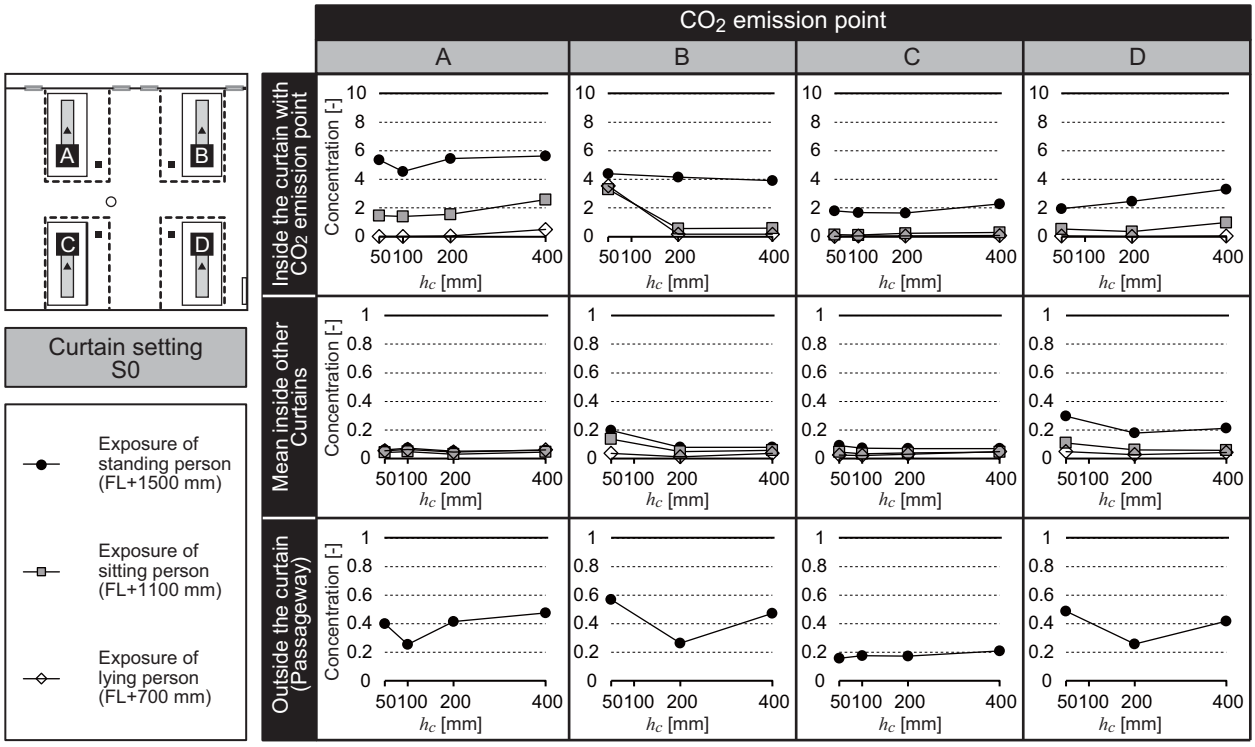


Figure 5.12 Contaminant concentration at the height of breathing zone (Curtain setting S0)

cases of h_c = 100 and 200 mm, as it was mentioned in Section 5.3.4. To provide enough fresh air into curtain, too large or too small space between the curtain and floor is undesirble.

Personal exposure in other curtains was low at every height. It means that the occupants inside the partition curtain would not easily perceive the odor generated in other curtain. All measured results of the case of S2 were worse than in other conditions. In the passageway (outside the curtain), personal exposure of standing

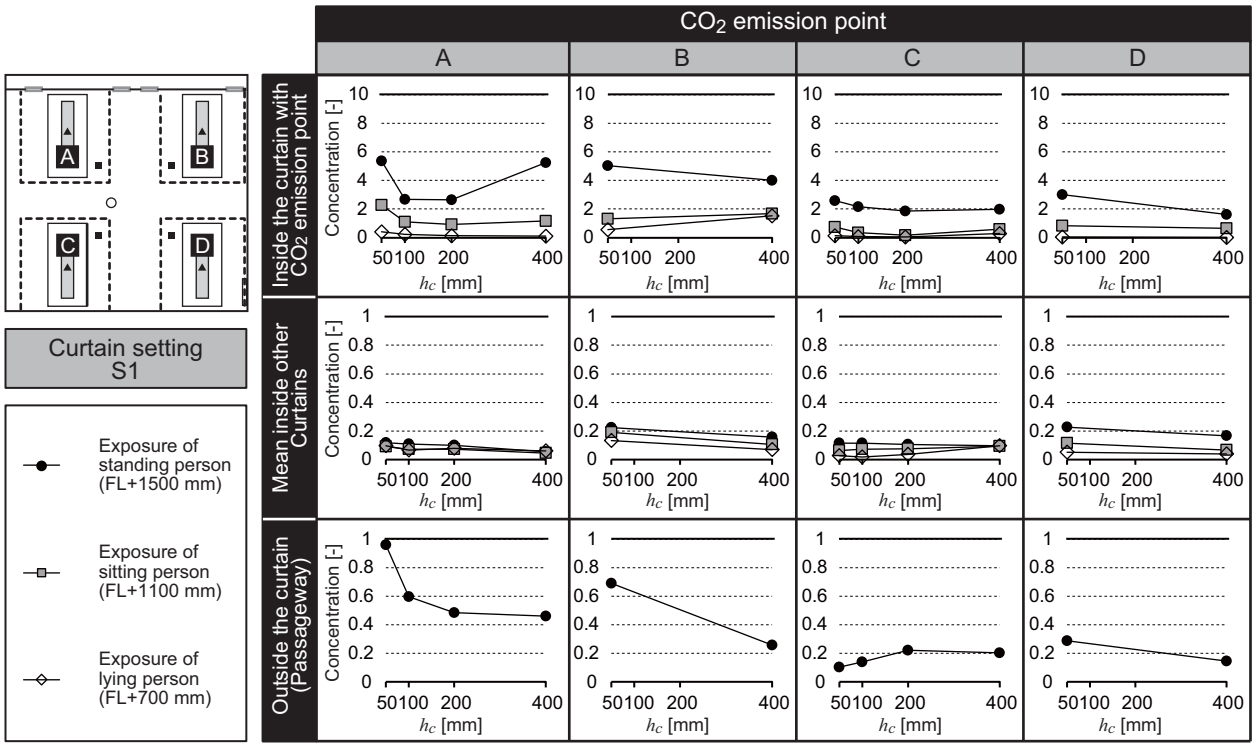


Figure 5.13 Contaminant concentration at the height of breathing zone (Curtain setting S1)

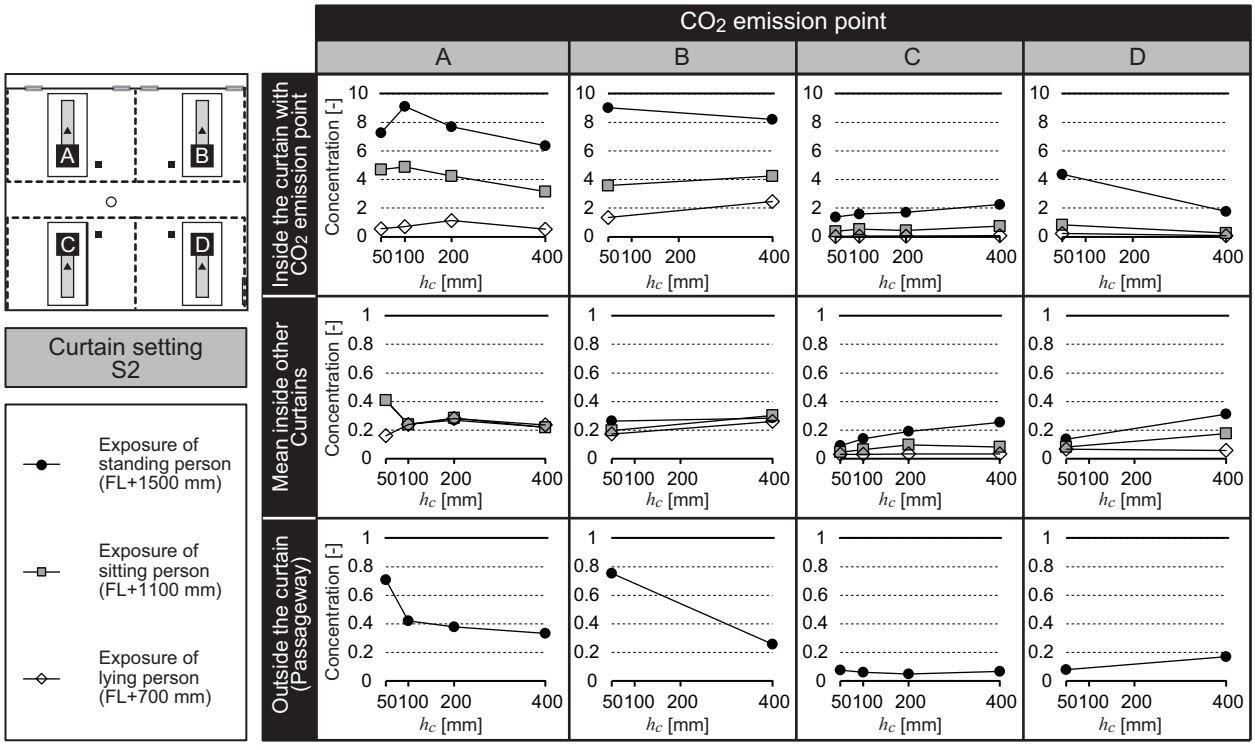


Figure 5.14 Contaminant concentration at the height of breathing zone (Curtain setting S2)

person was higher when the contaminant source was located in curtain A or B, rather than curtain C or D. If the contaminant is emitted inside the curtain with or near supply inlet, and supply inlets were unevenly distributed, the contaminated air could flow to outside the curtain. In case of h_c = 50 mm, the personal exposure of standing person outside the curtain was obviously higher than other cases.

The measured contaminant concentration at the height of breathing zone was slightly lower in case of curtain setting S0, rather than S1 and S2. It seems that it would be better to place the inlet outside the curtain. However, the more cases under different inlet arrangements and size of inlet should be investigated before drawing conclusions.

5.3.6 Supplied Airflow Rate into the Partition Curtains

The measured contaminant concentration profiles inside the curtain with contaminant source are shown in **Figure 5.15**. In nearly all cases, the contaminant interface formed apparently and the contaminant concentration in the lower part was close to the supply air.

As supplied airflow rate into the curtain increases, the height of contaminant interface would go up and the contaminant concentration in the upper part would decrease. If the normalized contaminant concentration in the upper part inside curtain ($C_{u\text{-}in}$) and the supply airflow rate (Q_s) are known, the supplied airflow rate inside the curtain with contaminant source ($Q_{s\text{-}in}$) can be expressed by

$$Q_{s-in} = \frac{Q_s}{C_{u-in}} \qquad \cdots(5\text{-}1)$$

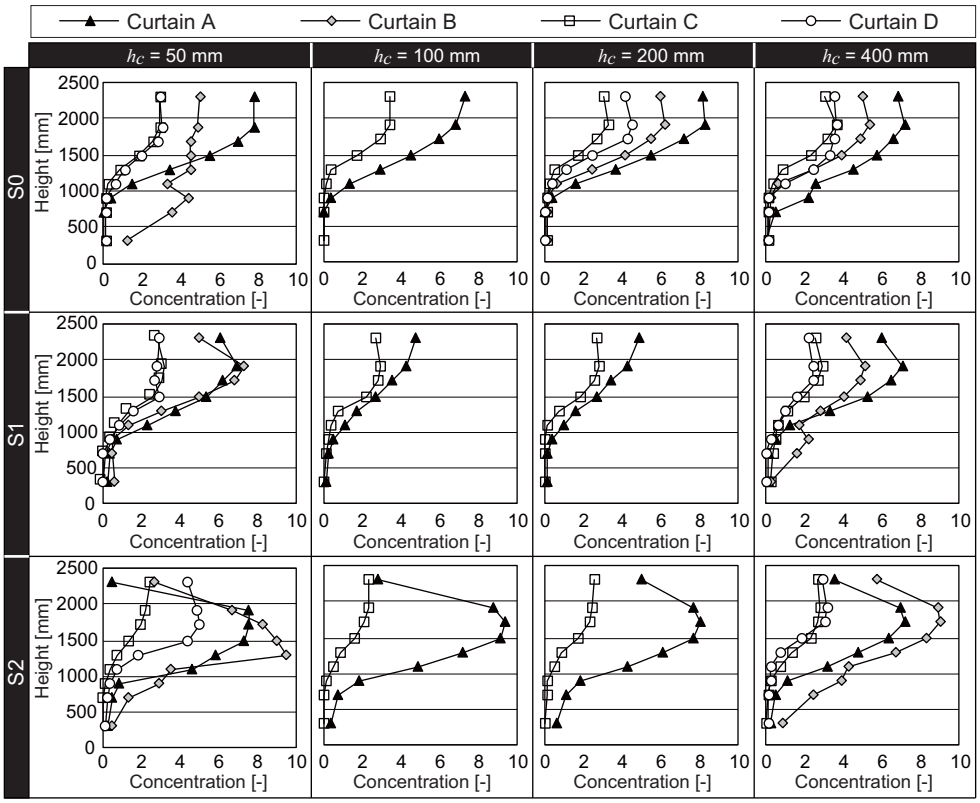


Figure 5.15 Contaminant concentration inside the curtain with CO_2 emission source

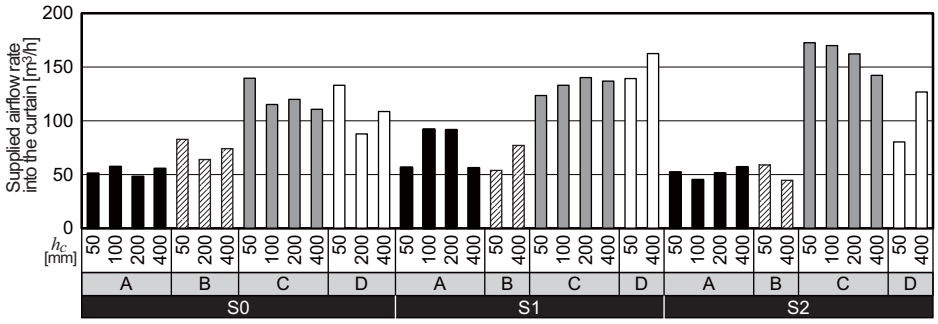


Figure 5.16 Supplied airflow rate into each curtain (Calculated using the contaminant concentration in the upper part inside curtain)

Figure 5.16 shows the calculated supplied airflow rate into the curtain with CO_2 emission. The supplied airflow rate is the total supply airflow rate divided by the normalized concentration of the upper part (1,900mm) inside the curtain. The supplied airflow rate into curtain C and D is larger than curtain A and B in every case. Because curtain C and D are far from the supply inlet, the supply air that passed through curtain A and B was accumulated in curtain C. When the supply inlets were located in both inside and outside the curtains (Case S1-100, S1-200), the supplied airflow rates into the curtain A and C were comparatively balanced. The experimental results implied that the location of suppy inlets and curtains had a greater impact to the contaminant concentration distribution in the room than the bottom height of the curtains.

5.3.7 Prediction of the Contaminant Concentration inside the Curtain with Contaminant Emission

Inversely, if the supplied airflow rate is known, the vertical contaminant concentration profile inside the curtain could be predicted. In this section, the vertical contamiant concetration was forecasted using the calculated supplied airflow rate and zonal model (**Figure 5.17**).

It was assumed that there was no vertical convection airflow along the curtain surface. The contaminant interface would form at the height where the supply airflow rate and the total plume rate (plume from the lying person simulator and black lamp in this experiment) are equal.

$$Q_s' = Q_p(y_i) + Q_{bl}(y_i) \quad \cdots(5\text{-}2)$$

The contaminant balance in zone (2) and (3) can be expressed by

Zone (2):

$$Q_{dr}(y_u)C_2 = Q_{dr}(y_u)C_u - (D + D_t)\frac{\partial C}{\partial y}A \quad \cdots(5\text{-}3)$$

Zone (3):

$$Q_{ur}(y_d)C_3 = (D + D_t)\frac{\partial C}{\partial y}A \quad \cdots(5\text{-}4)$$

The plume rates from the lying cylinder and the black lamp were calculated using equations in **Chapter 2**. However, in case of curtain setting S0, the lying person simulater was closer to the curtain surface compared to the curtain setting S1 and S2. In the previous study,

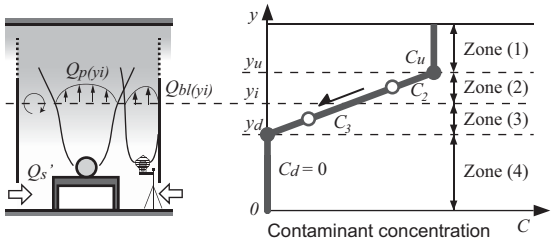


Figure 5.17 Zonal model for vertical contaminant concentration inside the curtain

it was found that if heat source is located near the wall or in a corner, the plume rate would be smaller than usual (Nielsen (1993)[5-6]). Hence, the contaminant concentration profile of S0 was also calculated using the plume rate from the lying cylinder reduced as 64% (Kosonen et al. (2017)[5-3], Nielsen (1993)[5-6]). The convection heat flux was assumed to be half of the total heat flux.

Figure 5.18 shows the calculated results of vertical contaminant concentration profiles inside the curtain with contaminant source. The supplied airflow inside the curtain estimated in Section 5.3.6 was used. In curtain C, the calculated results corresponded well with the measured contaminant concentration profiles. It indicates that the contaminant concentration inside the curtain could be predicted if the supplied airflow rate is known. In cases of curtain setting S0, the calculated results using reduced plume rate were closer to the measured results than using original plume rate. Because the heat source was located near the curtain, the plume could not spread as usual situation. In curtain A, the calculated results did not match well with the measured result, compared to the curtain C. The calculated contaminant interface tended to be lower than actual interface in all cases. The calculated contaminant interface layer existed near the height of 1,000 mm and it was approximately only 300 mm upper than the heat source. The plume rate near the top of the heat source might be overestimated in the used approximate equation, because the size of the heating cylinder was different from the previous study (Shinozaki et al. (2012)[5-7]). In order to predict the contaminant concentration more accurately, the plume rate near the lying cyliner should be studied in more detail.

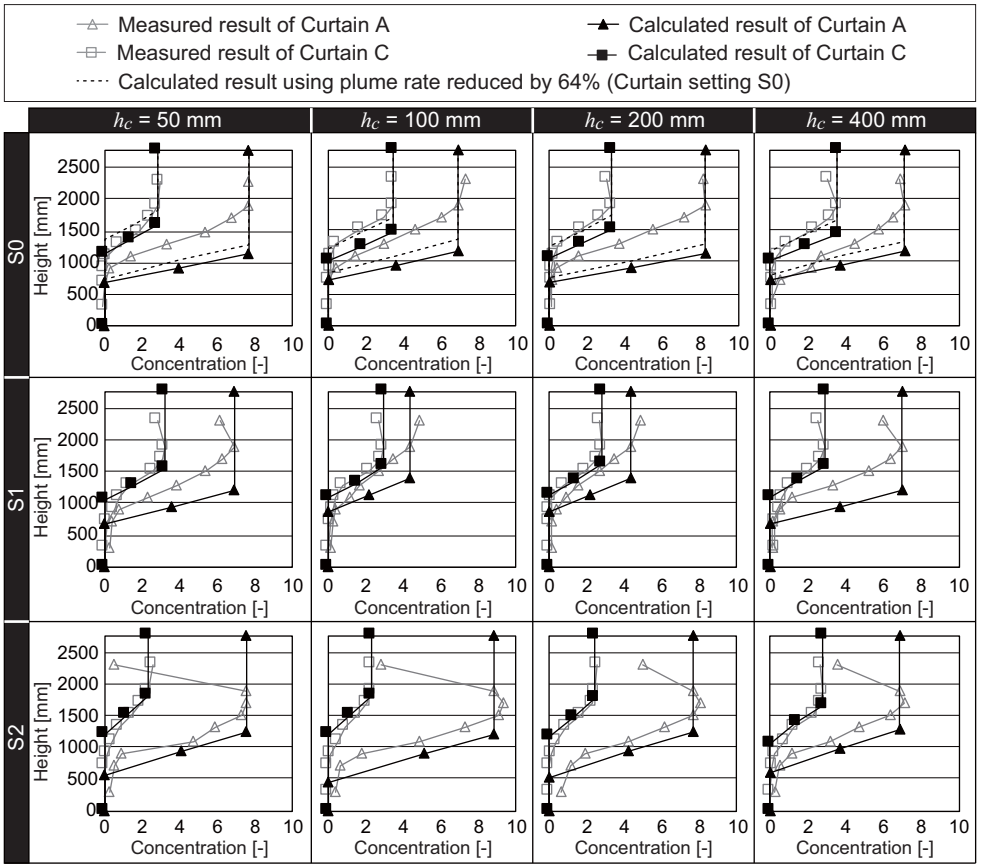


Figure 5.18 Predicted contaminant concentration inside the curtain with CO_2 emission source

5.3.8 Location of the Supply Inlet

The supply inlets were asymmetrically placed in the experiments and it greatly affected the temperature and the contaminant concentration profiles inside the curtain. However, if the DV is applied to a multiple-bed hospital ward, the supply inlets would be distributed as symmetrical as possible to avoid the unfairness in indoor environment inside each curtain. Hence, it is imperative to examine the influence of partition curtain when supply inlets are located symmetrically.

Since it was difficult to change the location of the supply inlets of the experimental chamber, the influece of location of the supply inlet was examined using Computational Fluid Dynamics (CFD). CFD has been often used to investigate the indoor environment in a room with DV. There are large amount of studies using CFD to investigate the indoor environment in a displacement-ventilated room. RNG k-ε model has been reported as the suitable model for the DV in some researches (Kobayashi and Chen (2003)[5-8], Lin et al. (2005)[5-9]). However, recent studies revealed that SST k-ε model has superior performance (Zhang et al. (2009), Gilani et al. (2015)[5-11]). Gilani et al. (2016)[5-11] studied the proper turbulence model for the stratified environment in a

Table 5.3 Summary of CFD setting

Tubulence Model	Standard k-ε Model	
Discretization Scheme	QUICK	
Boundary Conditions	Inlet	Velocity magnitude : 0.15645 m/s (392 m3/h in total)
		Turbulent intensity : 3%
		Turbulent length scale : 0.005 m
		Temperature : 16.408 °C(based on the measurement)
	Outlet	Velocity magnitude : 7.5617 m/s (392 m3/h in total)
	Wall (Heat)	Surface temperature (based on the measurement)
	Wall (Velocity)	Log-law
	Heat load	Heating surface
		(person simulator : 40 W each, black lamp : 60 W each)
Total Number of Cells	3,460,212	

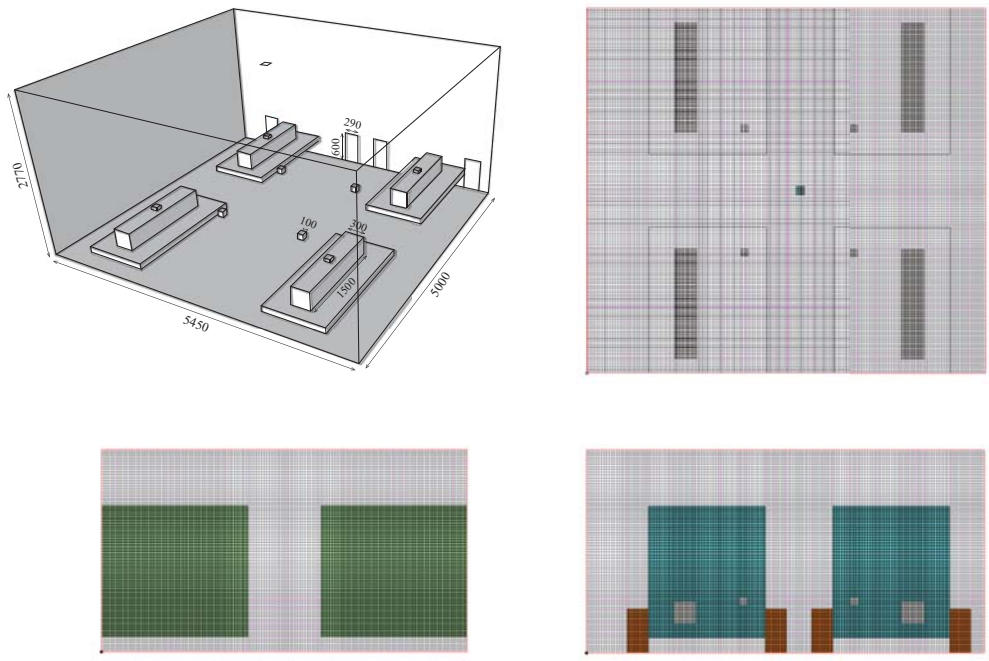
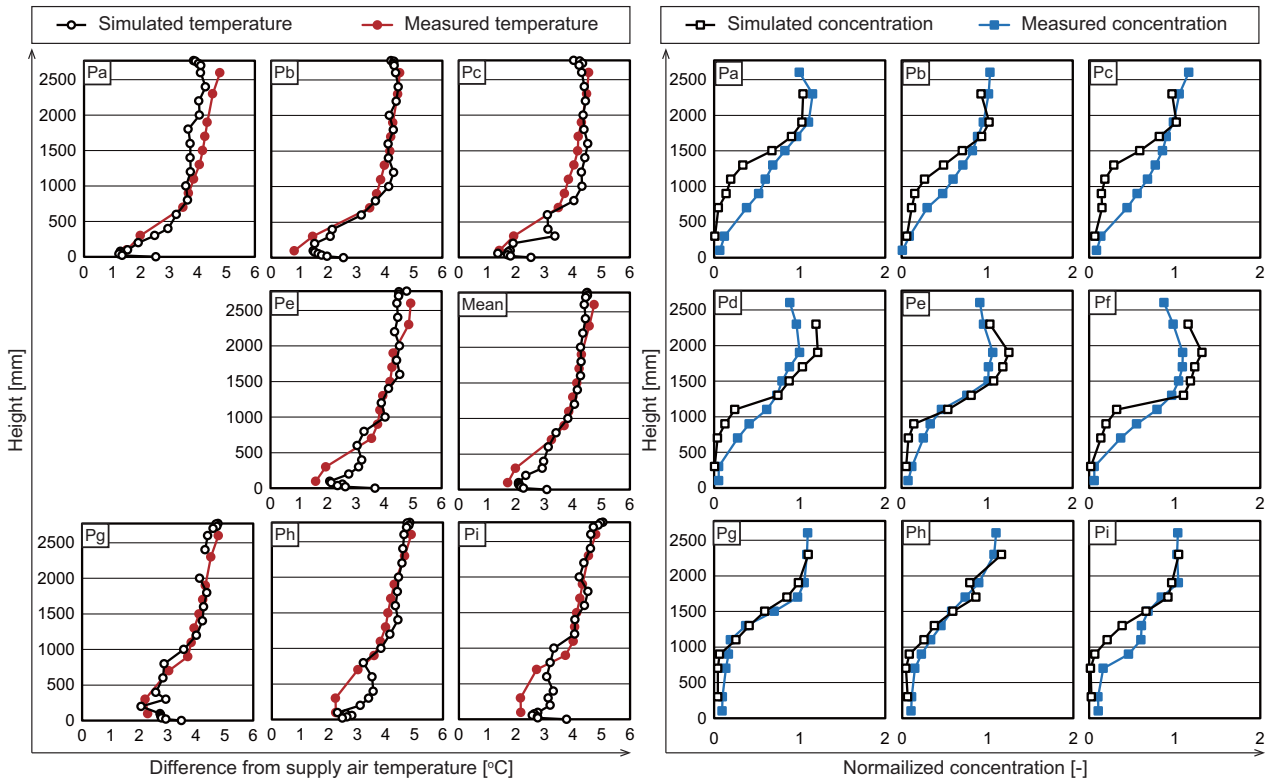


Figure 5.19 Computational domain and mesh layout

room with DV. Five models were compared and SST k-ω was considered to predict the vertical temperature distribution accurately. However, the aim of this simulation was not accurate prediction but spotting trend, standard *k*-ε model was adopted to simulate the differect conditions of the inlet locations. For a start, to assure the reliablity of the CFD simulation, the simulated result was compared with the measured result without curtain. CO_2 was emitted from all person simulator in the measurement. **Table 5.3** presents the summary of the CFD analysis. Turbulent intensity and turbulent length scale was set referring to the previous study (Inagaki et al. (2011)[5-12]). Inner surface temperatures of the floor, ceiling and walls were given based on the measurement and the radiation analysis was not performed. **Figure 5.19** shows the computational domain and grid layout. The shape of the person simulator was changed from cylinder (ϕ : 300 mm, L : 1,500 mm) to rectangular parallelopiped shape (L : 1,500 mm, W : 300 mm, H : 300 mm) for simplicity. A cube 100 mm on each side was adopted to simulate the black lamp.

The simulate and measured results are presented in **Figure 5.20**. Simulated vertical temperature profile was close to the measured results. Although the simulation overrated contaminant concentration in the lower part at Pa-Pb, the simulated results at other part roughly matched with the measured results. The simulation model was considered to be able to identify the trend of the temperature and contaminant concentraiton in a displacement-ventilated ward.

In the CFD simulation, four different conditions of inlets were chosen (**Figure 5.21**). In 'S0' case, four supply inlets were outside the curtain, while all supply inlets were inside the curtain (one inlet for one bed) in Case 'S1'. In Case '1', all inlets were placed on one wall, but four inlets were distributed on two walls symmetrically in Case '2'. Case S0-2m is similar to Case S0-2; however, the supply inlets were located in the



(a) Temperature ***(b) Contaminant concentration***

Figure 5.20 Simulated and measured results

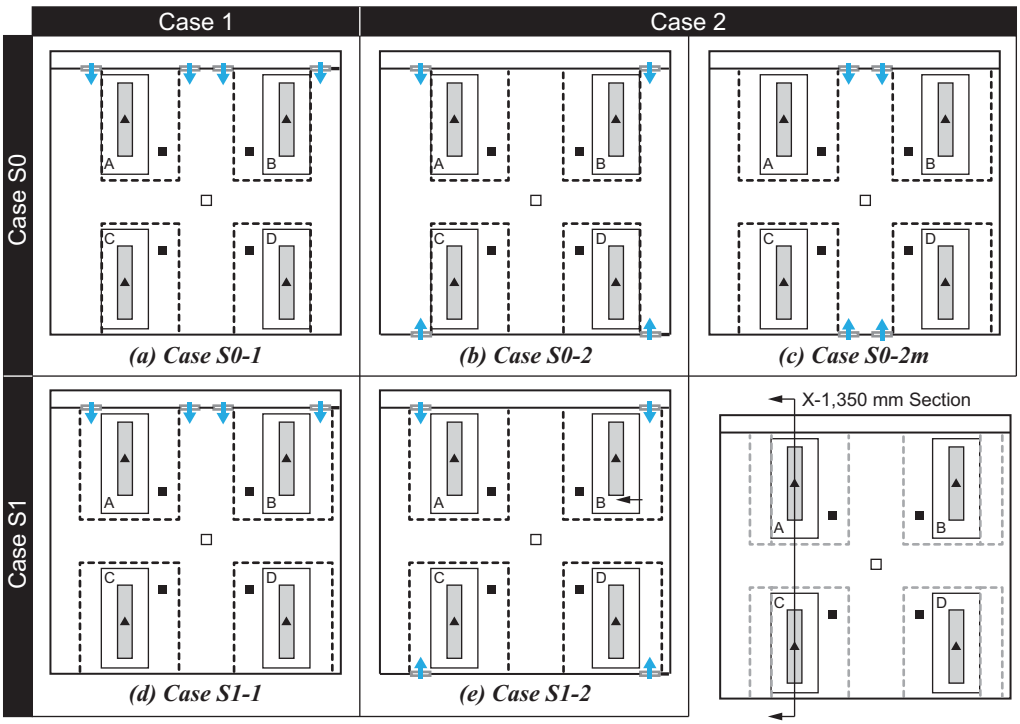


Figure 5.21 Simulated conditions

middle of the walls and the floor surface area inside the curtain was equal to Case S1-2. The simulation was performed with same setting of **Table 5.3**, except for the boundary condition of wall. The envelopes of the room were considered to be perfectly insulated. The exhaust outlet was moved to the middle of the room. The curtain was located at the height from 200 mm to 2,000 mm. There was no change in terms of the grid layout.

The simulated contaminant concentration distributions of Y-Z section at x = 1,350 mm are shown in **Figure 5.22**. As it was known from the experimental results, the height of the contaminant interface inside the Curtain A was lower than the Curtain C when the supply inlets were placed on only one wall. However, the contaminant concentration distributions in the Curtain A and C becomes close if the supply inlets were located symmetrically. When the supply inlets were inside the curtain, the contaminant interface tended to form at the lower height compared with the case of S0. It indicates that the supplied airflow rate into the curtain of Case S1 would be smaller than Case S0.

Figure 5.23, **5.24** and **5.25** present the simulated contaminant concentration distributions of X-Y section at z = 700 mm (breathing zone of lying person), 1,100 mm (sitting person) and 1,500 mm (standing person). The contaimant concentration distributions at height of 700 mm are not very different in all cases (**Figure 5.23**). High air quality is maintained in the lower part of the room. In **5.24** and **5.25**, when the supply inlets are placed on one wall (Case S0-1 and S1-1), the area with low contaminant concentration in the upper part is larger in Curtain C than A. It means that the supplied airflow rate is larger in Curtain C than A. However, the contaminant distributions inside each curtain are similar inside all curtains, if the supply inlets are located symmetrically. When the supply inlets were located outside the curtain (Case S0-2 and S0-2m), the contaminant concentration inside and outside the curtain is lower than Case S1-2. Once supplied air goes outside the curtain, it might hardly flow into the curtain again. On the other hand, the supplied air from

ouside to inside the curtain might not easily go out again. If supply inlet is inside the curtain, the supplied air would be It seems that the supply inlet would be better to be placed outside the partition curtain in the diplacement-ventilated ward. However, it should be noted that the radiative heat transfer is not considered and the condition of the curtain height was not varied in this simulation. More detailed and accurate simulation should be performed in further study.

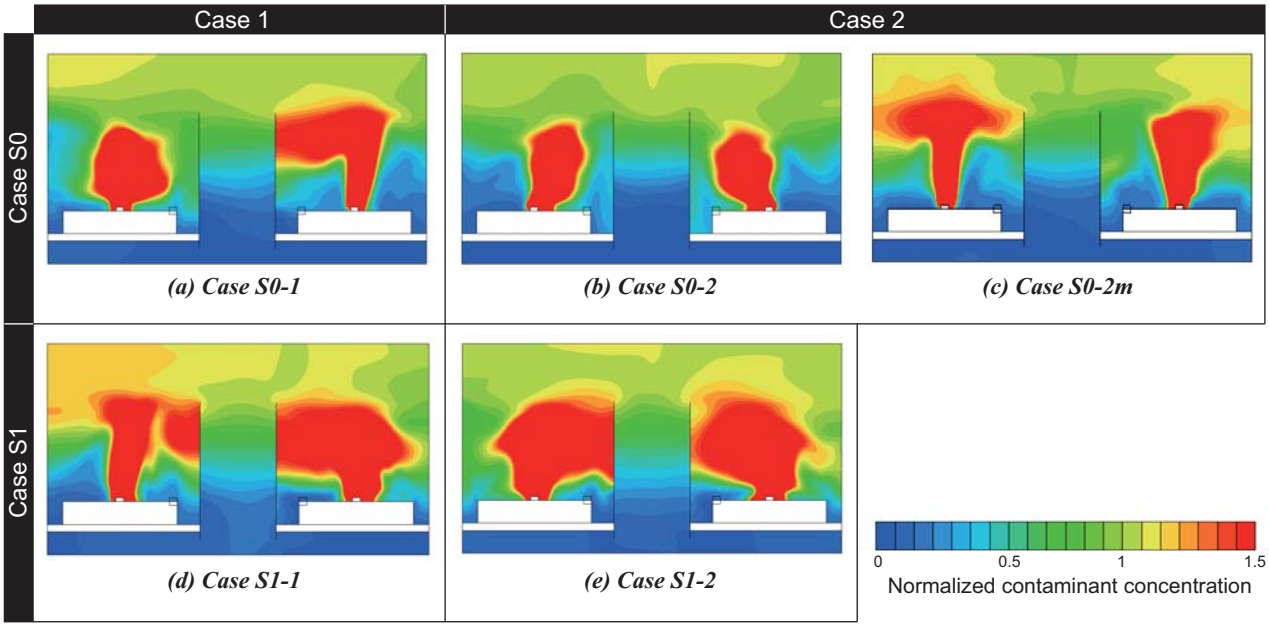


Figure 5.22 Simulated contaminant concentraion contours of Y-Z section (x = 1,350 mm)

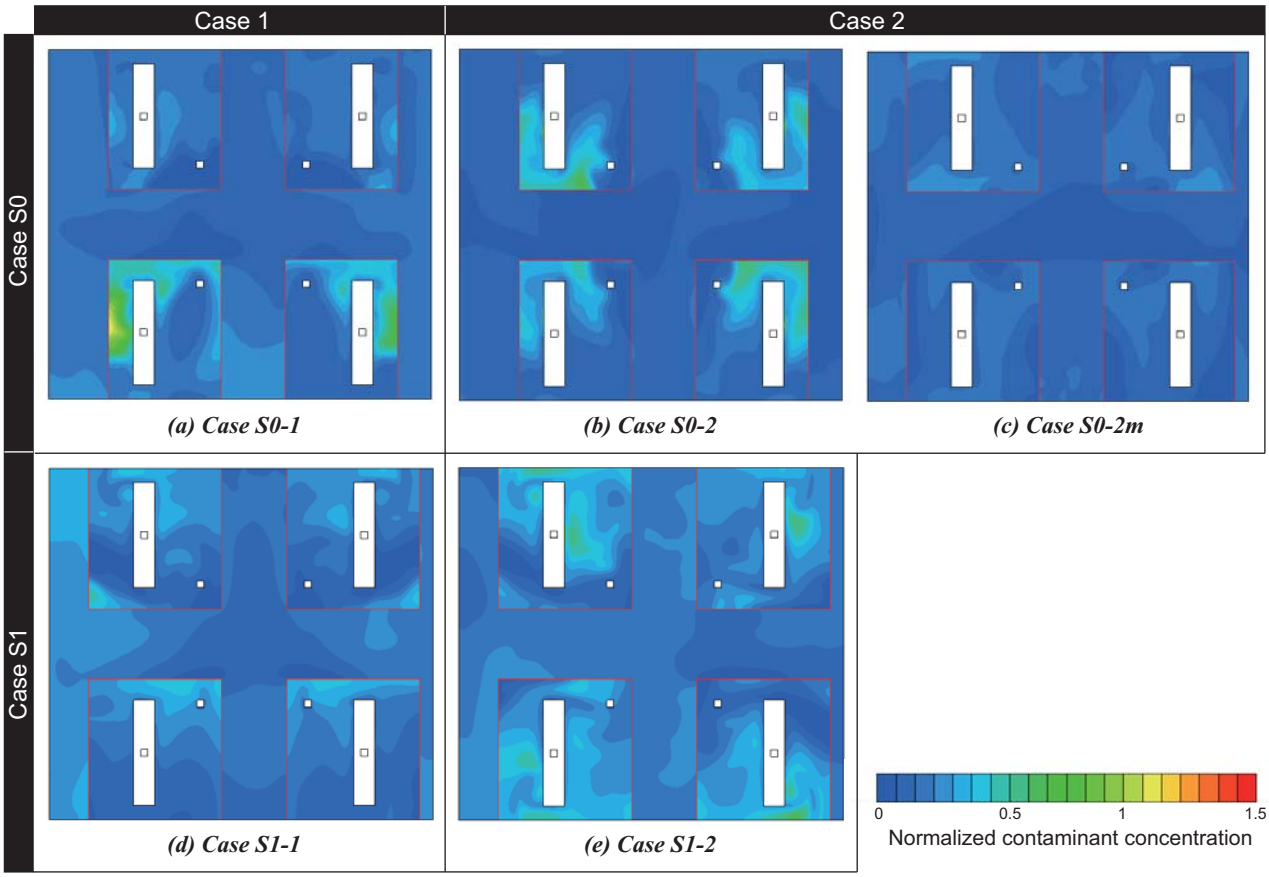


Figure 5.23 Simulated contaminant concentraion contours of X-Y section (z = 700 mm)

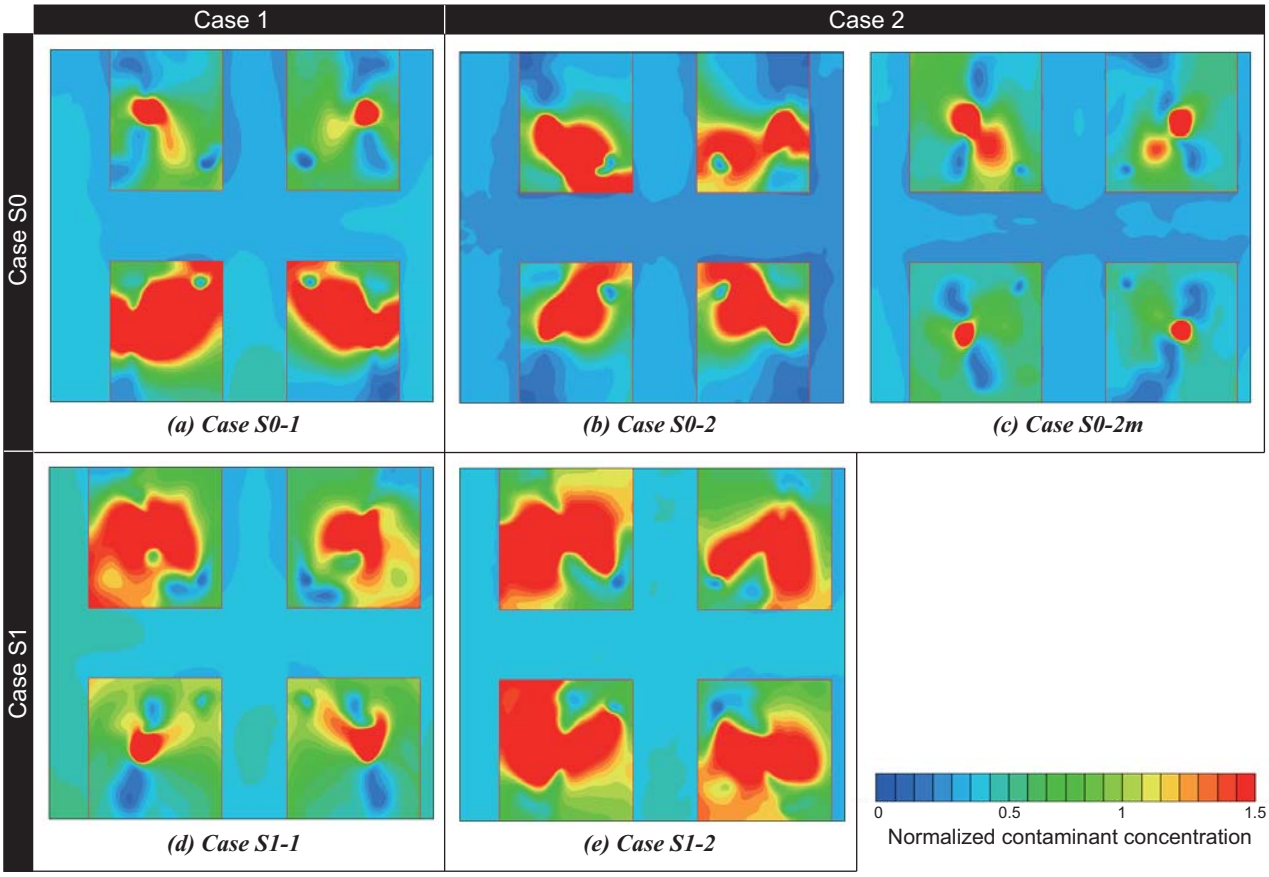


Figure 5.24 Simulated contaminant concentraion contours of X-Y section (z = 1,100 mm)

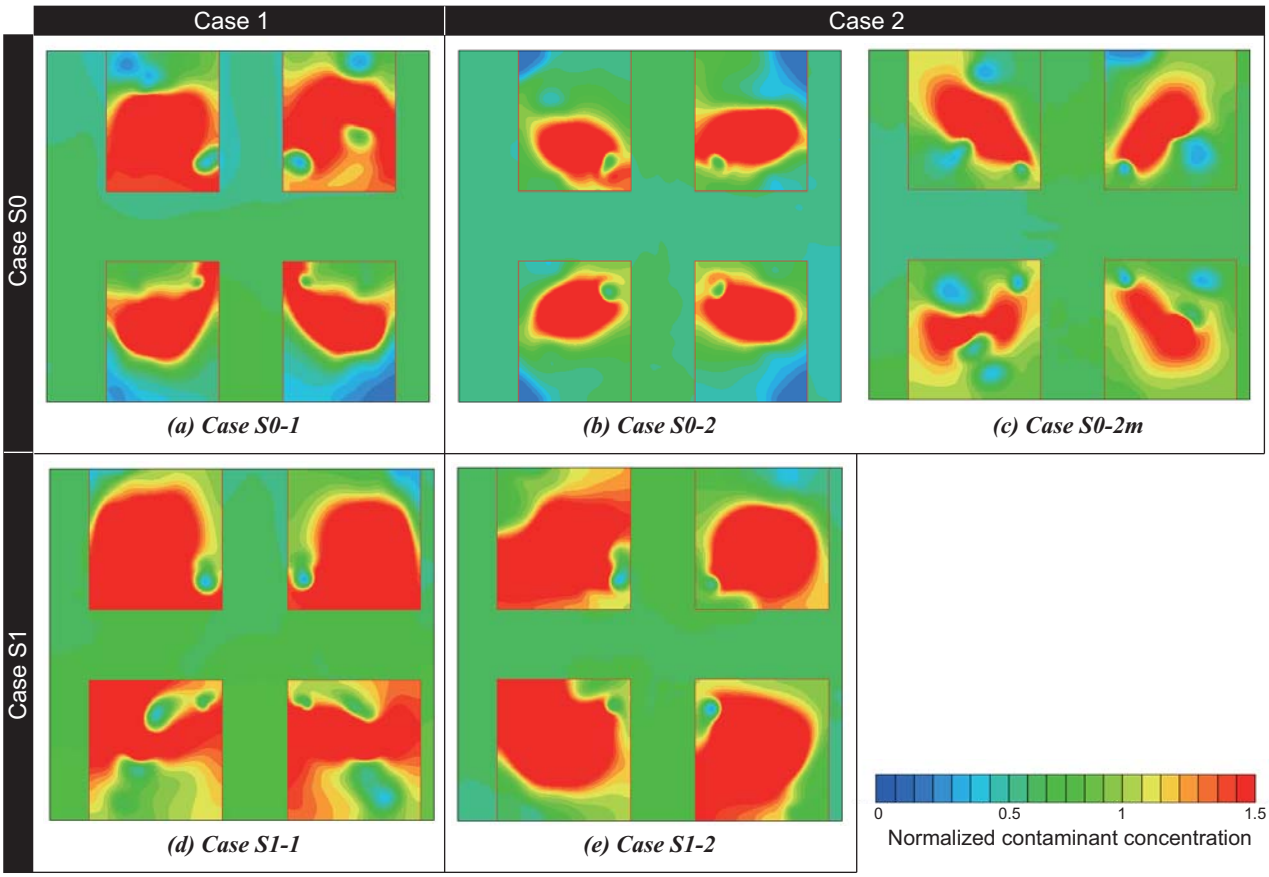


Figure 5.25 Simulated contaminant concentraion contours of X-Y section (z = 1,500 mm)

5.4 Chapter Discussion and Conclusion

The present study investigated the impact of the internal partition curtain in a four-bed hospital ward with DV. The temeprature and contaminant concentration distributions were investigated under the different bottom height of the curtains and the arrangement of the curtain and the supply inlet. Additionally, the supplied airflow rate into the curtain was estimated and the contaminant concentration was also predicted using zonal model. The following conclusions were obtained.

- It was revealed that the internal partition curtain could have a beneficial effect on removing contaminated air in a displacement-ventilated ward efficiently. When the partition curtain was installed, the contaminant concentration outside the curtain, where the contaminant source was located, was considerably lower than the results without curtain. If the unpleasant odor is emitted inside the curtain, the occupants inside other curtains or in the passageway would not easily perceive the odor in a multiple-bed ward with DV.
- When the space between the curtain and floor surface was small, the air temperature near the floor was different depend on the distance from the inlet. The air temperature near the inlet was lower , and the air temperature inside the far curtain from inlet was higher than the results without curtain. When all supply inlets were placed in the only one side of the curtains, the differences were particularly large.
- The curtain near the supply inlet had smaller supplied airflow rate than the curtain far from the inlet. The location of supply inlets considerably affected air distribution. When all supply inlets are located on only one side of the partition curtains, the air quality was worse than other supply inlet conditions. To distribute the supply airflow evenly, the supply inlets should be equally arranged from the curtains.
- The bottom height of the curtains did not have a significant impact on the contaminant concentration as long as there is a certain space between the floor and curtains. If the bottom height was small, the airflow could not pass under the curtain smoothly. However, if the space between the curtain and floor is too large, the airflow would pass through the curtain and go to outside the curtain. 200 mm was appropriate for the bottom height of the curtain in this experiment.
- The contaminant concentration in the curtain with contaminant source was significantly higher than the case without curtain or mixing ventilation. However, the air quality in the lower part was close to the supply air, because the contaminant concentration was stratified.
- It was proved that the vertical contaminant concentration profile inside the curtain with contaminant source could be predicted using zonal model, if the supplied airflow rate into the curtain is known.
- To avoid the disproportionate supply airflow rates into each curtain, the supply inlets should be symmetrically placed. Additionally, the supply inlet would be better to be located outside the curtain.

In this study, the experiment was carried out under limited supply inlet conditions. In order to decide the most appropriate curtain conditions for the displacement-ventilated ward, the more varied positions of curtain, inlet and outlet should be examined using CFD analysis in the subsequent study.

References

5-1) J. Noh, J. Lee, K. Noh, Y. Kim, S. Yook (2018) : Effects of Hospital Ward Curtains on Ventilation in a Four-bed Hospital Ward, *Aerosol and Air Quality Research*, 18, pp.2643–2653.

5-2) J. Hanada, T. Yamanaka, H. Kotani, Y. Momoi, K. Sagara, D. Tatsumi, S. Ueda, T. Maeda (2014) : Indoor Environment of Sickroom by Low Velocity Fabric Air Diffuser on Ceiling (Part3) Outline of Experiments and Effect of Curtain on Temperature and Contaminant Concentration Profiles, *Summaries of Technical Papers of Annual Meeting of AIJ,* pp.749-750 (In Japanese)

5-3) R. Kosonen, A. Melikov, E. Mundt, P. Mustakallio, P. V. Nielsen (2017) : REHVA Guidebook No. 23: Displacement Ventilation, REHVA, Brussels.

5-4) A. Iwamura, K. Sagara, T. Yamanaka, H. Kotani, T. Suzuki, T. Yamashita (2007) : Semi-Personal Air-conditioning System for Sickroom by Displacement Ventilation with Radiant Panel (Part 7) Influence of Exhaust Position on Distribution of Temperature and Contaminant Concentration, *Summaries of Technical Papers of Annual Meeting of AIJ*, pp.1301-1302 (In Japanese)

5-5) H. Brohus, P. V. Nielsen (1996) : Personal exposure in displacement ventilated rooms, *Indoor Air* 6 , pp.157–167.

5-6) P. V. Nielsen (1993), Displacement ventilation - Theory and design, Aalborg University, Aalborg, Denmark.

5-7) M. Shinozaki, T. Yamanake, K. Sagara, H. Kotani, Y. Momoi, T. Inagaki (2012) : Temperature and contaminant concentration profiles in four-beds sickroom with displacement ventilation (Part 3) Experiment results and thermal plume velocity above lying person simulator, *Proceedings of Technical Papers of Annual Meeting of SHASE*, pp.1747-1750. (In Japanese)

5-8) N. Kobayashi, Q. Chen (2003) : Floor-supply displacement ventilation in a small office, *Indoor and Built Environment*. 12(4), pp.281-291

5-9) Z. Lin, T. T. Chow, C. F. Tsang, K. F. Fong, L. S. Chan (2005) : CFD study on effect of the air supply location on the performance of the displacement ventilation system, *Building and Environment*. 40, pp.1051-1067.

5-10) T. Zhang, K. Lee, Q. Chen (2009) : A simplified approach to decribe complex diffusers in displacement ventilation for CFD simulations, Indoor Air. 19, pp.255-267.

5-11) S. Gilani, H. Montazeri, B. Blocken (2016) : CFD simulation of stratified indoor environment in displacement ventilation: Validation and sensitivity analysis, Building and Environment. 95, pp.299-313.

5-12) T. Inagaki, T. Yamanaka, K. Sagara, H. Kotani, Y. Momoi, T. Yamashita, N. Choi (2010) : Influence of Partition Curtain on Vertical Profile of Temperature and Contaminant Concentration in Sickroom with Displacement Ventilation, *AIVC International Conference*, In USB flash drive, D-2.

Published Papers related to Chapter 5

Conference Papers

*International Conference

1) T. Inagaki, T. Yamanaka, K. Sagara, H. Kotani, Y. Momoi, T. Yamashita, N. Choi (2010) : Influence of Partition Curtain on Vertical Profile of Temperature and Contaminant Concentration in Sickroom with Displacement Ventilation, *AIVC International Conference*, In USB flash drive, D-2.

*Papers for Archtectural Institute of Japan (AIJ)

1) N. Choi, T. Yamanaka, T. Kobayashi (2020) : Ventilation Performance in Four-Beds Sickroom with Displacement Ventilation (part7) Impact of Partition Curtains on Indoor Contaminant Concentration Distribution, *Proceedings of Technical Papers of Annual Meeting of AIJ Kinki branch*, pp.173-176. (In Japanese)

*Paper for The Society of Heating, Air-Conditioning and Sanitary Engineers of Japan (SHASE)

1) T. Inagaki, T. Yamanaka, K. Sagara, H. Kotani, Y. Momoi, N. Choi, T. Yamashita (2010) : Air-conditioning system for sickroom by displacement ventilation (Part 1) Effect of partition curtain on temperature and contaminant concentration profile, *Proceedings of Technical Papers of Annual Meeting of SHASE Kinki chapter*, pp.61-64. (In Japanese)
2) N. Choi, T. Yamanaka, K. Sagara, H. Kotani, Y. Momoi, T. Inagaki, T. Yamashita (2010) : Air-conditioning system for sickroom by displacement ventilation (Part 2) Effect of positional relation of curtain and inlet/outlet on temperature and contaminant concentration profile, *Proceedings of Technical Papers of Annual Meeting of SHASE Kinki chapter*, pp.65-68. (In Japanese)
3) T. Ihama, N. Choi, T. Yamanaka, T. Kobayashi (2020) : Temperature and contaminant concentration profiles in four-beds sickroom with displacement ventilation (Part 8) Influence of internal partition curtains on contaminant concentration profiles, *Proceedings of Technical Papers of Annual Meeting of SHASE Kinki chapter*, A-13. (In Japanese)

Original Papers

1) T. Inagaki, T. Yamanaka, K. Sagara, H. Kotani, Y. Momoi, T. Yamashita, N. Choi (2011) : Study on influence of partition curtain in sickroom with displacement ventilation, *Journal of Environmental Engineering (Transaction of AIJ)*, Volume 76, No. 662, pp.377-383. (In Japanese)
2) N. Choi, T. Yamanaka, T. Kobayashi, T. Ihama (2020) : Impact of partition curtains on temperature and contaminant concentration in a displacement ventilated four-bed hospital ward, *Transactions of the Society of Heating, Air-conditioning and Sanitary Engineers of Japan*, Vol. 45, No. 283, pp.31-39. (In Japanese)

Chapter 6.
Conclusions

6 Conclusions

Unpleasant odor in a ward has been a troublesome issue to spoil the hospital indoor environment. Although displacement ventilation (DV) is known for its high efficiency, it has been rarely installed in a hospital ward. This study focused on using DV to solve the unpleasant odor problem in the hospital ward or nursing facilities. Since the hospital ward is the living space for inpatients and is also a workplace for the hospital staff, the indoor environment in a ward should be clean and comfortable. To explore the appropriateness of DV for the ward, the temperature and contaminant concentration distributions were examined under various conditions. Additionally, the several prediction models were validated to find the proper model to predict the vertical temperature and concentration distribution in a ward with DV. The outcome of this study on the influence of radiant panel, vertical aiflow and partition in the displacement-ventilated room could also be applied to other types of indoor spaces than a ward. The main finding obtained in this study are summarized in the sections below.

6.1 Temperature Distribution in a Displacement-ventilated Ward

Vertical temperature profile in a displacement-ventilated room is varied depending on the type and location of heat source. There is large amount of data about the temperature distribution and thermal comfort in a room with DV. However, most of researches focused on office and classroom and DV has been still rarely introduced in a ward. The dominant heat source in a ward is a lying person, while the main heat source in office or classroom is a sitting person. Hence, the temperature distribution characteristics in a ward with DV would be different from office. This study examined the temperature distribution in both of single-bed and four-bed (multiple-bed) ward with DV. It was known that the temperature distribution is stratified rather than being linearized, if heat sources are distributed in the lower part of the room such as office. Similarly, the vertical temperature distribution in ward with DV tends to be stratified. The temperature gradient in the lower part of the neutral height is sharper than the upper part. The temperature distribution in the upper part was nearly constant, and it was close to mixing ventilation.

The vertical temperature distribution in a ward with DV could be predicted using the zonal model. When the temperature gradient was obviously positive, the relative air temperature near the floor κ was nearly 0.5 in the experiment results. It indicates that "50% rule" could be applied to the displacement-ventilated ward. Because the air temperature in the upper part of the neutral height is nearly constant, the temperature distribution can be roughly forecasted using this "50% rule", if the netural height can be calculated. However, when the supply airflow rate is very large, the temperature stratification gets weaker and nearly linearized. Hence, the two-node model (Mundt model or Xu model) might have better accuracy in this case.

6.2 Contaminant Concentration in a Displacement-ventilated Ward

As with general displacement-ventilated room, the contaminant concentration is stratified in a ward with DV. The room is vertically divided into two zone and the air quality in lower zone of the contaminant interface can be maintained as fresh as supply air. It indicates that person in the lower part (lying and sitting person) might not perceive the unpleasant smell in a ward with DV. A standing person would smell the odor; however, the concentration of the odor would not be as high as it is in the ambient air due to the convective airflow layer around the body. It was revealed that the contaminant concentration of inhaled air of the standing person is lower that the ambient air. The entrained airflow rate to the boundary layer of the standing person was expected to be larger at the chest than the leg. However, if there is another heat source with significantly stronger plume than lying person, the contaminated plume would be locked-up without reaching the ceiling. In this case, the contaminant concentration at the stagnation height is higher than the mixing ventilation and personal exposure also increase. Hence, the location of strong heat source should be carefully detemined.

The contaminant interface forms at the height where the supply airflow rate and the sum of upward and downward convection airflow rate are equal (neutral height). Although several previous study suggested the equation to predict this neutral height, it could not be applied to the ward, because the plume rate of the lying person is larger than the sitting person. However, in this study, it was proven that the neutral height in a ward with DV if the convection airflow rate of heat sources inside the ward can be calculated. The validity of the zonal model was confirmed in this paper. When the contaminated air is locked-up, the improved zonal model can be used. The contaminant concentration of the room with DV could be predicted with these models.

6.3 Radiant Panel as a Complementary Heating and Cooling System

The vertical radiant panel should be used carefully with DV. When the vertical radiant panel is utilized as a heating system, the air in the lower part would be still clean. However, the contaminant air could be locked up in the upper part of the room if there is space between the panel and the bed. In order to remove the odor efficiently in the hospital ward, the radiant panel should be placed as close to the bed as possible. On the other hand, using a radiant panel as a cooling system is not recommended. If the surface temperature of the radiant panel is lower than the supply air, the contaminant air in the upper part would be transported to the lower part of the room, and the contaminant interface could not exist. In this case, the contaminant concentration distribution in a room is close to the mixing ventilation, and the air quality in the lower part could even worse than the mixing ventilation.

6.4 Influence fo Vertical airflow along a Vertical Surface

Downward airflow along the vertical surface considerably affects the air quality of the lower zone, and the upward airflow could cause contaminant stagnation in the upper part of the room with DV. Hence, the walls of the displacement-ventilated room should be insulated well. If there is a window in a ward, the radiator near the window would be helpful to reduce the downward airflow from the cold window. As it approaches

the cooled or heated vertical surface, the influence of convection airflow also becomes greater. Because downward airflow has a significant influence on the contaminant concentration in the lower occupant zone, it should be more seriously considered than the upward airflow along the wall. In this study, the wall temperature was changed to generate different amount of convection airflow. However, the convection airflow rate could not be accurately predicted because the measurement point of the air temperature was not close enough to the wall. As the wall became cooler, more downward airflow was generated, and the heat loss in the room also increased. To avoid the decreased air quality in the occupied zone, The sufficient heat gain should be exist in a ward with DV. Although the increase in the downward airflow caused the higher contaminant concentration in the lower part, it was still lower than the mixing ventilated room, as long as the positive concentration gradient was maintained. However, if the heat gain in the room was small, the temperature and contaminant concentration in the entire room were no longer stratified, and air quality in the occupied zone became close to that of the exhaust air. The results from this experiment and previous studies showed that when the temperature difference between the supply and exhaust air was larger than 1 °C, the contaminant concentration in the lower part increased sharply and became close to mixing ventilation. The influence of the stability of temperature stratification should be further examined in subsequent studies.

6.5 Influence of Internal Partition Curtain

Internal partition curtain has a beneficial effect on the contaminant concentration distribution in a ward with DV. The contaminated air emitted from the heat source inside the curtain can be removed efficiently without spreading outside the curtain. The bottom height of the curtain influences the supplied airflow rate inside the curtain. If the space between the floor and curtain is too small, the supply air would not be easy to flow into the curtain. However, if the space is too large, the supplied air into the curtain would flow out from the curtain. Hence, the partition curtain should be installed at the appropriate height. The location of the supply inlets also affect the contaminant concentration distribution greatly. To provide equal air quality into all curtains, the supply inlets should be placed asymmetrically. If the inlets are one-sided, the further curtain is located from the inlets, the more supply air flow into the curtain. In this study, the air quailty inside and outside the curtain was better when the supply inlets were located outside the curtain, rather than being located inside the curtain.

6.6 Future Perspectives

For a goal of removing unpleasant odor from the patient's body and bodily excharges, DV might be an appropriate ventilation system for a ward. Because the body is a contaminant source as well as heat source, the odor can be effectively exhausted in a room with DV. However, it should be noted that the suitability of DV for wards is still controversial if there is a risk of droplet or airborne infection. In this study, the target contaminant was passive gaseous pollutant and the contaminant source was simulated using tracer gas. The infectious pollutants would be distributed differently, because it is denser than the room air and emitted with positive momentum. For this reason, the further study on the distribution of various sizes of particles should

be performed if DV is expected to reduce the nosocomial infection risk in a ward.

Plume interaction should be further examined. It was assumed that the plumes above the heat sources go up individually when the neutral height was calculated in this study. However, the the plumes would merged if heat sources are located closely. In this case, the plume rate would be overestimated if it is calculated individually. The plume interaction is also a key of lock-up phenomenon. It should be studied under various types and locations of heat sources to predict the neutral height accurately and to avoid the stagnation of the contaminated air.

In this study, the influence of heat loss and gain through the walls was examined. Since heat loss or gain causes the convection airflow along the wall, it had a great influence on the contaminant concentration in a ward with DV. On the other hand, heat loss through the ceiling or floor has a different influence than does heat loss through a wall. In cases with heat loss through the ceiling or floor, there was no significant increase in the contaminant concentration, whereas heat loss through a vertical surface directly affected the contaminant concentration because of the downward airflow. Differences among the effects of heat loss or gain through walls, floors and ceilings on contaminant concentration require further study.

Thermal environment is also an important factor to create the comfortable indoor environment of the wards. However, this study focused on the contaminant concentration (indoor air quality), rather than thermal comfort. In subsequent study, thermal comfort of the patients and staff in the hospital wards with DV should be investigated under different heat generation and supply airflow rate conditions.

The experiments in this study were carried out with limited supply airflow conditions. Supply airflow rate also considerably affect the temperature and contaminant concentration in a room with DV, and the proper supply airflow rate for a ward is still unknown. This should be investigated in further study.

Original Papers

1) N. Choi, T. Yamanaka, K. Sagara, Y. Momoi, T. Suzuki (2019) : Displacement ventilation with radiant panel for hospital wards: Measurement and prediction of the temperature and contaminant concentration profiles, *Building and Environment*, Volume 160, 106197.
2) N. Choi, T. Yamanaka, T. Kobayashi (2020) : Influence of vertical airflow along walls on temperature and contaminant concentration distributions in a displacement-ventilated four-bed hospital ward, *Building and Environment*, Volume 183, 107181.
3) N. Choi, T. Yamanaka, T. Kobayashi, T. Ihama (2020) : Impact of partition curtains on temperature and contaminant concentration in a displacement ventilated four-bed hospital ward, *Transactions of the Society of Heating, Air-conditioning and Sanitary Engineers of Japan*, Vol. 45, No. 283, pp.31-39. (In Japanese)